Kinetics of Carbon Dioxide Absorption into Aqueous Solutions of 4-(Diethylamino)-2-Butanol and Blended Monoethanolamine and 4-(Diethylamino)-2-Butanol

A Thesis

Submitted to the Faculty of Graduate Studies and Research

In Partial Fulfillment of the Requirements

for the Degree of

Doctor of Philosophy

in Engineering

University of Regina

By

Teerawat Sema

Regina, Saskatchewan

January, 2012

UNIVERSITY OF REGINA

FACULTY OF GRADUATE STUDIES AND RESEARCH

SUPERVISORY AND EXAMINING COMMITTEE

Teerawat Sema, candidate for the degree of Doctor of Philosophy in Engineering**,** has presented a thesis titled, ***Kinetics of Carbon Dioxide Absorption into Aqueous Solutions of 4-(Diethylamino)-2-Butanol and Blended Monoethanolamine and 4-(Diethylamino)-2-Butanol,*** in an oral examination held on December 20, 2011. The following committee members have found the thesis acceptable in form and content, and that the candidate demonstrated satisfactory knowledge of the subject material.

External Examiner:	*Dr. Firoz A. Chowdhury, Research Institute of Innovative Technology for the Earth (RITE)
Supervisor:	Dr. Raphael Idem, Industrial Systems Engineering
	Dr. Paitoon Tontiwachwuthikul, Industrial Systems Engineering
Committee Member:	Dr. Hussameldin Ibrahim, Process Systems Engineering
Committee Member:	Dr. Gang Zhao, Process SYstems Engineering
Committee Member:	Dr. Iqbal Husain, Department of Mathematics & Statistics
Chair of Defense:	Dr. R. Nicholas Carleton, Department of Psychology

*Not present at defense

Abstract

Recently, global warming and climate change problems have begun to receive attention globally. One of the urgent policies is to control greenhouse gas emissions to the atmosphere. Among the greenhouse gases, CO_2 is considered to be a major contributor due to its abundance. The absorption of CO_2 into chemical solvents is one of the most promising technologies for capturing CO_2 due to its capability of handling large amounts of exhaust stream. One of the key parameters for this technology is to use effective solvents. A newly developed amino alcohol solvent, 4-(diethylamino)-2-butanol (DEAB), is now being considered as a promising alternative solvent for capturing CO_2 due to its energy efficiency for regeneration and high absorption capacity.

The primary focus of this research is on developing comprehensive reaction rate/kinetics models that take into account the coupling between the chemical equilibrium, mass transfer, and chemical kinetics of all possible chemical reactions for the absorption of CO_2 into aqueous solutions of DEAB and blended MEA-DEAB in order to explore the potential of these new formulated solvents for capturing CO_2 in terms of reaction kinetics. The fundamental knowledge required for the kinetics study, such as the physical solubility of CO_2 (Henry's law constant), the physical diffusivity of CO_2, the equilibrium solubility of CO_2, and the CO_2-amines equilibria, are also considered in this research.

The physical solubility and physical diffusivity of CO_2 in aqueous solutions of DEAB and blended MEA-DEAB were estimated via a N_2O analogy, which consists of measuring the solubility and diffusivity of N_2O instead of CO_2. The developed predictive

correlations for the solubility and diffusivity of N_2O in these new formulated solvents provide good predictive results compared to the experimental results.

The absorption capacity in terms of the equilibrium solubility of CO_2 in aqueous solutions of DEAB was found to be very high (comparable with PZ) and higher than that of AMP, MDEA, MEA, and DEA. Furthermore, the equilibrium solubility of CO_2 in an aqueous solution of blended MEA-DEAB was observed to be higher than that of MEA. This research also established the mathematical models for calculating the equilibrium solubility of CO_2 in an aqueous solution of these new formulated solvents. The calculated CO_2 equilibrium solubility results were found to fit well with the experimental results.

Finally, the comprehensive reaction rate/kinetics models for CO_2 absorption into aqueous solutions of DEAB and blended MEA-DEAB were successfully developed. The predicted CO_2 absorption rates obtained from the models favourably fit with the experimental results. The reaction kinetics results show that: (i) the rate of CO_2 absorption into DEAB is higher than that into MDEA, is comparable with that into AMP and DEA, and is lower than that into MEA and PZ, and (ii) the rate of CO_2 absorption into blended MEA-DEAB is higher than that into MEA.

Based on the results obtained from this research in terms of reaction kinetics and absorption capacity, it can be concluded that the aqueous solutions of DEAB and blended MEA-DEAB have good potential to be used as the alternative solvents for capturing CO_2.

Acknowledgements

Foremost, I would like to express my appreciation and acknowledgement to my supervisors, Dr. Raphael Idem and Dr. Paitoon Tontiwachwuthikul, for their invaluable guidance, support, and encouragement throughout my study. I appreciate all their contributions of time and their passion, which exceptionally inspire and enrich my growth as a researcher and an engineer.

My acknowledgement also extends to Dr. Mohamed Edali for his guidance on setting up the laminar jet absorber.

Many thanks go, in particular, to Mr. Derek Gervais and Mr. Ross Brice for their exceptional work on the liquid jet receiver.

Financial support from the International Test Centre for CO_2 Capture (ITC), the Faculty of Engineering and Applied Science, the Faculty of Graduate Studies and Research at the University of Regina, and the Natural Sciences and Engineering Research Council of Canada (NSERC), through funding received by my supervisors, is greatly acknowledged and sincerely appreciated.

Dedication

This work is dedicated to

My beloved parents,

Wattanaphong and Napaporn Sema

My brother,

Pirattapong Sema

And my grandmother,

Bang-On Charoenruaywattana

Also, many thanks to my girlfriend,

Pathamaporn Wattanaphan

Table of Contents

List of Tables

List of Figures

Nomenclature

a_i	coefficient for temperature dependence coefficient
A_i	temperature dependence coefficient
C	molar concentration (mol/L)
C_e^*	equilibrium concentration of gas at interface (mol/L)
C_j^0	bulk concentration for species j (mol/L)
C_{N_2O}	concentration of N_2O at equilibrium (mol/L)
d	jet diameter (m)
D	diffusivity of gas in liquid (m^2/s)
$D_{CO_2-amine}$	physical diffusivity of CO_2 in aqueous amine solution (m^2/s)
$D_{N_2O-amine}$	diffusivity of N_2O in aqueous amine solution (m^2/s)
$D_{CO_2-H_2O}$	physical diffusivity of CO_2 in water (m^2/s)
$D_{N_2O-H_2O}$	diffusivity of N_2O in water (m^2/s)
E	enhancement factor
h	jet height (m)
He_{N_2O}	solubility of N_2O (kPa m^3/kmol)
$He_{CO_2-amine}$	physical solubility of CO_2 in aqueous amine solution (kPa m^3/kmol)
$He_{N_2O-amine}$	solubility of N_2O in aqueous amine solution (kPa m^3/kmol)
$He_{N_2O-DEAB}$	solubility of N_2O in DEAB solvent (kPa m^3/kmol)

$He_{CO_2-H_2O}$	physical solubility of CO_2 in water (kPa m^3/kmol)
$He_{N_2O-H_2O}$	solubility of N_2O in water (kPa m^3/kmol)
k_{2i}	second order forward rate coefficient for reaction i (m^3/kmol s)
k_L^0	liquid phase mass transfer coefficient for physical absorption of CO_2 (m/s)
K_i	chemical equilibrium constant for reaction i
L	liquid flow rate (m^3/s)
n_{N_2O}	moles of N_2O fed to the stirred reactor (mol)
$n_{N_2O}^g$	moles of N_2O in gas phase at equilibrium (mol)
$n_{N_2O}^l$	moles of N_2O in liquid phase at equilibrium (mol)
N	local CO_2 absorption rate per unit area (kmol/m^2 s)
N_{ave}	average CO_2 absorption rate per unit area (kmol/m^2 s)
P	pressure (kPa)
P_{CO_2}	equilibrium partial pressure of CO_2 (kPa)
P_{N_2O}	partial pressure of N_2O (kPa)
P_V	vapour pressure (kPa)
P_T	total pressure at equilibrium (kPa)
R	gas constant (kPa L/mol K)
R_A	rate of CO_2 absorption (mol/s)
$[R_3N]$	free amine concentration (mol/L)
$[R_3N]_0$	initial amine concentration (mol/L)

t	temperature (^{o}C)
T	temperature (K)
V_g	volume of gas container (L)
V_l	volume of liquid in container (L)
Z_{N_2O}	compressibility factors

Greek symbols

α	CO_2 loading (mol of CO_2 per mol of amine)
ΔH_{abs}	heat of CO_2 absorption (kJ/mol)
ϕ_i	volume fraction of species i
η	viscosity (Pa.s)
τ	contact time (s)
χ_i	mole fraction of species i

Abbreviations

AMP	2-amino-2-methyl-1-propanol
AMPD	2-amino-2-methyl-1,3-propanediol
CFCs	chlorofluorocarbons
CO_2	carbon dioxide
DEA	diethanolamine
DEAB	4-(diethylamino)-2-butanol
DETA	diethylenetriamine

DGA	diglycolamine
DIPA	diisopropanolamine
DMMEA	dimethylmonoethanolamine
EDA	ethylenediamine
EG	ethylene glycol
FDM	finite different method
FEM	finite element method
H_2S	hydrogen sulfide
HCl	hydrochloric acid
IPCC	intergovernmental panel on climate change
IR	infrared
MDEA	methyldiethanolamine
MEA	monethanolamine
MIPA	monoisopropanolamine
N_2	nitrogen
N_2O	nitrous oxide
ODE	ordinary differential equation
PDE	partial differential equation
PZ	piperazine
TBAE	2-(*tert*-butylamino)-ethanol
TEA	triethanolamine
TMS	tetramethylene sulphone
VLE	vapour-liquid equilibrium

Chapter 1 Introduction

1.1 General

Recently, a fundamental change in governments' policies on energy-related environmental issues, especially on combating global warming and climate change problems, has been witnessed globally. The Intergovernmental Panel on Climate Change (IPCC) pointed out that the drastic increase of greenhouse gases, such as carbon dioxide (CO_2), methane, and chlorofluorocarbons (CFCs), can be mainly attributed to emission from human activities. These emissions will enhance the greenhouse effect, resulting in an increased earth surface temperature, which directly affects human activities in many ways through the rapid melting of polar ice caps, the presence of heat waves, drought, and severe weather (Houghton et al., 1990; IEA, 2005).

Among the greenhouse gases, CO_2 is considered to be a major contributor due to its abundance (IEA, 2009). Almost 60% of CO_2 emissions are from coal-fired power generation plants and other industrial processes such as those associated with refineries and natural gas processing plants. Thus, the removal of CO_2 from these large point exhausted gas streams is essential in order to make any mitigation impact on CO_2 emission. In addition to the environmental reasons for CO_2 removal, there are some industrial processes, such as ammonia production and hydrogen production, that also require the removal of CO_2. Currently, there are several technology options for capturing CO_2 based on different physical and chemical processes including absorption, adsorption, membrane, and cryogenics (Rao and Rubin, 2002).

In the absorption technology, CO_2 is absorbed chemically, physically, or both chemically and physically by the solvent. After the absorption process, the solvent is regenerated by applying heat or reducing pressure for CO_2 desorption; then, the regenerated solvent is recycled for the absorption process again. Physical absorption is generally suitable for processes that have a high partial pressure of CO_2 such as that associated with natural gas processing plants. On the other hand, absorption using chemical solvents, such as aqueous amine solutions, is suitable for processes that have a low partial pressure of CO_2 such as in coal fired power generation plants. The adsorption process relies on the attraction between CO_2 and the solid adsorbent. Generally, used adsorbents consist of activated carbon (Maroto-Valer et al., 2005), a molecular sieve (Stewart and Hessami, 2005), or lithium compounds (Fauth et al., 2005). For the membrane technology, there are two approaches applied in the literature, which are: (i) a membrane that can be used for separating CO_2 from the stream and (ii) a membrane that is used to increase the CO_2-amine interface (deMontigny, 2004; Brunetti et al., 2010). In the cryogenics separation, CO_2 in the stream is liquefied by refrigeration. Generally, cryogenics separation is applied to a stream that has a high CO_2 concentration of at least 70% (Plasyski and Chen, 2002). The advantages and disadvantages of each technology are summarized in Table 1.1.

Table 1.1 Advantages and disadvantages of absorption, adsorption, membrane, and cryogenics technologies (Figueroa et al., 2008; Yang et al., 2008; Brunetti et al., 2010)

Technologies	Advantages	Disadvantages
Post combustion amine based CO_2 absorption	• technology is proven and commercially available • able to handle large amounts of exhausted stream	• high energy consumption for regeneration • solvent degradation • solvent corrosiveness
Adsorption	• uncomplicated technology • high thermal and chemical resistance	• high operation cost • low efficiency
Membrane	• high thermal and chemical resistance • high gas-liquid interface	• significant capital cost • requires more research and development
Cryogenics	• suitable for high CO_2 concentration stream (>70%) • liquid CO_2 is obtained directly from the process	• requires significant energy for refrigeration • high capital cost

Base on Table 1.1, it can be concluded that the post combustion amine-based CO_2 absorption technology has been recently accepted as one of the most cost effective options among the others (Devid and Herzog, 2000; Rao and Rubin, 2002).

Typically, the principal amines in commercial CO_2 absorption processes are monoethanolamine (MEA), diethanolamine (DEA), methyldiethanolamine (MDEA), and 2-amino-2-methyl-1-propanol (AMP) (Sartori and Savage, 1983; Tontiwachwuthikul et al., 1991; Kohl and Nielsen, 1997). It is generally accepted that primary and secondary amines, such as MEA and DEA, react rapidly with CO_2 to form carbamates. However, there is a relatively high heat of CO_2 absorption associated with carbamate formation; thus, the cost of regenerating MEA and DEA is high. MEA and DEA also have the disadvantage of a limited CO_2 absorption capacity at 0.5 mol of CO_2 per mol of amine. On the other hand, tertiary amines, such as MDEA, do not react with CO_2 directly. It acts as base that promotes the hydrolysis of CO_2 to form bicarbonate and protonated amine. This reaction is much slower than the direct reactions of MEA and DEA. However, the heat associated with bicarbonate formation is much lower than that with carbamate formation; thus, the regeneration cost for MDEA is much lower than that of MEA and DEA. MDEA also has an advantage over MEA and DEA on the CO_2 absorption capacity, which is limited to 1 mol of CO_2 per mol of amine. The primary sterically hindered amine, such as AMP, is also reactive with CO_2. Similar to MEA and DEA, AMP reacts directly with CO_2 to form carbamate. However, the carbamate generated from the CO_2-AMP reaction is not stable because of the high branches of AMP. The instable carbamate is easily hydrolyzed to form bicarbonate and free AMP. The released free AMP can then react with CO_2 again. Therefore, the CO_2 absorption capacity of AMP is limited to 1 mol

of CO_2 per mol of amine, which is higher than that of MEA and DEA (Sartori and Savage, 1983; Tontiwachwuthikul et al., 1991).

Chakravarty et al. (1985) first suggested mixing a primary or secondary amine with a tertiary amine to capitalize on the advantages of each amine and to compensate for the undesirable properties of one amine using the second amine. By mixing a primary or secondary amine with a tertiary amine, the CO_2 absorption rate can be enhanced and the energy requirement for regeneration process can be reduced. The benefits of a blended amine system have been proven widely in the literature (Critchfield and Rochelle, 1987; Kohl and Nielsen, 1997; Zhang et al., 2002; Choi et al., 2007; Edali et al., 2007). The examples of blended amine systems are MEA-MDEA, DEA-MDEA, and AMP-MDEA. However, MEA has been selected to be mixed with MDEA rather than DEA and AMP due to the higher reactivity of MEA over DEA and AMP.

According to Tontiwachwuthikul et al. (2008) and Maneeintr et al. (2009), who studied the rational molecular deign and placement of functional groups of amino alcohol compounds, a newly developed amino alcohol solvent, 4-(diethylamino)-2-butanol (DEAB), is being considered as a promising solvent for capturing CO_2 due to its energy efficiency for regeneration and very high absorption capacity. However, it was mentioned by Maneeintr et al. (2010), who studied the CO_2 absorption performance of MEA and DEAB in terms of the overall mass transfer coefficient, that the overall mass transfer coefficient of aqueous DEAB solutions is lower than that of aqueous MEA solutions. The results also show that the reaction between CO_2 and DEAB is probably slower than that of MEA. This is because DEAB is a tertiary amine since it has 3 carbon atoms attached to the nitrogen atom (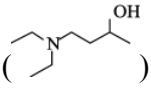

).

Based on the suggestion of Chakravarty et al. (1985), it is worthwhile to blend MEA with DEAB in order to (1) counter the high regeneration energy of MEA, (2) compensate the low CO_2 absorption capacity of MEA, and (3) enhance the CO_2 absorption rate of DEAB. Therefore, the primary focus of this research is on studying the kinetics of CO_2 absorption into aqueous solutions of the new formulated solvents (i.e., DEAB and blended MEA-DEAB) because the reaction kinetics data is one of the key parameters required for the process simulation and design of the absorber for a CO_2 treating plant (Rochelle, 1991). Furthermore, the performance of these new formulated solvents in terms of the equilibrium solubility of CO_2 (absorption capacity) is also considered in this research.

1.2 Research Objectives

The overall objective of this research is to develop and study, in comparison with the conventional solvents, the potential of the new formulated solvents (i.e., DEAB and blended MEA-DEAB) that can be used for capturing CO_2 in terms of reaction kinetics. In order to achieve this primary goal, fundamental knowledge of the new formulated solvents, such as the physical solubility of CO_2 (Henry's law constant), the physical diffusivity of CO_2, the equilibrium solubility of CO_2, and the equilibrium constant that governs the CO_2-DEAB reaction, are required. Therefore, the main objectives of this research can be summarized as follows:

1. To experimentally determine and establish the predictive correlations for the physical solubility of CO_2 (Henry's law constant) and the physical diffusivity of CO_2 in aqueous solutions of DEAB and blended MEA-DEAB.

2. To experimentally determine and develop mathematical models that can be used to predict the equilibrium solubility of CO_2 in aqueous solutions of DEAB and blended MEA-DEAB.
3. To establish the predictive correlation for calculating the equilibrium constant that governs the CO_2-DEAB reaction.
4. To obtain the experimental kinetics data for CO_2 absorption into aqueous solutions of DEAB and blended MEA-DEAB.
5. To develop comprehensive reaction rate/kinetics models for CO_2 absorption into aqueous solutions of DEAB and blended MEA-DEAB that take into account the coupling between the chemical equilibrium, mass transfer, and chemical kinetics of all possible chemical reactions.

1.3 Thesis Outline

This thesis consists of an integrated-article format in which Chapters 4, 5, 6, 7, and 8 are actual manuscripts for publication; each of the five chapters is a standalone manuscript with separate relevant introductions, results and discussion, and summaries. Chapter 1 provides an overall introduction, while Chapter 2 provides a general literature review of the overall subject matter. All the experimental apparatuses and procedures that have been used throughout this research are presented in Chapter 3. Finally, the thesis is summarized in Chapter 9, which includes overall conclusions and recommendations for future research.

1.4 References

1. Brunetti, A.; Scura, F.; Barbieri, G.; Drioli, E. Membrane technologies for CO_2 separation. Journal of Membrane Science 2010, 359, 115-125.

2. Chakravaty, T.; Phukan, U.K.; Weiland, R.H. Reaction of acid gases with mixtures of amines. Chem. Engng. Prog. 1985, 81, 32-36.

3. Choi, W.J.; Cho, K.C.; Lee, S.S.; Shim, J.G.; Hwang, H.R., Park, S.W.; Oh, K.J. Removal of carbon dioxide by absorption into blended amines: kinetics of absorption into aqueous AMP/HMDA, AMP/MDEA, and AMP/piperazine solutions. Green Chem. 2007, 9, 594-598.

4. Critchfield, J.; Rochelle, G.T. Absorption of carbon dioxide in aqueous MDEA and MDEA/MEA solutions. The AIChE National Meeting, Houston, Texas, 1987.

5. deMontigny, D. Comparing packed column and membrane absorber for CO_2 capture; Ph.D. thesis, University of Regina, Regina, Canada, 2004.

6. Devid, J.; Herzog, H. The cost of carbon capture. The fifth International Conference on Greenhouse gas Control Technologies, Australia, 2000.

7. Edali, M.; Aboudheir, A.; Idem, R. Kinetics of carbon dioxide absorption into mixed aqueous solutions of MDEA and MEA using laminar jet apparatus and numerically solved absorption-rate/kinetic model. The COMSOL Conference, Boston, 2007.

8. Fauth, D.J.; Frommell, E.A.; Hoffman, J.S.; Reasbeck, R.P.; Pennline, H.W. Eutectic salt promoted lithium zirconate: novel high temperature sorbent for CO_2 capture. Fuel Processing Technology 2005, 86, 1503-1521.

9. Figueroa, J.D.; Fout, T.; Plasyski, S.; McIlvried, H.;Srivastava, R.D. Review advances in CO_2 capture technology-the U.S. department of energy's carbon sequestration program. International Journal of Greenhouse gas control 2008, 2, 9-20.

10. Houghton, R.; Jenkins, G.J.; Ephraums, E. Climate Change: the IPCC Scientific Assessment; Cambridge University Press: Cambridge 1990.

11. International Energy Agency (IEA) Emission Trading for Climate Policies; IEA head of publication service: France 2005.

12. International Energy Agency (IEA) CO_2 Emissions from fuel combustion; IEA head of publication service: France 2009.

13. Kohl, A.L.; Nielsen, R.B. Gas Purification: 5th Edition; Gulf Publishing Company: Houston, Texas, USA, 1997.

14. Maneeintr, K.; Idem, R. O.; Tontiwachwuthikul, P.; Wee, A. G. H. Synthesis, solubilities, and cyclic capacity of amino alcohols for CO_2 Capture from flue gas streams. Energy procedia 2009, 1, 1327-1334.

15. Maneeintr, K.; Idem, R. O.; Tontiwachwuthikul, P.; Wee, A. G. H. Comparative mass transfer studies of CO_2 absorption into aqueous solutions of DEAB and MEA. Ind. Eng. Chem. Res. 2010, 49, 2857-2863.

16. Maroto-Valer, M.M.; Tang, Z.; Zhang,Y. CO_2 capture by activated and impregnated anthracites. Fuel Processing Technology 2005, 86, 1487-1502.

17. Plasyski, S.I.; Chen, Z.Y. Review of CO_2 capture technologies and some improvement opportunities. Sympasia-Americal Chemical Society 2002, 644.

18. Rao, A.B.; Rubin, E.S. A technical, economical, and environmental assessment of amine based CO_2 capture technology for power plant greenhouse gas control. Environ. Sci. Technol. 2002, 36, 4467-4475.

19. Rochelle, G.T. Research needs foe acids gas kinetics and equilibria in alkanolamine systems. 70th GPA annual convention 1991, 66-82.

20. Sartori, G.; Savage, D.W. Sterically hindered amines for CO_2 removal from gases. Ind. Eng. Chem. Fundam. 1983, 22, 239-249.

21. Stewart, C.; Hessami, M. A study of methods of carbon dioxide capture and sequestration-the sustainability of a photosynthetic bioreactor approach. Energy Conversion and Management 2005, 46, 403-420.

22. Tontiwachwuthikul, P.; Meisen, A.; Lim, J.C. Solubility of CO_2 in 2-amino-2methyl-1-propanol solutions. J. Chem. Eng. Data 1991, 36, 130-133.

23. Tontiwachwuthikul, P.; Wee, A. G. H.; Idem, R. O.; Maneeintr, K.; Fan, G. J.; Veawab, A.; Aroonwilas, A.; Chakma, A. Method for capturing carbon dioxide from gas streams. US Patent Application. US Patent Application, No. US 2008/0050296 A1, 2008.

24. Yang, H.; Xu, Z.; Fan, M.; Gupta, R.; Slimane, R.B.; Bland A.E.; Wright, I. Progress in carbon dioxide separation and capture: a review. Journal of Environmental Sciences 2008, 20, 14-27.

25. Zhang, X.; Zhang, C.F.; Liu, Y. Kinetics of absorption of CO_2 into aqueous solution of MDEA blended with DEA. Ind. Eng. Chem. Res. 2002, 41, 1135-1141.

Chapter 2 General Literature Review

2.1 The screening of novel structured amines for CO_2 capture

Novel amines for capturing carbon dioxide (CO_2) have been developed based on the approach of rational molecular design and synthesis by appropriate substitution of the hydroxyl group into the structure of amino alcohol. The newly developed amines are 4-diethylamino-2-butanol (DEAB), 4-isopropylamino-2-butanol, 4-piperidino-2-butanol, 4-propylamino-2-butanol, and 4-(ethyl-methyl-amino)-2-butanol (Tontiwachwuthikul et al., 2008). Maneeintr et al. (2009) studied the performance of these amines for capturing CO_2 in terms of the equilibrium solubility of CO_2 and the cyclic capacity at an amine concentration of 2 M, a temperature range of 313 K to 353 K, and a CO_2 partial pressure range of 15 kPa to 100 kPa. They concluded that DEAB is an effective solvent for capturing CO_2 due to its very high absorption capacity and cyclic capacity.

2.2 Physical solubility and physical diffusivity of CO_2

Both physical solubility and physical diffusivity of CO_2 in aqueous amine solutions at various temperatures and amine concentrations are essential for developing the reaction rate/kinetics model for CO_2 absorption. However, the physical solubility and physical diffusivity of CO_2 in aqueous amine solutions cannot be measured directly because CO_2 reacts chemically with the aqueous amine solutions. Due to the similarity of molecular weight, chemical configuration, volume, and electronic structure between CO_2 and nitrous oxide (N_2O), Clarke (1964) assumed that the ratios of the solubility or diffusivity of CO_2 and N_2O in water and in an aqueous solution of organic solvents are

similar at the same temperature (Clarke, 1964; Liu et al., 1999). Then, Sada et al. (1977 and 1978) and Versteeg and van Swaaij (1988a) applied this concept for estimating the physical solubility and physical diffusivity of CO_2 in aqueous amine solutions. This methodology is called the N_2O analogy and is shown in Equations 2.1 and 2.2.

$$He_{CO_2-amine} = He_{N_2O-amine}\left(\frac{He_{CO_2-H_2O}}{He_{N_2O-H_2O}}\right) \tag{2.1}$$

$$D_{CO_2-amine} = D_{N_2O-amine}\left(\frac{D_{CO_2-H_2O}}{D_{N_2O-H_2O}}\right) \tag{2.2}$$

where $He_{CO_2-amine}$ and $He_{CO_2-H_2O}$ are the physical solubility of CO_2 (Henry's law constant) in amine solution and water, respectively. $He_{N_2O-amine}$ and $He_{N_2O-H_2O}$ are the solubility of N_2O in amine solution and water, respectively. $D_{CO_2-amine}$ and $D_{CO_2-H_2O}$ are the physical diffusivity of CO_2 in amine solution and water, respectively. Lastly, $D_{N_2O-amine}$ and $D_{N_2O-H_2O}$ are the diffusivity of N_2O in amine solution and water, respectively.

The N_2O analogy is widely accepted for estimating the physical solubility and physical diffusivity of CO_2 in aqueous amine solutions via measuring the solubility and diffusivity of N_2O (Versteeg and van Swaaij, 1988a; Xu et al., 1991;Wang et al., 1992; Browning and Weiland, 1994; Li and Lee, 1996; Ko et al., 2001).

Generally, the solubility of N_2O is measured in a temperature-controlled stirred reactor (glass flask or stainless steel reactor). The solubility of N_2O is measured through the pressure change in the system. The solubility of N_2O has been measured in various aqueous amine systems, such as (1) single amine systems of monoethanolamine (MEA), diethanolamine (DEA), triethanolamine (TEA), methyldiethanolamine (MDEA), 2-

amino-2-methyl-1-propanol (AMP), monoisopropanolamine (MIPA), diisopropanolamine (DIPA), ethylenediamine (EDA), diethylenetriamine (DETA), dimethylmonoethanolamine (DMMEA), and 2-(*tert*-butylamino)-ethanol (TBAE) and (2) blended amine systems of MEA-MDEA, MEA-AMP, AMP-MDEA, AMP-tetramethylene sulphone (TMS), and DEA-ethylene glycol (EG) (Sada et al., 1978; Haimour and Sandall, 1984; Versteeg and van Swaaij, 1988a; Xu et al., 1991; Wang et al., 1992; Saha et al., 1993; Li and Lai, 1995; Munder et al., 2000; Park and Sandall, 2001; Hartono et al., 2008).

In order to predict the solubility of N_2O in aqueous amine solutions, various predictive models have been applied such as the polynomial model (Versteeg and Van Swaaij, 1988a), the semiempirical model (Wang et al., 1992; Li and Lai, 1995), and the Redlich-Kister equation (Hartono et al., 2008). Versteeg and van Swaaij (1988a) reported that the solubility of N_2O is considered to be a polynomial function with respect to the amine concentration at a specific temperature. They also mentioned that the polynomial model is applicable for the prediction of the solubility of N_2O in aqueous solutions of DMMEA, DEA, TEA, MIPA, and DIPA at various temperatures and amine concentrations.

Wang et al. (1992) considered the solubility of N_2O in terms of excess Henry's quantity, which is a function of the temperature, the volume fraction of individual species in the solutions, the solubility of N_2O in water, and the solubility of N_2O in the individual amine. This semiempirical model can be used for binary (single amine aqueous solution) and tertiary (blended amine aqueous solution) systems. Wang et al. (1992) and Li and Lai (1995) reported that the semiempirical model gives a good estimation of the N_2O

solubility of various aqueous amine solutions of MEA, DEA, MDEA, AMP, DIPA, MEA-MDEA, MEA-AMP, AMP-MDEA, AMP-TMS, and DEA-EG.

The Redlich-Kister equation is widely used to correlate physical properties of binary and ternary solutions such as density, viscosity, and refractive index. Hatono et al. (2008) applied the Redlich-Kister equation for the prediction of the solubility of N_2O in aqueous solutions of DETA over various ranges of temperatures and amine concentrations. They mentioned that the solubility of N_2O depends on the mole fraction of amine in the solutions and the solubility of N_2O in the individual amine at a specific temperature. It was reported that the predicted results from the Redlich-Kister equation correlate well with the experimental results.

On the contrary, concerning the solubility of N_2O, the measurements of the diffusivity of N_2O were performed using various equipments such as a single-sphere absorber (Xu et al., 1991), a wetted wall column (Li and Lai, 1995; Li and Lee, 1996), a stirred cell reactor (Versteeg and van Swaaij, 1988a), and a laminar jet absorber (Aboudheir et al., 2004). The diffusivity of N_2O has been measured in various aqueous amine systems such as (1) single amine systems of MEA, DEA, TEA, MDEA, AMP, DIPA, and DMMEA and (2) blended amine systems of MEA-MDEA, MEA-AMP, DEA-MDEA, and DEA-AMP (Versteeg and van Swaaij, 1988a; Xu et al., 1991; Li and Lai, 1995; Li and Lee, 1996; Ko et al., 2001).

In order to predict the diffusivity of N_2O in aqueous amine solutions, two predicted models have been applied such as the semiempirical model (Ko et al., 2001) and the modified Stokes-Einstein model (Versteeg and van Swaaij, 1988a). The semiempirical model considers the diffusivity of N_2O in aqueous amine solution to be a

function of temperature and amine concentration. It has been mentioned that the semiempirical model provides a good estimation of the N_2O diffusivity into aqueous amine solutions of MEA, DEA, DIPA, MDEA, TEA, AMP, MEA-MDEA, MEA-AMP, DEA-MDEA, and DEA-AMP.

On the other hand, the modified Stokes-Einstein model correlates N_2O diffusivity in aqueous amine solutions via viscosity. The model describes the dependence of N_2O diffusivity in terms of viscosity. Versteeg and van Swaaij (1988a) found that the modified Stokes-Einstein model was applicable for the estimation of N_2O diffusivity into aqueous amine solutions of MEA, DEA, TEA, MIPA, and DIPA.

2.3 Vapour-liquid equilibria and chemical equilibrium constant

The vapour-liquid equilibria of the aqueous CO_2-amine system are essential for reaction rate/kinetics model development, which is required for process simulation and design for CO_2 treatment plants (Rochelle, 1991; Li and Shen, 1993). Kent and Eisenberg (1976) proposed a predictive method for determining the correlation representing the vapour-liquid equilibria of hydrogen sulphide (H_2S) and CO_2 in aqueous solutions of MEA and DEA. In this method, (1) the equilibrium solubility of acid gas (in their case, H_2S and CO_2) at various acid gas partial pressures and temperatures, (2) all involved equilibrium constants, and (3) Henry's constant are all used in the mathematical modeling. Then, the equilibrium constant governing amine reaction is determined by fitting to the experimental equilibrium solubility results at various temperatures, partial pressures of acid gas, and amine concentrations. They found that the proposed equilibrium constant, which is a function of only temperature in Kelvin, and the predicted

equilibrium solubility of acid gas, which is obtained from the modeling, can be used to represent the vapour-liquid equilibria of acid gas in aqueous amine solutions.

Austgen et al. (1989 and 1991) proposed the thermodynamic model for the equilibrium constant for the prediction of H_2S and CO_2 solubility in aqueous solutions of MEA, DEA, blended MEA-MDEA, and blended DEA-MDEA using the electrolyte-NRTL equation. In their model, the activity coefficient was applied as a representative of long-range ion-ion interaction and short-range binary interaction. The model is also a function of only temperature in Kelvin. They concluded that the equilibrium solubility of CO_2 calculated from the proposed model correlated well with the experimental results.

However, it has been mentioned by various researchers (Hu and Chakma, 1990; Tontiwachwuthikul et al., 1991; Li and Shen, 1993; Beak and Yoon, 1998; Beak et al., 2000) that in order to predict the equilibrium solubility of acid gas in an aqueous amine solution, the equilibrium constant, which governs amine reaction, should not only be considered as a function of temperature but also as a function of other parameters such as acid gas loading, free amine concentration, and physically dissolved CO_2 concentration. Li and Shen (1993) proposed predicted correlations for the equilibrium constant governing amine reaction in aqueous CO_2-blended MEA-MDEA systems. The predicted correlation for the equilibrium constant is also determined by fitting the correlation to the experimental CO_2 equilibrium solubility results. The Li-Shen model is a function of temperature, CO_2 loading, and free amine concentration. The results show that predicted equilibrium solubility of CO_2 in aqueous solutions of blended MEA-MDEA fit reasonably well with the experimental results.

Hu and Chakma (1990) proposed the predictive models for equilibrium constants governing amine reactions in an aqueous H_2S and CO_2-diglycolamine (DGA) system. The proposed model is a function of temperature, physically dissolved CO_2 concentration, and free amine concentration. They concluded that the proposed model works well for the prediction of the equilibrium solubility of H_2S and CO_2 in aqueous solutions of DGA.

2.4 Kinetics of CO_2 absorption into aqueous amine solutions

The kinetics of CO_2 absorption into aqueous amine solutions have been studied for a number of years with a wide variety of aqueous amine solutions such as MEA, DEA, MDEA, AMP, MDEA-MEA, MEA-AMP, MDEA-PZ, and AMP-PZ (Versteeg and van Swaaij, 1988b; Saha and Bandyopadhyay, 1995; Mandal et al., 2001; Zhang et al., 2001; Sun et al., 2005; Edali et al., 2009).

Saha and Bandyopadhyay (1995) conducted the experiment for measuring the rate of CO_2 absorption into aqueous AMP solutions using a wetted wall column over temperature and AMP concentration ranges of 294 K to 318 K and 0.5 M to 2 M, respectively. The zwitterion mechanism was applied in their work. The reaction rate constant and the order of reaction with respect to concentration of CO_2 and AMP were determined using a graphical method.

Ramachandran et al. (2006) performed an experiment using a laminar jet absorber for studying the kinetics of CO_2 absorption into an aqueous solution of CO_2 loaded, blended MEA-MDEA. Based on Hugbie's penetration theory, the experimental apparent

rate constants were fitted with the zwitterion mechanism rate expression or the termolecular mechanism rate expression to obtain the rate constants.

One of the very first numerical comprehensive reaction rate/kinetics models, which takes into account the coupling between chemical equilibrium, mass transfer, and chemical kinetics of all possible chemical reactions, was developed by Hagewiesche et al. (1995). They measured the rate of CO_2 absorption into an aqueous solution of unloaded, blended MEA-DEAB using a laminar jet absorber. The developed model is governed by a system of partial differential-nonlinear algebraic equations. The method of lines was used to transform the partial differential equations (PDEs) into the ordinary differential equations (ODEs); they were then solved using the code DDASSL in FORTRAN. Their developed reaction rate/kinetics model is capable of predicting the CO_2 absorption rate, the enhancement factor, and the rate coefficient of reaction between CO_2 and MEA. However, the experiment was performed with unloaded solution and at only 313 K.

Rinker et al. (1995 and 2000) studied the kinetics of CO_2 absorption in aqueous unloaded solutions of MDEA and blended DEA-MDEA using a wetted sphere absorber over a temperature range of 293 K to 342 K and concentration range of 10% to 30% mass MDEA. Their comprehensive reaction rate/kinetics models also take into account the coupling between chemical equilibrium, mass transfer, and chemical kinetics of all possible chemical reactions. The system of PDEs was developed. Then, the method of lines was used to transform the PDEs into ODEs. The system of ODEs was solved numerically using the code DDASSL in FORTRAN. Their predicted CO_2 absorption rates were found to agree reasonably well with the experimental results.

The more comprehensive reaction rate/kinetics model was developed by Aboudheir et al. (2003), who measured the rates of CO_2 absorption into an aqueous solution of loaded MEA using a laminar jet absorber over a temperature range of 293 K to 333 K, a concentration range of 3 M to 9 M, and a CO_2 loading range of 0.1 to 0.49. In their study, the partial differential-nonlinear algebraic equations were solved using the finite difference method (FDM) based on the Barakat-Clark scheme. They reported that the developed comprehensive reaction rate/kinetics model favourably predicted CO_2 absorption rates. Also, the absorption rate constant obtained from the model is in good agreement with the literature's values.

Recently, the comprehensive reaction rate/kinetics model has been extended to other promising amines systems such as blended MEA-MDEA and blended MDEA-piperazine (PZ) (Edali et al., 2007 and 2009). In their studies, the partial differential-nonlinear algebraic equations have been solved using two numerical techniques: the FDM based on the Barakat-Clark scheme and the finite element method (FEM) based on COMSOL software. They have found that both FDM and FEM produce very accurate predictions of CO_2 absorption rate results. Also, no significant difference between the results obtained from FDM and FEM were observed. Therefore, Edali (2010) suggested that the FEM based on COMSOL software could be used for the numerical solution of the partial differential-algebraic equations because coding the program of the numerical scheme can be eliminated.

2.5 References

1. Aboudheir, A.; Tontiwachwuthikil, P.; Chakma, A.; Idem, R. Kinetics of reactive absorption of carbon dioxide in high CO_2-loaded concentrated aqueous MEA solutions. Chem. Eng. Sci. 2003, 58, 5195-5210.

2. Austgen, D.M.; Rochelle, G.T.; Peng, W.; Chen, C.C. Model of vapor-liquid equilibria for aqueous acid gas-alkanolamine systems using the electrolyte-NRTL equation. Ind. Eng. Chem. Res. 1989, 26, 1060-1073.

3. Austgen, D.M.; Rochelle, G.T.; Chen, C.C. Model of vapor-liquid equilibria for aqueous acid gas-alkanolamine system. 2. Representation of H_2S and CO_2 solubility in aqueous MDEA and CO_2 solubility in aqueous mixtures of MDEA with MEA or DEA. Ind. Eng. Chem. Res. 1991, 30, 543-555.

4. Beak, J.I.; Yoon, J.I. Solubility of carbon dioxide in aqueous solutions of 2-amino-2-methyl-1,3-propanediol. J. Chem. Eng. Data 1998, 43, 635-637.
5. Browning, G.J.; Weiland, R.H. Physical solubility of carbon dioxide in aqueous alkanolamines via nitrous oxide analogy. J. Chem. Eng. Data 1994, 39, 817-822
6. Clarke, J. K. A. Kinetics of absorption of carbon dioxide in monoethanolamine solutions at short contact times. Ind. Eng. Chem. Fundam. 1964, 3, 239-245.
7. Edali, M. Kinetics, modeling, and simulation of carbon dioxide absorption into mixed aqueous loaded solution blendes of methyldiethanolamine with monoethanolamine and with piperazine; Ph.D. thesis, University of Regina, Regina, Canada, 2010.

8. Edali, M.; Aboudheir, A.; Idem, R. Kinetics of carbon dioxide absorption into mixed aqueous solutions of MDEA and MEA using laminar jet apparatus and numerically solved absorption-rate/kinetic model. The COMSOL Conference, Boston, 2007

9. Edali, M.; Aboudheir, A.; Idem, R. Kinetics of carbon dioxide into mixed aqueous solutions of MDEA and MEA using laminar jet apparatus and a numerically solved 2D absorption rate/kinetics model. International Journal of Greenhouse Gas Control 2009, 3, 550-560.

10. Hagewiesche, D.P.; Ashour, S.S.; Al-Ghawas, H.A.; Sandall, O.C. Absorption of carbon dioxide into aqueous blends of monoethanolamine and N-methyldiethanolamine. Chem Eng. Sci. 1995, 50, 1071-1079.

11. Haimour, N.; Sandall, O.C. Absorption of carbon dioxide into aqueous methyldiethanolamine. Chemical Engineering Science 1984, 39, 1791-1796.

12. Hartono, A.; Juliussen, O.; Svendsen, F.H. Solubility of N_2O in aqueous solution of diethylenetriamine. J. Chem. Eng. Data 2008, 53, 2696-2700.

13. Hu, W.; Chakma, A. Modelling of equilibrium solubility of CO_2 and H_2S in aqueous diglycolamine (DGA) solutions. The Canadian Journal of Chemical Engineering 1990, 68, 523-525.

14. Ko, J.; Tsai, T.; Lin, C.; Wang, H.; Li, M. Diffusivity of nitrous oxide in aqueous alkanolamine solutions. J. Chem. Eng. Data 2001, 46, 160-165.

15. Li, M.H.; Lai, M.D. Solubility and diffusivity of N_2O and CO_2 in (monoethanolamine + N-methyldiethanolamine + water) and in (monoethanolamine + 2-amino-2-methyl-1-propanol + water). J. Chem. Eng. Data 1995, 40, 486-492.

16. Li, M.H.; Lee, W.C. Solubility and diffusivity of N_2O and CO_2 in (diethanolamine+N-methyldiethanolamine+water) and in (diethanolamine+2-amino-2-methyl-1-propanol+water). J. Chem. Eng. Data 1996, 41, 551-556.

17. Li, M.H.; Shen, K.P. Calculation of equilibrium solubility of carbon dioxide in aqueous mixtures of monoethanolamine and methyldiethanolamine. Fluid Phase Equilibria 1993, 85, 129-140.

18. Liu, Y.; Zhang, L.; Watanasiri, S. Representing vapor-liquid equilibrium for an aqueous MEA-CO_2 system using the electrolyte nonrandom-two-liquid model. Ind. Eng. Chem. Res. 1999, 38, 2080-2090.

19. Mandal, B.P.; Guha, M.; Biswa, A.K., Bandopadhyay, S.S. Removal of carbon dioxide by absorption in mixed amines modeling of absorption in aqueous MDEA/MEA and AMP/MEA solutions. Chem. Eng. Sci. 2001, 51, 6217-6244.

20. Maneeintr, K.; Idem, R. O.; Tontiwachwuthikul, P.; Wee, A. G. H. Synthesis, solubilities, and cyclic capacity of amino alcohols for CO_2 Capture from flue gas streams. Energy procedia 2009, 1, 1327-1334.

21. Munder, B.; Lidal, H.; Sandall, O. C. Physical solubility of hydrogen sulfide in aqueous solutions of 2-(tert-Butylamino) ethanol. J. Chem. Eng. Data 2000, 45, 1201-1204.

22. Park, M. K.; Sandall, O. C. Solubility of carbon dioxide and nitrous oxide in 50 mass % Methyldiethanolamine. J. Chem. Eng. Data 2001, 46, 166-168.
23. Rinker, E.B.; Ashour, S.S.; Sandall, O.C. Kinetics and modeling of carbon dioxide absorption into aqueous solutions of N-methyldiethanolamine. Chem. Eng. Sci. 1995, 50, 755-768.
24. Rinker, E.B.; Ashour, S.S.; Sandall, O.C. Absorption of carbon dioxide into aqueous blends of diethanolamine and methyldiethanolamine. Ind. Eng. Chem. Res. 2000, 39, 4346-4356.
25. Rochelle, G.T. Research needs foe acids gas kinetics and equilibria in alkanolamine systems. 70th GPA annual convention 1991, 66-82.
26. Sada, E.; Kumazawa, H.; Butt M.A. Solubilities of gases in aqueous solutions of amine. J. Chem. Eng. Data 1977, 22, 277-278.
27. Sada, E.; Kumazawa; H.; Butt M.A. Solubilities of hydrogen sulfide and carbon dioxide in a diglycolamine solution. J. Chem. Eng. Data 1978, 23, 161-163.
28. Saha, A, K.; Bandyopadhyay, S.S. Kinetics of absorption of CO_2 into aqueous solutions of 2-amino-2-methyl-1-propanol. Chemical Engineering Science 1995, 50, 3587-3598.
29. Saha, A, K.; Bandyopadhyay, S.S.; Biwas, A.K. Solubility and Diffusivity of N_2O and CO_2 in aqueous 2-amino-2-methyl-1-propanol. J. Chem. Eng. Data 1993, 38, 78-82.
30. Sun, W.C.; Yong, C.B.; Li, M.H.; Kinetics of the absorption of carbon dioxide into mixed aqueous solutions of 2-amino-2-methyl-1-propanol and piperazine. Chem. Eng. Sci. 2005, 60, 503-516.

31. Tontiwachwuthikul, P.; Meisen, A.; Lim, J.C. Solubility of CO_2 in 2-amino-2methyl-1-propanol solutions. J. Chem. Eng. Data 1991, 36, 130-133.

32. Tontiwachwuthikul, P.; Wee, A. G. H.; Idem, R. O.; Maneeintr, K.; Fan, G. J.; Veawab, A.; Aroonwilas, A.; Chakma, A. Method for capturing carbon dioxide from gas streams. US Patent Application. US Patent Application, No. US 2008/0050296 A1, 2008.

33. Versteeg, G. F.; van Swaaij W.P.M. Solubility and diffusivity of acid gases (CO_2, N_2O) in aqueous alkanolamine solutions. J. Chem. Eng. Data 1988a, 33, 29-34.

34. Versteeg, G. F.; van Swaaij W.P.M. On the kinetics between CO_2 and alkanolamines both in aqueous and non-aqueous solutions-I. primary and secondary amines. Chemical Engineering Science 1988b, 43, 573-585.

35. Wang, Y. W.; Xu, S.; Otto, F. D.; Mather, A. E. Solubility of N_2O in alkanolamines and in mixed solvents. The Chemical Engineering Journal 1992, 48, 31-40.

36. Xu, S.; Otto, F.D.; Mather, A.E. Physical properties of aqueous AMP solutions. J. Chem. Eng. Data 1991, 36, 71-75

37. Zhang, X.; Zhang, C.F.; Qin, S.J.; Zheng, Z.S. A kinetics study on the absorption of carbon dioxide into a mixed aqueous solution of methyldiethanolamine and piperazine. Ind. Eng. Chem. Res. 2001, 40, 3785-3791.

Chapter 3 Experimental Procedure

3.1 Chemicals

4-diethylamino-2-butanol (DEAB) was synthesized according to the procedure described by Tontiwachwuthikul et al. (2008) in our solvent synthesis laboratory in the International Test Centre for CO_2 Capture (ITC) at the University of Regina. The purity of synthesized DEAB was determined using GC-MS and found to be in the range of 91-93%. ReagentPlus grade monoethanolamine (MEA) and methyldiethanolamine (MDEA) with a purity of ≥99% were supplied by Sigma-Aldrich Co., Canada. Aqueous solutions of MEA and blended MEA-DEAB of desired concentrations were prepared by adding a known amount of de-ionized water and predetermined amounts of MEA and DEAB. Carbon dioxide (CO_2), nitrogen (N_2), and nitrous oxide (N_2O) with purities of 99.9% were supplied by Praxair Inc, Canada.

3.2 Solubility of N_2O

The apparatus and experimental technique used for determining N_2O solubility were modified from the works of Munder et al. (2000) and Park et al. (2001). The solubility experiment was performed in a rotary-type 600 ml stainless steel autoclave reactor (model Parr 5500, Parr Instrument Co., Moline, IL) connected to a controller (model Parr 4843, Parr Instrument Co., Moline, IL) as shown in Figure 3.1. The reactor consisted of a variable-speed impeller, a heating mantle, a cooling coil, a gas feed port, a thermocouple, and a pressure transducer.

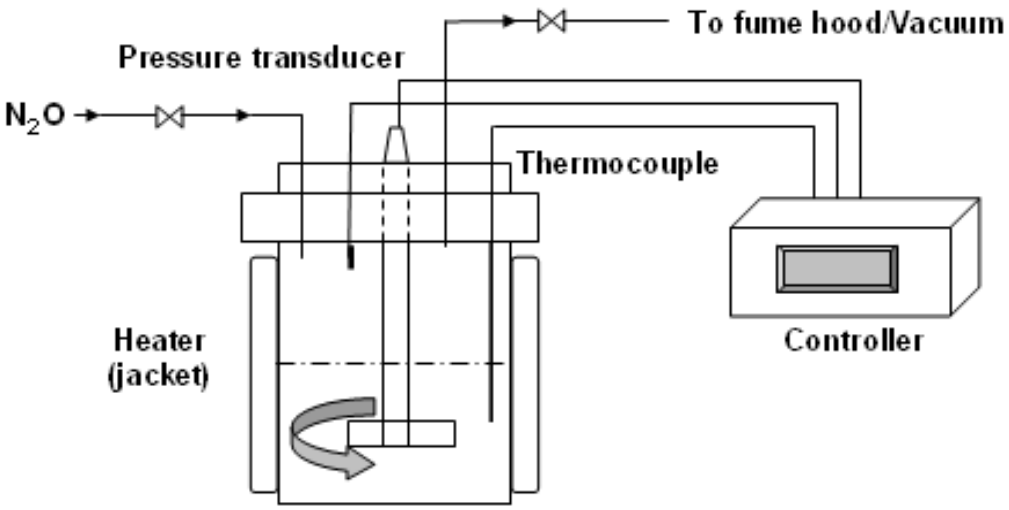

Figure 3.1 Experimental set up for N_2O solubility measurement.

Initially, the amine solution was degassed using an ultrasonic bath (VWR model 75D, VWR international, ON, Canada), and then 300 ml of the degassed amine solution was introduced into the reactor. The desired temperature was set and controlled by the controller and then the vacuum was turned on. After shutting down the vacuum pump, the liquid was under a certain pressure due to liquid vaporization. The pressure, P_V (kPa), was measured at equilibrium. Then, a certain amount of N_2O (n_{N_2O}; kmol) was fed to the reactor. The amount of n_{N_2O} can be determined by measuring the pressure in the reactor before N_2O injection (P_1; kPa) and after N_2O injection (P_2; kPa).

$$n_{N_2O} = (P_2 - P_1)\frac{V_g}{Z_{N_2O}RT} \tag{3.1}$$

where V_g is volume of the gas container (m^3), R is the gas constant, and Z_{N_2O} is compressibility factors of N_2O, which can be calculated using the Peng-Robinson equation of state (Peng and Robinson, 1976). After the system had reached equilibrium, the equilibrium pressure (P_T; kPa) was measured. The partial pressure of N_2O (P_{N_2O}; kPa) at equilibrium is:

$$P_{N_2O} = P_T - P_V \tag{3.2}$$

The number of moles of N_2O in the gas phase at equilibrium ($n^g_{N_2O}$; kmol) can be determined using:

$$n^g_{N_2O} = \frac{P_{N_2O}V_g}{Z_{N_2O}RT} \tag{3.3}$$

The number of moles of N_2O dissolved in the liquid phase at equilibrium ($n^l_{N_2O}$; kmol) can be determined using:

$$n^l_{N_2O} = n_{N_2O} - n^g_{N_2O} \tag{3.4}$$

The concentration of N_2O at equilibrium (C_{N_2O}; kmol/m^3) is:

$$C_{N_2O} = \frac{n^l_{N_2O}}{V_l} \tag{3.5}$$

Then, the N_2O solubility (He_{N_2O}; kPa m^3/kmol) is defined as:

$$He_{N_2O} = \frac{P_{N_2O}}{C_{N_2O}} \tag{3.6}$$

The equipment and calculation procedure for the N_2O solubility were validated with MEA and MDEA within a temperature range of 298 K to 343 K as shown in Figure 3.2. It was found that the experimental results are in good agreement with the literature works (Wang et al., 1992) with an absolute average deviation (AAD) of 2.3%, which confirms that the N_2O solubility data obtained from this work are accurate. Some experimental works were tested for repeatability; the results show that the deviation of the N_2O solubility measurement is 1.4%.

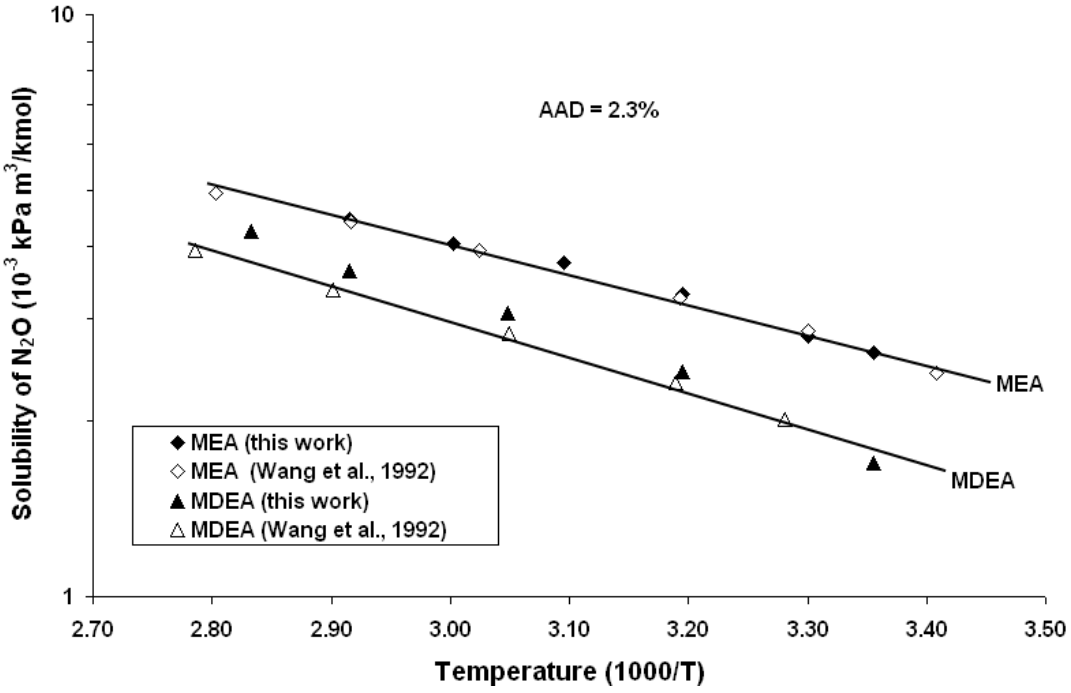

Figure 3.2 N_2O solubility in MEA and MDEA; solid lines are predicted results obtained from Wang et al. (1992).

3.3 Diffusivity of N_2O

The N_2O diffusivities were measured using the laminar jet absorber as shown in Figure 3.3. A detailed description of the laminar jet absorber and its operation can be seen in Al-Ghawas et al. (1989) and Aboudheir et al. (2004). Briefly, the amine solution was degassed by spraying it into a vacuum, and then the degassed amine solution was passed through the temperature-controlled water jacket in order to reach the desired temperature. The degassed amine solution was then passed through the jet nozzle in order to continuously generate a smooth-surfaced rod-like jet in the absorption chamber. The soap-film meter was used to measure the rate of absorption (R_A; mol/s). The two dimensional microscope was used to measure jet height (h; cm) and jet diameter (d; cm). Finally, the discharged liquid was collected and liquid flow rate (L; cm^3/s) was measured. According to the penetration theory for physical absorption, R_A can be defined as:

$$R_A = 4C_e^*(DLh)^{1/2} \tag{3.7}$$

where C_e^* is the equilibrium concentration of gas at the interface (mol/cm^3), D is the diffusivity of gas in the liquid (cm^2/s), L is the liquid flow rate (cm^3/s), and h is jet height (cm). A plot of R_A and $(Lh)^{1/2}$ at various flow rates and jet heights should provide a straight line through the origin with a slope of $4C_e^*D^{1/2}$. C_e^* can be determined using:

$$C_e^* = \frac{P_{N_2O}}{He_{N_2O}} \tag{3.8}$$

The laminar jet absorber was validated with 1 M MEA for the diffusivity of N_2O at 298 K, which was found to be 1.72×10^{-5} cm/s (while Sada et al. (1978) and Aboudheir et al. (2004) found it to be 1.69×10^{-5} cm/s and 1.70×10^{-5} cm/s, respectively). Also, some

N_2O diffusivity measurements were tested for repeatability. The results show that the deviation of the N_2O diffusivity measurement is 0.8%.

3.4 Absorption rate of CO_2

The CO_2 absorption rate was also measured using a laminar jet absorber. The detailed description is the same as in Section 3.3. The equipment was validated with water for the diffusivity of CO_2 at 298 K, which was found to be 1.97×10^{-5} cm/s (while Al-Ghawas et al. (1989) and Aboudheir et al. (2004) found it to be 1.96×10^{-5} cm/s and 1.95×10^{-5} cm/s, respectively). Also, some CO_2 diffusivity measurements were tested for repeatability. The results show that the deviation of the CO_2 diffusivity measurement is 0.7%.

3.5 Equilibrium solubility of CO_2

The apparatus and experimental technique used for determining the equilibrium solubility of CO_2 were similar to those in the work of Tontiwachwuthikul et al. (2008). The experimental setup is shown in Figure 3.4. The main features are a saturation cell, an absorption reactor, a mass flow meter, and a water bath with a temperature controller. For each experiment, the saturated cell and the absorption reactor were immersed in a water bath (Cole-Parmer) with a temperature controller (Cole-Parmer, within a temperature range of –20°C to 200°C with a ± 0.01°C accuracy). Two gas streams (CO_2 and N_2) were mixed and controlled by a flow controller (electronic Aalborg GFM-17 gas flow meters ranging from 5 mL/min to 5 L/min with a ± 0.15% /°C accuracy) and fed to the system. Initially, the amine solution of the desired concentration was introduced into the

absorption reactor. Then, the mixed gas stream of the desired CO_2 partial pressure was introduced into the saturation cell and bubbled into the absorption reactor at atmospheric pressure. The water-saturated stream from the absorption reactor was then passed through a condenser in order to recover all condensable species back to the system. The condenser was continually fed with cold water in order to keep the amine loss at a minimum. The CO_2 concentration in the mixed gas stream was measured by a portable infrared (IR) CO_2 gas analyzer (Nova Analytical System Inc. (Hamilton, ON), model 302 HWP ranging from 0.0-100.0% CO_2 with a ±1% accuracy). The liquid sample was then taken for the measurement of CO_2 loading using the acidification technique (Horwitz, 1975). The amine concentration was determined using titration with a 1 M HCl solution to the 0.1% wt. methyl orange end point. For the CO_2 loading measurement, the amine sample was also treated with the excess 1 M HCl solution and then the released absorbed CO_2 was collected in a gas burette containing the displacement solution. The CO_2 loading measurement was repeated every 2 hours until the system reached equilibrium. The equipment was validated with 2 M MEA, 2 M diethanolamine (DEA), 2 M MDEA, and 2 M 2-amino-2-methyl-1-propanol (AMP). The results were found to be in good agreement with the literature (Austgen et al., 1991; Tontiwachwuthikul et al., 1991; Jou et al., 1992; Benamar and Aroua, 2005; Maneeintr et al., 2009) with an AAD of 3.2% as shown in Figure 3.5. Therefore, it can be concluded that the equipment and procedures for this study are considered to be properly applicable for measuring the equilibrium solubility of CO_2. Also, some experiments were tested for repeatability. It was found that the deviation of the equilibrium solubility measurement is 0.6%.

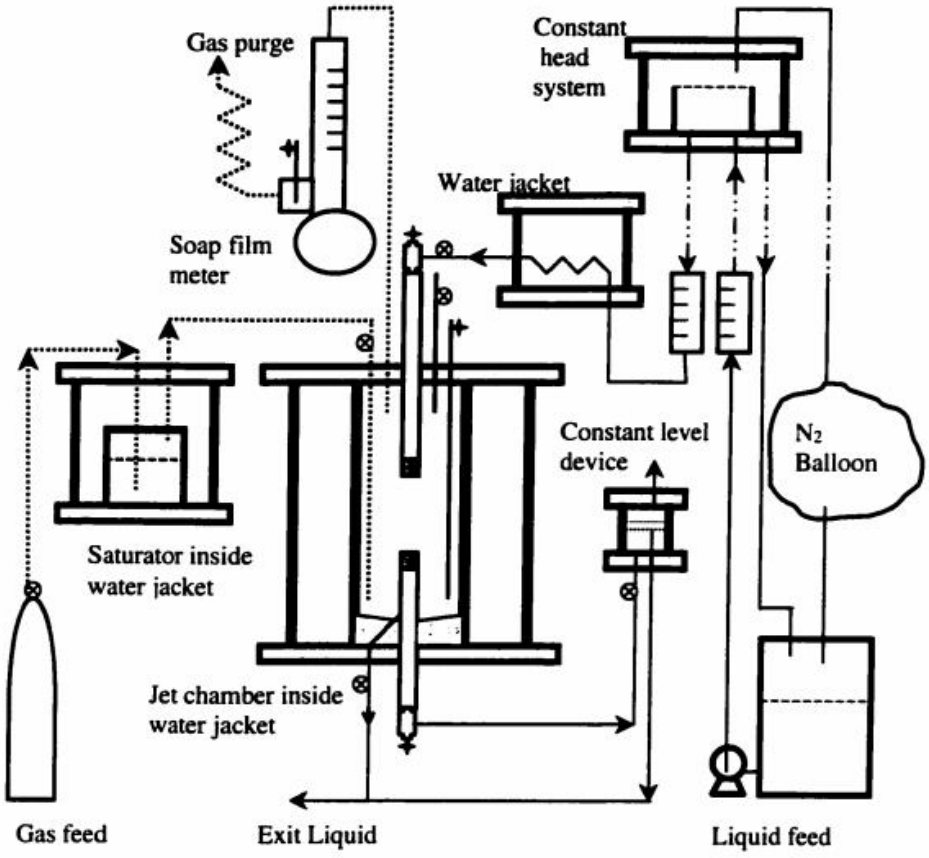

Figure 3.3 Experimental setup for laminar jet absorber (Aboudheir et al., 2004).

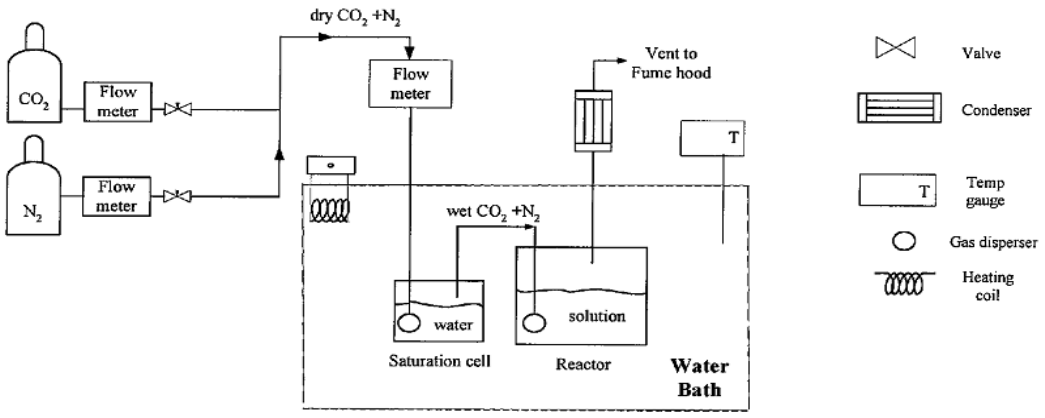

Figure 3.4 Experimental setup for CO_2 equilibrium solubility experiment (Tontiwachwuthikul et al., 2008).

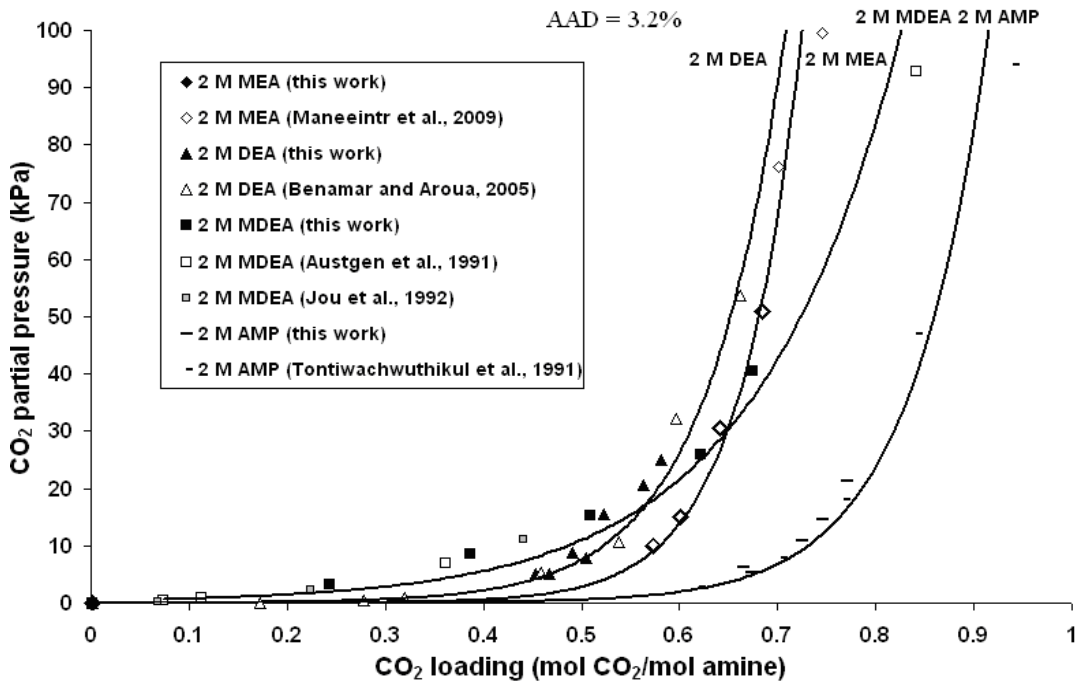

Figure 3.5 Equilibrium solubility of CO_2 in aqueous solutions of 2 M MEA, 2 M DEA, 2 M MDEA, and 2 M AMP (lines are trend lines of the experimental results obtained from this study).

3.6 References

1. Aboudheir, A.; Tontiwachwuthikul, P.; Chakma, A.; Idem, R. A novel design for the nozzle of laminar jet absorber. Ind. Eng. Chem. Res. 2004, 43, 2568-2574.

2. Al-Ghawas, H. A.; Ruiz-Ibanez, G.; Sandall, O. C. Absorption of carbonyl sulphide in aqueous methyldiethanolamine. Chem. Eng. Sci. 1989, 44, 631-639.

3. Austgen, D.M.; Rochelle, G.T.; Chen, C.C. Model of vapor-liquid equilibria for aqueous acid gas-alkanolamine system. 2. Representation of H_2S and CO_2 solubility in aqueous MDEA and CO_2 solubility in aqueous mixtures of MDEA with MEA or DEA. Ind. Eng. Chem. Res. 1991, 30, 543-555.

4. Benamar, A.; Aroua, M.K. Modeling of CO_2 solubility and carbamate concentration in DEA, MDEA and their mixtures using the Deshmukh-Mather model. Fluid Phase Equilibria 2005, 231, 150-162.

5. Horwitz, W., Association of Official Analytical Chemists (AOAC) Methods; George Banta Co.: Menasha, WI, 1975.

6. Jou, F.Y.; Mather, A.E.; Otto, F.D. Solubility of H_2S and CO_2 in aqueous methyldiethanolamine solutions. Ind. Eng. Chem. Process Des. Dev. 1992, 21, 539-544

7. Maneeintr, K.; Idem, R. O.; Tontiwachwuthikul, P.; Wee, A. G. H. Synthesis, solubilities, and cyclic capacity of amino alcohols for CO_2 Capture from flue gas streams. Energy procedia 2009, 1, 1327-1334.

8. Munder, B.; Lidal, H.; Sandall, O. C. Physical solubility of hydrogen sulfide in aqueous solutions of 2-(tert-Butylamino) ethanol. J. Chem. Eng. Data 2000, 45, 1201-1204.

9. Park, M. K.; Sandall, O. C. Solubility of carbon dioxide and nitrous oxide in 50 mass % Methyldiethanolamine. J. Chem. Eng. Data 2001, 46, 166-168.

10. Peng, D.; Robinson D.B. A new two-constant equation of state. Ind. Eng. Chem. Fundam. 1976, 15, 59-64.

11. Sada, E.; Kumazawa; H.; Butt M.A. Solubilities of gases in aqueous solutions of amine. J. Chem. Eng. Data 1978, 23, 161-163.

12. Tontiwachwuthikul, P.; Meisen, A.; Lim, J.C. Solubility of CO_2 in 2-amino-2methyl-1-propanol solutions. J. Chem. Eng. Data 1991, 36, 130-133.

13. Tontiwachwuthikul, P.; Wee, A. G. H.; Idem, R. O.; Maneeintr, K.; Fan, G. J.; Veawab, A.; Aroonwilas, A.; Chakma, A. Method for capturing carbon dioxide from gas streams. US Patent Application. US Patent Application, No. US 2008/0050296 A1, 2008.

14. Versteeg, G. F.; van Swaaij W.P.M. Solubillity and diffusivity of acid gases (CO_2, N_2O) in aqueous alkanolamine solutions. J. Chem. Eng. Data 1988, 33, 29-34

15. Wang, Y. W.; Xu, S.; Otto, F. D.; Mather, A. E. Solubility of N_2O in alkanolamines and in mixed solvents. The Chemical Engineering Journal 1992, 48, 31-40.

Chapter 4 Solubility and Diffusivity of N_2O in Aqueous 4-(Diethylamino)-2-Butanol Solutions

4.1 Introduction

A newly developed amino alcohol solvent, 4-(diethylamino)-2-butanol (DEAB), is considered to be a promising alternative solvent for capturing carbon dioxide (CO_2) due to its energy efficiency for regeneration and high absorption capacity for CO_2 removal (Tontiwachwuthikul et al., 2008; Maneeintr et al., 2009). However, a better solvent for capturing CO_2 should not only provide energy efficiency, high absorption capacity, and cyclic capacity, but should also have a fast absorption rate (reaction kinetics), low degradation rate, and low corrosion rate.

In order to develop the reaction kinetics model, several physical, chemical, and thermodynamic properties of the aqueous amine solution are required, such as the physical solubility of CO_2 or Henry's law constant, physical diffusivity of CO_2, density, viscosity, an equilibrium constant that governs CO_2-amine reaction, and CO_2 absorption rate data (Rochelle, 1991). Even though the physical solubility and physical diffusivity of CO_2 at various temperatures and concentrations are essential for developing the reaction kinetics model, they cannot be measured directly because CO_2 reacts chemically with aqueous amine solutions. Thus, the measurements of nitrous oxide (N_2O) solubility and diffusivity through the N_2O analogy can be used to determine the solubility and the diffusivity of CO_2 in aqueous amine solutions (Clarke, 1963; Sada et al., 1977 and 1978). This is due to the similarity of molecular weight, chemical configuration, volume, and electronic structure between CO_2 and N_2O (Liu et al., 1999).

In this chapter, new experimental results on the N_2O solubility and N_2O diffusivity of aqueous solutions of DEAB are presented over various ranges of temperatures and concentrations. Then, these results are used to establish correlations for the N_2O solubility and N_2O diffusivity of aqueous solutions of DEAB.

4.2 Results and discussion

4.2.1 N_2O solubility in DEAB solvent

The solubility data for the DEAB solvent over the temperature range of 298 K to 343 K are presented in Table 4.1 and also plotted in Figure 4.1. It was reported by Wang et al. (1992) that the solubility of N_2O in pure amine solvent is an exponential function with temperature in Kelvin (T), as shown in Equation 4.1.

$$He_{N_2O-amine} = b_1 \exp\left(\frac{b_2}{T}\right) \tag{4.1}$$

It can also be written as:

$$\ln He_{N_2O-amine} = \ln b_1 + \left(\frac{b_2}{T}\right) \tag{4.2}$$

A semi-log plot of $He_{N_2O-amine}$, and $1000/T$ should be a straight line, as shown in Figure 4.1. As expected, the N_2O solubility of DEAB solvent increases as temperature increases (Versteeg and van Swaaij, 1988; Wang et al., 1992).

The predictive correlation for the solubility of N_2O in DEAB solvent ($He_{N_2O-DEAB}$; kPa m^3/kmol) can be established as:

$$He_{N_2O-DEAB} = (1.188 \times 10^7) \exp\left(\frac{-2460.3}{T}\right) \tag{4.3}$$

The parity chart comparing the measured $He_{N_2\backslash O-DEAB}$ and predicted $He_{N_2\backslash O-DEAB}$ from Equation 4.3 is shown in Figure 4.2. The predicted values fit well with the experimental values with an absolute average deviation (AAD) of 3.6%.

Table 4.1 Solubility of N_2O in DEAB solvent

Temperature (K)	Solubility (kPa m^3/kmol)
298	3179
303	3553
313	4423
323	5484
333	7894
343	9043

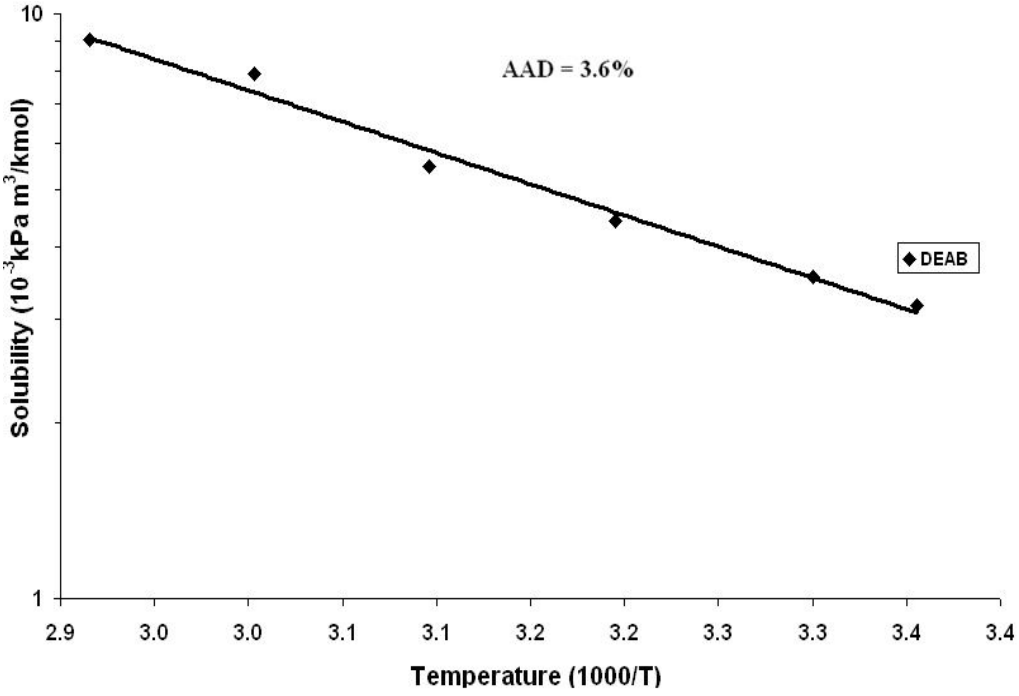

Figure 4.1 N_2O solubility in DEAB solvent; solid lines are predicted results.

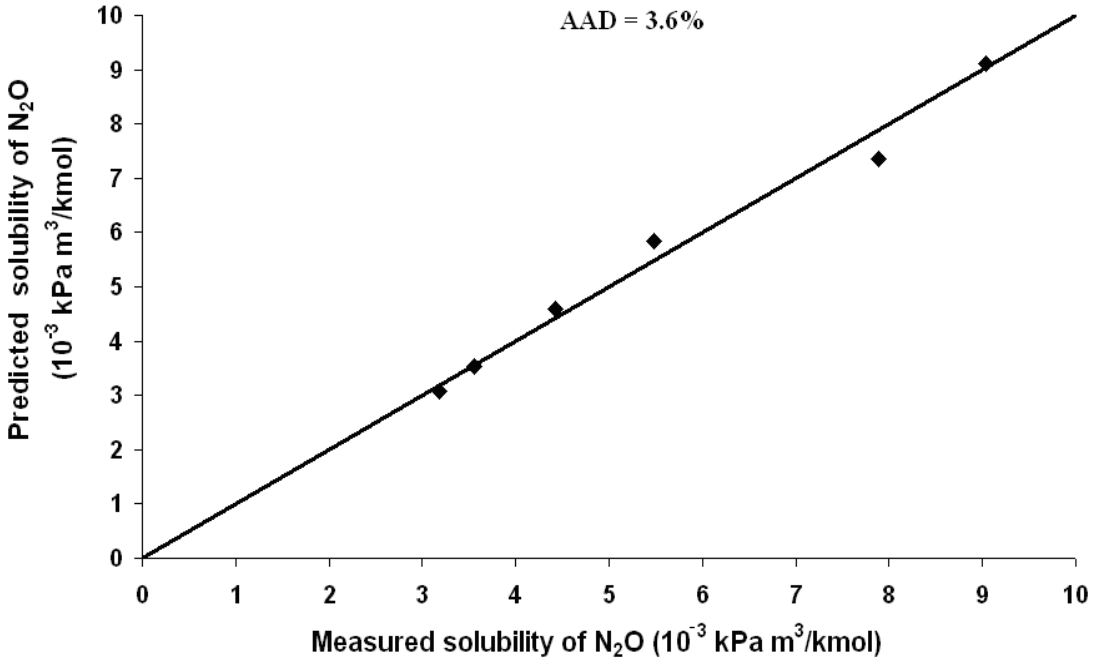

Figure 4.2 Parity chart comparing experimental and predicted values of N_2O solubility in DEAB solvent.

4.2.2 N_2O solubility in aqueous DEAB solutions

The N_2O solubility measurements of aqueous DEAB solutions were done over a temperature range of 298 K to 343 K and a DEAB concentration range of 0.68 M to 3.77 M. The results are shown in Table 4.2 and plotted in Figures 4.3, 4.4, and 4.5. It can be observed that N_2O solubility increases as temperature increases and decreases as DEAB concentration increases. In this study, the N_2O solubility or He_{N_2O} is defined as a ratio of the partial pressure of N_2O at equilibrium (P_{N_2O}) and concentration of dissolved N_2O at equilibrium (C_{N_2O}) as shown in Equation 3.6. As temperature increases, the concentration of dissolved N_2O tends to decrease, which leads to the increasing of N_2O solubility as can be seen in Figures 4.3, 4.4, and 4.5 and Table 4.2. The N_2O solubility decreases as DEAB concentration increases because of the effect of the solution density. At low density, there are more free spaces for N_2O to be dissolved, which means that C_{N_2O} would be high (in other words, N_2O solubility or He_{N_2O} would be low at low solution density). In the case of aqueous DEAB solution, it has been found by Maneeintr et al. (2008) that the solution density decreases as DEAB concentration increases; thus, the N_2O solubility in aqueous DEAB solutions decreases as DEAB concentration increases.

To correlate the N_2O solubility results at various DEAB concentrations and temperatures, there are several models that have been applied in the literature such as the semiempirical model (Wang et al., 1992), Redlich-Kister equation (Hartono et al., 2008), and polynomial model (Versteeg and van Swaaij, 1988). In this study, these three different models were used to develop the predictive models for the N_2O solubility in aqueous DEAB solution.

4.2.2.1 Semiempirical model

It was reported by Wang et al. (1992) that the semiempirical model gives a good estimation of the N_2O solubility of various aqueous amine solutions of MEA, diethanoalamine (DEA), MDEA, 2-amino-2-methyl-1-propanol (AMP), and diisopropanolamine (DIPA). The model can be written as:

$$\ln He_{N_2O-Solution} = \phi_{H_2O}\phi_{DEAB}\left(k_1 + k_2 t + k_3 t^2 + k_4 \phi_{H_2O}\right) + \phi_{H_2O} \ln He_{N_2O-H_2O} + \phi_{DEAB} \ln He_{N_2O-DEAB} \tag{4.4}$$

where ϕ_i is volume fraction of species i and t is temperature in degrees centigrade.

$$He_{N_2O-H_2O} = \left(8.55 \times 10^6\right) \exp\left(\frac{-2284}{T}\right) \tag{4.5}$$

$He_{N_2O-DEAB}$ is given in Equation 4.3.

The N_2O solubility results of the aqueous DEAB solution, which are shown in Table 4.2, were correlated with Equation 4.4 using a non-linear regression analysis package (NLREG program). The unknown parameters $\left(k_1, k_2, k_3, k_4\right)$ are listed in Table 4.3. As can be seen in Figure 4.3, the predicted results from the semiempirical model correlate moderately well with the experimental results with an AAD of 6.9%, which is in an acceptable range of AAD less than 10%.

Table 4.2 Solubility of N_2O in aqueous DEAB solutions

Temperature (K)	N_2O solubility (kPa m^3/kmol)				
	0.68 M	1.34 M	1.97 M	3.19 M	3.77 M
298	6676	5285	3965	2699	2416
313	7103	5706	4228	2884	2665
323	7600	5918	4457	3077	2868
333	8102	6354	4857	3410	3184
343	8623	6808	5274	3824	3640

Table 4.3 Parameters for the semiempirical model in Equation 4.4

Parameters	Value
k1	-0.564
k2	-0.1452
k3	7.31×10^{-4}
k4	6.65

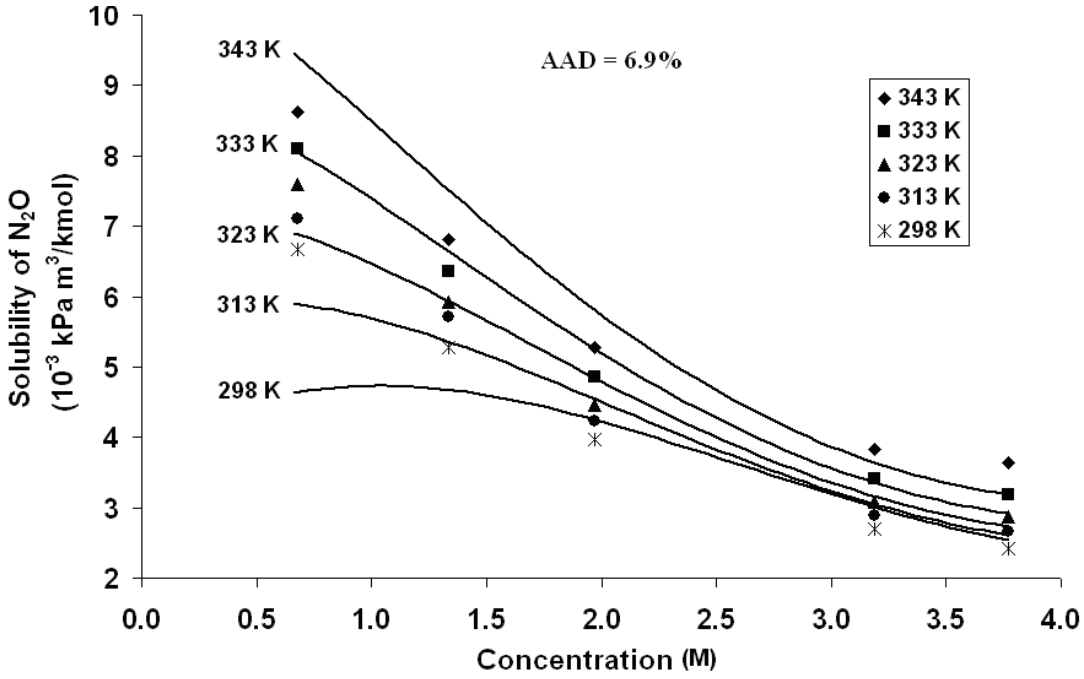

Figure 4.3 Solubility of N_2O in aqueous DEAB solutions; solid lines are calculated from the semiempirical model in Equation 4.4.

4.2.2.2 Redlich-Kister equation

The Redlich-Kister equation (Redlich and Kister, 1948) is widely used to correlate properties of binary solutions, such as the density, viscosity, refractive index, and N_2O solubility, in aqueous amine solutions (Hartono et al., 2008; Maneeintr et al., 2008). In this study, the Redlich-Kister equation was used as the predictive correlation for N_2O solubility in aqueous DEAB solutions. For a specific temperature, the Redlich-Kister equation can be written as:

$$\ln He_{N_2O-Solution} = x_{H_2O} \ln He_{N_2O-H_2O} + x_{DEAB} \ln He_{N_2O-DEAB} + x_{H_2O} x_{DEAB} \left[A_0 + A_1 (2x_{DEAB} - 1) + A_2 (2x_{DEAB} - 1)^2 + A_3 (2x_{DEAB} - 1)^3 + A_4 (2x_{DEAB} - 1)^4 \right] \quad (4.6)$$

where x_i is mole fraction of species i.

A_i is the temperature dependent coefficient, which can be determined at a specific temperature by regression analysis using the NLREG program. The regression results are shown in Table 4.4. In addition, the temperature dependent coefficients (A_i) can also be correlated using a polynomial function, as shown in Equation 4.7 (Hartono et al., 2008). Regression analysis using the NLREG program was then used to correlate A_i over the temperature range of 298 K to 343 K. The a_i coefficients are reported in Table 4.5.

$$A_i = a_0 + a_1 T + a_2 T^2 + a_3 T^3 + a_4 T^4 \quad (4.7)$$

The predicted results using the Redlich-Kister equation are plotted in Figure 4.4. It is found that the predicted results fit well with the experimental results with an AAD of 1.7%.

Table 4.4 Temperature dependence coefficient (A_i) for the Redlich-Kister equation in Equation 4.6

Temperature (K)	A0	A1	A2	A3	A4
298	11275.5645	58980.4612	115354.7140	100000.3800	32416.3803
313	9759.6709	49999.7800	95794.1557	81388.0183	25868.3751
323	5855.3836	30242.4758	58395.7231	50000.1500	16006.7291
333	803.0325	4792.1097	10466.9748	10000.2000	3519.0595
343	-176.2587	-703.8725	-1000.1300	-545.4710	-91.2443

Table 4.5 Coefficient a_i for calculating A_i using Equation 4.7 for the Redlich-Kister equation

	A0	A1	A2	A3	A4
a0	1.50778×10^{8}	-1.92852×10^{6}	9.23838×10^{3}	-1.96405×10^{1}	1.56331×10^{-2}
a1	1.01844	-2.27532×10^{5}	2.14007×10^{3}	-6.68140	6.92738×10^{-3}
a2	1.04274	-4.09869×10^{5}	3.85801×10^{3}	-1.20516×10^{1}	1.25002×10^{-2}
a3	1.17025×10^{9}	-1.49265×10^{7}	7.13199×10^{4}	-1.51259×10^{2}	1.20124×10^{-1}
a4	3.61518×10^{8}	-4.60683×10^{6}	2.19924×10^{4}	-4.66043×10^{1}	3.69828×10^{-2}

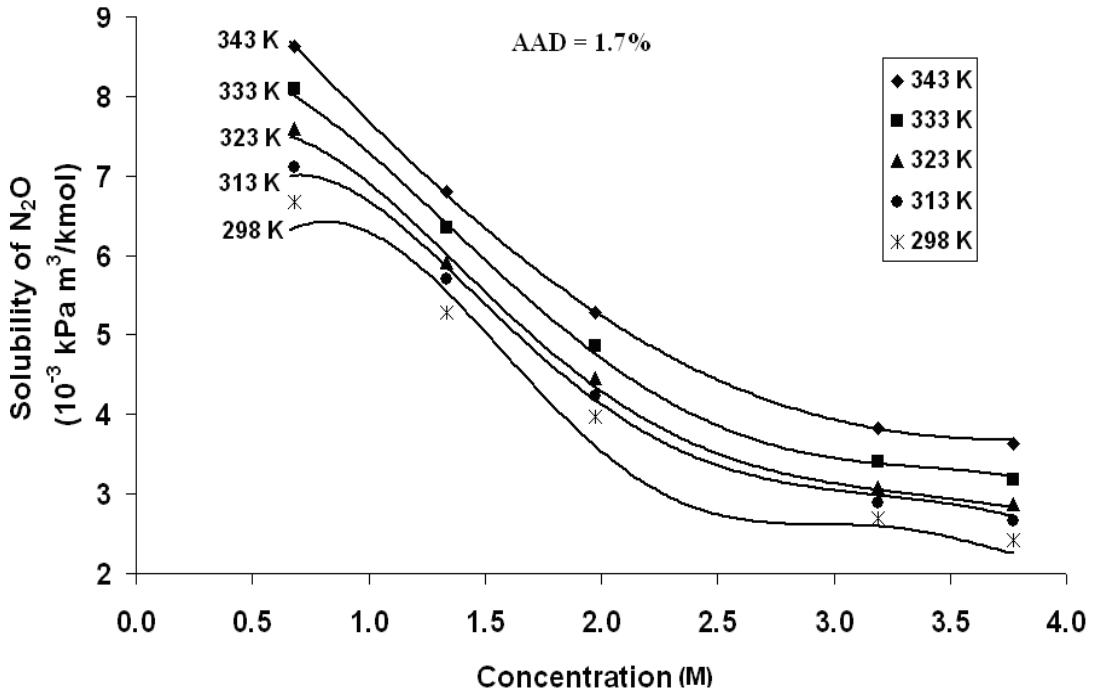

Figure 4.4 Solubility of N_2O in aqueous DEAB solutions; solid lines are calculated using the Redlich-Kister equation in Equation 4.6.

4.2.2.3 Polynomial model

Versteeg and van Swaaij (1988) mentioned that the polynomial model could be used to predict the N_2O solubility in aqueous solutions of dimethylmonoethanolamine (DMMEA), DEA, triethanolamine (TEA), monoisopropanolamine (MIPA), and DIPA. In this study, the polynomial model is defined as follows:

$$He_{N_2O-Solution} = A_0 + A_1C + A_2C^2 + A_3C^3 + A_4C^4 \quad (4.8)$$

As mentioned earlier, A_i is the temperature dependence coefficient, which can be determined for a specific temperature through regression analysis using the NLREG program. The A_i coefficients can also be correlated with temperature using the polynomial function, as shown in Equation 4.7. The regression results for A_i and a_i coefficients are shown in Tables 4.6 and 4.7, respectively.

The predicted results using the polynomial model are plotted in Figure 4.5 where it can be seen that they fit perfectly well with the experimental results. A parity chart that compares the experimental and predicted results is shown in Figure 4.6 with an AAD of 0.1%.

In this study, three predictive models (the semiempirical model, Redlich-Kister equation, and polynomial model) were used to correlate the experimental results of N_2O solubility in aqueous DEAB solution as shown in Equations 4.4, 4.6, and 4.8, respectively. By comparing the predicted results with the experimental results as shown in Figure 4.6, it was found that the polynomial model provides the best predicted results with an AAD of 0.1%. The semiempirical model also provides very good predicted results with an AAD of 1.7%. Lastly, the Redlich-Kister equation gives moderately well-fitted results with an AAD of 6.9%.

The Redlich-Kister equation correlates N_2O solubility at a specific temperature in terms of the mole fraction of DEAB in the solution and N_2O solubility in the individual species in the solution, which are water and DEAB as shown in Equations 4.6. It can be seen from Figures 4.4 and 4.6 that the predicted results are slightly deviated from the experimental results (AAD is 1.7%). This is because of the deviation from the calculations of N_2O solubility in water and DEAB solvent.

The semiempirical model correlates N_2O solubility with the volume fraction of DEAB in the solution, temperature, and also N_2O solubility in the individual species in the solution, which are water and DEAB as shown in Equation 4.4. It is found that the predicted results obtained from the semiempirical model fit moderately well with the experimental results with an AAD of 6.9% as shown in Figures 4.3 and 4.6. Table 4.8 shows the AAD for N_2O solubility in aqueous solutions of MEA, AMP, DEA, MDEA, and DEAB obtained from the semiempirical model. It can be observed that the semiempirical model works very well in the case of small chemical structure such as MEA and AMP (with AAD of 1.0% and 1.4%, respectively). The deviation from the experimental results seems to increase as the complexity of molecular structure increases as can be seen in Table 4.8. This is because the solution tends to be more nonideality as increasing the complexity of the amine molecule; thus, the larger deviation from the experimental results is obtained. Therefore, the largest deviation from the experimental results is observed in the case of DEAB, which has the most complexity molecular structure as shown in Table 4.8.

Similar to the Redlich-Kister equation, the polynomial model correlates N_2O solubility at a specific temperature. However, the polynomial model considers N_2O

solubility in terms of DEAB concentration, as shown in Equation 4.8. The predicted results obtained from the polynomial model, which is an empirical model, are found to fit perfectly with the experimental results because the N_2O solubility at a specific temperature is a polynomial relation with respect to the DEAB concentration, as can be seen in Figure 4.5. Even though the polynomial model provides very good predicted N_2O solubility results in the case of aqueous DEAB solutions, it might not provide perfectly fitted results for the other amine systems. However, this present study is focused on the N_2O solubility in aqueous DEAB solutions; thus, the polynomial model, which provides the best predicted results among the three, is considered as a predictive correlation for N_2O solubility in aqueous DEAB solutions.

Table 4.6 Temperature dependence coefficient (A_i) for the polynomial model in Equation 4.8

Temperature (K)	A0	A1	A2	A3	A4
298	7192.6862	586.9998	-2574.5698	932.7205	-100.8690
313	7690.1553	475.1385	-2499.9985	877.2504	-90.5170
323	8767.6254	-768.6242	-1869.2141	741.2947	-79.9785
333	9423.7316	-1099.5165	-1682.0268	686.4953	-74.1191
343	10063.2768	-1322.3503	-1598.5036	667.8243	-71.7936

Table 4.7 Coefficient a_i for calculating A_i using Equation 4.7 for the polynomial model

	A0	A1	A2	A3	A4
a0	5.212153×10^{7}	-9.715676×10^{7}	4.568702×10^{7}	-7.504659×10^{6}	3.179821×10^{5}
a1	-6.444611×10^{5}	1.202471×10^{6}	-5.649038×10^{5}	9.265523×10^{4}	-3.919161×10^{3}
a2	2.985272×10^{3}	-5.574765×10^{3}	2.616163×10^{3}	-4.283690×10^{2}	1.807481×10^{1}
a3	-6.139722	1.147464×10^{1}	-5.378946	8.791127×10^{-1}	-3.698447×10^{-2}
a4	4.731089×10^{-3}	-8.848154×10^{-3}	4.142989×10^{-3}	-6.757754×10^{-4}	2.833489×10^{-5}

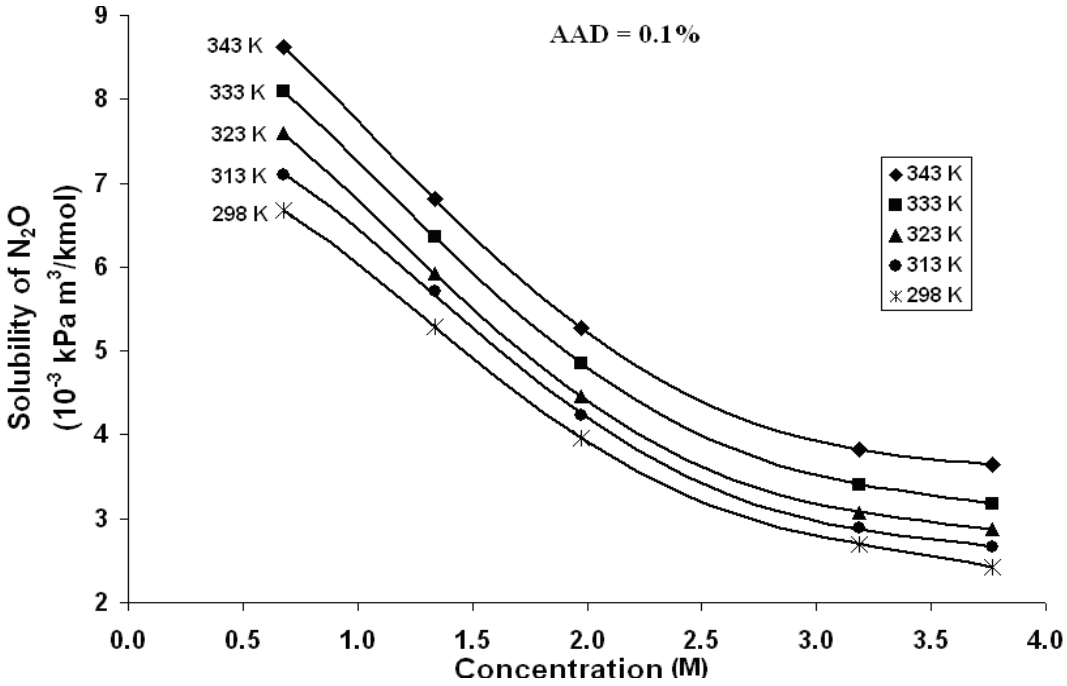

Figure 4.5 Solubility of N_2O in aqueous DEAB solutions; solid lines are calculated from the polynomial model in Equation 4.8.

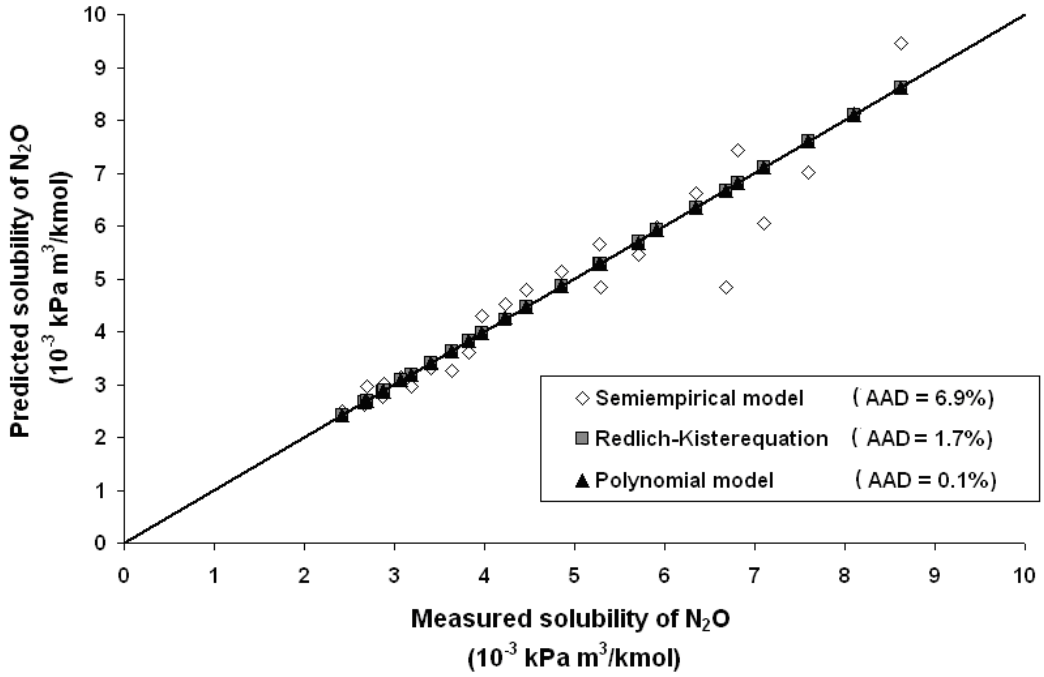

Figure 4.6 Parity chart comparing experimental and predicted results of N_2O solubility of aqueous DEAB solutions.

Table 4.8 AAD for N_2O solubility in aqueous amine solutions of MEA, AMP, DEA, MDEA, and DEAB obtained from the semiempirical model

Amine	Molecular weight (g/mol)	Chemical structure	%AAD for N_2O solubility obtained from semiempirical model (Wang et al., 1992)
MEA (1 M-6 M)	61	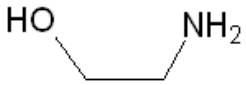	1.0
AMP (0.2 M-3 M)	89	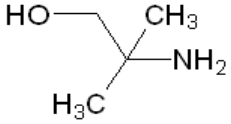	1.4
DEA (0.2 M-8.5 M)	105	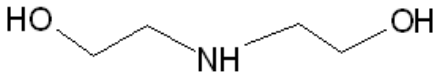	2.8
MDEA (0.3 M-4.5 M)	119	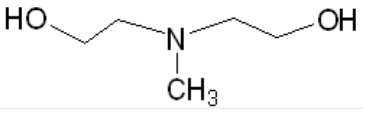	4.3
DEAB (0.68 M-3.77 M)	145	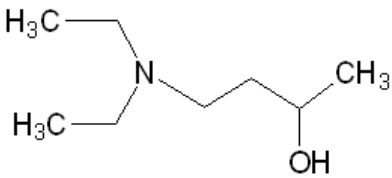	6.9 (this work)

4.2.3 N_2O diffusivity in aqueous DEAB solutions

The diffusivity of N_2O in aqueous DEAB solutions was measured using a laminar jet absorber over a temperature range of 298 K to 318 K and a concentration range of 1 M to 2.5 M. The experimental values obtained from this study are shown in Table 4.9 and plotted in Figure 4.7. The results show that the diffusivity increases as temperature increases and decreases as DEAB concentration increases, which corresponds well with the results of Tamimi et al. (1994) and Ko et al. (2001) who used water and aqueous amine solutions of MEA, DEA, DIPA, MDEA, TEA, and AMP. It is generally accepted that both temperature and viscosity play an important role in N_2O diffusivity (Li and Lee, 1996). As temperature increases, the N_2O molecule gains more energy, which leads to the higher diffusivity of N_2O. For the effect of viscosity, there will be a higher resistivity for N_2O to diffuse into high viscosity solution compared to low viscosity solution; thus, the diffusivity decreases as viscosity increases. In the case of aqueous solutions of DEAB, it was observed by Maneeintr et al. (2009) that the viscosity of the solutions increases as DEAB concentration increases but decreases as temperature increases. Therefore, the N_2O diffusivity in aqueous solutions of DEAB decreases as amine concentration increases and increases as temperature increases, as can be seen in Figure 4.7 and Table 4.9.

In order to develop a predictive model for the diffusivity of N_2O at various concentrations and temperatures, two models (modified Stokes-Einstein and semiempirical models) that have been used in the literature were applied. In this study, these two models were used to establish which would provide the better predictive

models for the N_2O diffusivity of aqueous DEAB solutions that correlated well with experimental results.

Table 4.9 Diffusivity of N_2O in aqueous DEAB solutions

Concentration (M)	Temperature (K)	Diffusivity (10^9 m^2/s)
1	298	1.89
1	308	2.16
1	318	2.49
2	298	1.04
2	308	1.31
2	318	1.59
2.5	298	0.68
2.5	308	0.91
2.5	318	1.22

4.2.3.1 Modified Stokes-Einstein model

The first model is the modified Stokes-Einstein model as used by Versteeg and van Swaaij (1988). They found that the modified Stokes-Einstein model is applicable to estimating the N_2O diffusivity into aqueous amine solutions of MEA, DEA, TEA, MIPA, and DIPA. The modified Stokes-Einstein model considers the N_2O diffusivity (D_{N_2O}) to be a function of viscosity $(\eta; Pa \cdot s)$. For various aqueous amine solutions (Versteeg and van Swaaij, 1988), the modified Stokes-Einstein model can be written as:

$$D_{N_2O} \cdot \eta^{0.8} = \text{Constant} \tag{4.9}$$

The viscosity of the aqueous DEAB solution was calculated based on the results of Maneeintr et al. (2009). By determining the constant value in Equation 4.9 using the NLREG program, the modified Stokes-Einstein model was found to be:

$$D_{N_2O} \cdot \eta^{0.8} = 1.219 \times 10^{-11} \tag{4.10}$$

The predicted N_2O diffusivity in aqueous DEAB solutions are shown in Figure 4.7 as dashed lines. It was found that the predicted results from modified Stokes-Einstein model correlate fairly well with the experimental results with an AAD of 10.2%.

4.2.3.2 Semiempirical model

The semiempirical model for the N_2O diffusivity of aqueous amine solution was proposed by Ko et al. (2001). It was found that this model provides a good estimation of the N_2O diffusivity in aqueous amine solutions of MEA, DEA, DIPA, MDEA, TEA, and AMP. The semiempirical model takes both concentration and temperature into account, as shown in Equation 4.11.

$$D_{N_2O} = \left(b_0 + b_1 C + b_2 C^2\right)\exp\left(\frac{b_3 + b_4 C}{T}\right) \tag{4.11}$$

where C is DEAB molar concentration and T is temperature in Kelvin.

After regression analysis using the NLREG program, the predictive correlation for the diffusivity of N_2O in aqueous DEAB solution can be written as:

$$D_{N_2O} = \left[(4.64\times10^{-8}) + (8.74\times10^{-8})C + (2.86\times10^{-8})C^2\right]\exp\left(\frac{(-9.50) + (-3.81C)}{T}\right) \tag{4.12}$$

The predicted results are shown in Figure 4.7 as solid lines. It can be seen that the predicted values fit well with the experimental values. This can also be confirmed by a parity chart, as presented in Figure 4.8 with an AAD of 3.4%.

By comparing the semiempirical and the modified Stokes-Einstein models as shown in Figures 4.7 and 4.8, it is clear that the semiempirical model provides better predicted results for the N_2O diffusivity in aqueous solutions of DEAB. This is because the semiempirical model takes both temperature and amine concentration into account. Since both temperature and amine concentration directly control the solution viscosity (it was mentioned by Li and Lee (1996) that the temperature and the viscosity play an important role on the N_2O diffusivity), the semiempirical model seems to be adequate for predicting N_2O diffusivity in aqueous solutions of DEAB. Even though the modified Stokes-Einstein model correlates N_2O solubility directly with solution viscosity, the predicted results do not fit very well with the experimental results. This could be because the DEAB aqueous solution behaves differently from the modified Stokes-Einstein relation.

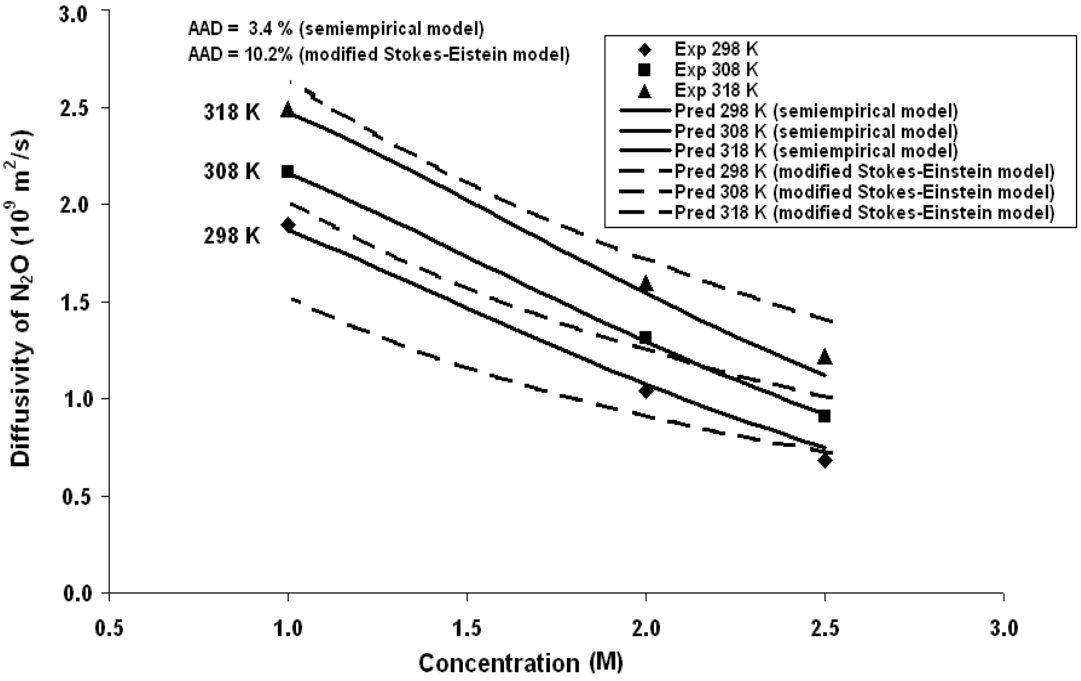

Figure 4.7 Diffusivity of N_2O in aqueous DEAB solutions; dashed lines are calculated from the modified Stokes-Einstein model in Equation 4.10 and the solid lines are calculated from the semiempirical model in Equation 4.12.

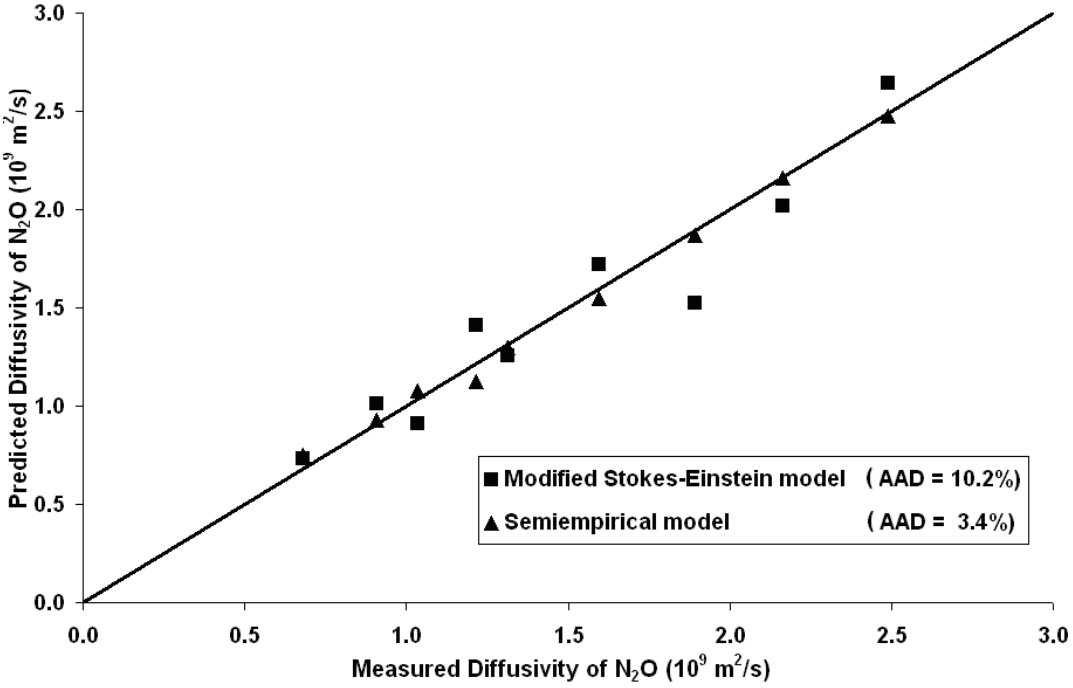

Figure 4.8 Parity chart comparing experimental and predicted results of N_2O diffusivity in aqueous DEAB solutions.

4.3 Summaries

1. The N_2O solubility in DEAB solvent increases as temperature increases over a temperature range of 298 K to 343 K. Also, the N_2O solubility in DEAB solvent can be calculated by:

$$He_{N_2O-DEAB} = (1.188 \times 10^7) \exp\left(\frac{-2460.3}{T}\right)$$ with an AAD of 3.6%.

2. The N_2O solubility in aqueous DEAB solutions increases as temperature increases and decreases as DEAB concentration increases over a temperature range of 298 K to 343 K and a DEAB concentration range of 0.68 M to 3.77 M. The predicted N_2O solubility obtained from the polynomial model in Equation 4.8 fit very well with the experimental results with an AAD of 0.1%.

3. The diffusivity of N_2O in aqueous DEAB solutions increases as temperature increases and decreases as DEAB concentration increases over a temperature range of 298 K to 318 K and a concentration range of 1 M to 2.5 M. The semiemipirical model of Equation 4.12 provides good agreement with the experimental results with an AAD of 3.4%.

4. The physical solubility and physical diffusivity of CO_2 in aqueous DEAB solutions can then be estimated using the N_2O analogy.

4.4 References

1. Aboudheir, A.; Tontiwachwuthikul, P.; Chakma, A.; Idem, R. A novel design for the nozzle of laminar jet absorber. Ind. Eng. Chem. Res. 2004, 43, 2568-2574.

2. Al-Ghawas, H. A.; Ruiz-Ibanez, G.; Sandall, O. C. Absorption of carbonyl sulphide in aqueous methyldiethanolamine. Chem. Eng. Sci. 1989, 44, 631-639.

3. Clarke, J. K. A. Kinetics of absorption of carbon dioxide in monoethanolamine solutions at short contact times. Ind. Eng. Chem. Fundam. 1963, 3, 239-245.

4. Hartono, A.; Juliussen, O.; Svendsen, F.H. Solubility of N_2O in aqueous solution of diethylenetriamine. J. Chem. Eng. Data 2008, 53, 2696-2700.

5. Ko, J.; Tsai, T.; Lin, C.; Wang, H., Li, M. Diffusivity of nitrous oxide in aqueous alkanolamine solutions. J. Chem. Eng. Data 2001, 46, 160-165.

6. Li, M.H.; Lee, W.C. Solubility and diffusivity of N_2O and CO_2 in (diethanolamine+N-methyldiethanolamine+water) and in (diethanolamine+2-amino-2-methyl-1-propanol+water). J. Chem. Eng. Data 1996, 41, 551-556.

7. Liu, Y.; Zhang, L.; Watanasiri, S. Representing vapor-liquid equilibrium for an aqueous MEA-CO_2 system using the electrolyte nonrandom-two-liquid model. Ind. Eng. Chem. Res. 1999, 38, 2080-2090.

8. Maneeintr, K.; Amr, H.; Idem, R. O.; Tontiwachwuthikul, P.; Wee, A. G. H. Physical and transport properties of aqueous amino alcohol solutions for CO_2 capture from flue gas streams. Process Safety and Environmental Protection 2008, 86, 291-295.

9. Maneeintr, K.; Idem, R. O.; Tontiwachwuthikul, P.; Wee, A. G. H. Synthesis, solubilities, and cyclic capacity of amino alcohols for CO_2 Capture from flue gas streams. Energy procedia 2009, 1, 1327-1334.

10. Munder, B.; Lidal, H.; Sandall, O. C. Physical solubility of hydrogen sulfide in aqueous solutions of 2-(tert-Butylamino) ethanol. J. Chem. Eng. Data 2000, 45, 1201-1204.

11. Park, M. K.; Sandall, O. C. Solubility of carbon dioxide and nitrous oxide in 50 mass % Methyldiethanolamine. J. Chem. Eng. Data 2001, 46, 166-168.

12. Peng, D.; Robinson D.B. A new two-constant equation of state. Ind. Eng. Chem. Fundam. 1976, 15, 59-64.

13. Redlich, O.; Kister, A.T. Algebraic representation of thermodynamic properties and the classification of solutions. Industrial and Engineering Chemistry, 1948, 40, 345-348.

14. Rochelle, G.T. Research needs foe acids gas kinetics and equilibria in alkanolamine systems. 70th GPA annual convention 1991, 66-82.

15. Sada, E.; Kumazawa, H.; Butt M.A. Solubilities of gases in aqueous solutions of amine. J. Chem. Eng. Data 1977, 22, 277-278.

16. Sada, E.; Kumazawa; H.; Butt M.A. Solubilities of hydrogen sulfide and carbon dioxide in a diglycolamine solution. J. Chem. Eng. Data 1978, 23, 161-163.

17. Tamimi, A.; Rinker, E.W.; Sandall, O. C. Diffusivity coefficient for hydrogen sulfide, carbon dioxide, and nitrous oxide in water over temperature range 293-368 K. J. Chem. Eng. Data 1994, 39, 330-332.

18. Tontiwachwuthikul, P.; Wee, A. G. H.; Idem, R. O.; Maneeintr, K.; Fan, G. J.; Veawab, A.; Aroonwilas, A.; Chakma, A. Method for capturing carbon dioxide from gas streams. US Patent Application. US Patent Application, No. US 2008/0050296 A1, 2008.

19. Versteeg, G. F.; van Swaaij W.P.M. Solubility and diffusivity of acid gases (CO_2, N_2O) in aqueous alkanolamine solutions. J. Chem. Eng. Data 1988, 33, 29-34.

20. Wang, Y. W.; Xu, S.; Otto, F. D.; Mather, A. E. Solubility of N_2O in alkanolamines and in mixed solvents. The Chemical Engineering Journal 1992, 48, 31-40.

Chapter 5 Correlations for Equilibrium Solubility of CO_2 in Aqueous 4-(Diethylamino)-2-Butanol Solutions

5.1 Introduction

The vapour-liquid equilibria of the carbon dioxide (CO_2) and 4-(diethylamino)-2-butanol (DEAB) aqueous system is essential for reaction kinetics model development, which is required for process simulation and design for the CO_2 treating plant (Rochelle, 1991; Li and Shen, 1993). In order to obtain the vapour-liquid equilibria of the CO_2-DEAB aqueous system, the chemical equilibrium constant that governs the CO_2-DEAB-water reaction is required. However, it is difficult and costly to obtained chemical equilibrium constants experimentally. Kent and Eisenberg (1976) proposed a predictive method for determining the chemical equilibrium constant via the predicting of the equilibrium solubility of acid gas at various temperatures, partial pressures of acid gas, and amine concentrations.

In order to develop the mathematical model for predicting equilibrium solubility of CO_2 in aqueous DEAB solutions, equilibrium solubility of CO_2 at various operating conditions including temperature, DEAB concentration, and CO_2 partial pressure are required. Moreover, the development of correlations to predict the equilibrium solubility of CO_2 in aqueous DEAB solutions is also important because experimental measurements are not only costly but also time consuming.

In this chapter, the experimental results of the equilibrium solubility of CO_2 in aqueous DEAB solutions are reported over ranges of temperatures, DEAB concentrations, and CO_2 partial pressures. These results were then used to test existing

mathematical correlations for predicting the equilibrium solubility and chemical equilibrium constant of CO_2 absorption in aqueous DEAB solutions for different conditions.

5.2 Calculating equilibrium solubility of CO_2 in aqueous DEAB solutions

The chemical equilibria of CO_2/DEAB aqueous system is governed by the following equations:

$$RR_2'N + H^+ \xleftrightarrow{K_1} RR_2'NH^+ \tag{5.1}$$

$$CO_2 + RR_2'N + H_2O \xleftrightarrow{K_2} RR_2'NH^+ + HCO_3^- \tag{5.2}$$

$$H_2O + CO_2 \xleftrightarrow{K_3} H^+ + HCO_3^- \tag{5.3}$$

$$CO_2 + OH^- \xleftrightarrow{K_4} HCO_3^- \tag{5.4}$$

$$HCO_3^- \xleftrightarrow{K_5} H^+ + CO_3^{2-} \tag{5.5}$$

$$H_2O \xleftrightarrow{K_6} H^+ + OH^- \tag{5.6}$$

$RR_2'N$ represents DEAB where R is $(CH_2)_2CH(CH_3)OH$ and R' is CH_2CH_3 and K_i is the chemical equilibrium constant for reaction i. DEAB is considered to be a tertiary amine since it has 3 carbon atoms attached to the nitrogen atom. In this case, DEAB does not react directly with CO_2, but it acts as a base, which catalyzed the hydration of CO_2 (Kohl and Nielsen, 1997), as presented in Equation 5.2.

The expressions for the chemical equilibrium constants can be described as follow:

$$K_1 = \frac{[RR_2'NH^+]}{[H^+][RR_2'N]} = \frac{K_2}{K_3} \tag{5.7}$$

$$K_2 = \frac{\left[RR_2^{/}NH^+\right]\left[HCO_3^-\right]}{\left[CO_2\right]\left[RR_2^{/}N\right]} \tag{5.8}$$

$$K_3 = \frac{\left[H^+\right]\left[HCO_3^-\right]}{\left[CO_2\right]} \tag{5.9}$$

$$K_4 = \frac{\left[HCO_3^-\right]}{\left[CO_2\right]\left[OH^-\right]} \tag{5.10}$$

$$K_5 = \frac{\left[H^+\right]\left[CO_3^{2-}\right]}{\left[HCO_3^-\right]} = \frac{K_2}{K_1 K_6} \tag{5.11}$$

$$K_6 = \left[H^+\right]\left[OH^-\right] \tag{5.12}$$

Based on Equations 5.7-5.12, it can be seen that not all of the chemical equilibrium constants are independent. Only 4 chemical equilibrium constants (K_2, K_3, K_4, and K_6) are independent. The remaining two (K_1 and K_5) can be obtained by the combination of the independent chemical equilibrium constants, as shown in Equations 5.7 and 5.11. Also, water concentration is considered to be constant due to the presence of excess amount of water in the solution (the water concentration is much higher than the DEAB concentration).

The total DEAB balance, total carbon balance, and the charge balance based on the chemical equilibrium equations (Equations 5.1-5.6) can be expressed as follows:

$$\left[RR_2^{/}N\right]_0 = \left[RR_2^{/}NH^+\right] + \left[RR_2^{/}N\right] \tag{5.13}$$

$$\alpha\left[RR_2^{/}N\right]_0 = \left[CO_2\right] + \left[HCO_3^-\right] + \left[CO_3^{2-}\right] \tag{5.14}$$

$$\left[RR_2^{/}NH^+\right] + \left[H^+\right] = \left[OH^-\right] + \left[HCO_3^-\right] + 2\left[CO_3^{2-}\right] \tag{5.15}$$

where $\left[RR_2^{/}N\right]_0$ and α are the initial DEAB concentration and CO_2 loading in the aqueous DEAB solution, respectively.

In addition, the physical solubility of CO_2 in aqueous DEAB solution, which is described in Chapter 4, can be related to Henry's law as:

$$P_{CO_2} = He_{CO_2}[CO_2] \tag{5.16}$$

where P_{CO_2} and He_{CO_2} represent the partial pressure of CO_2 in the gas phase and Henry's law constant of CO_2 in aqueous DEAB solution, respectively.

5.2.1 Correlation for K_2 with various operating parameters using existing models

A solution of the 8 coupled nonlinear algebraic equations (i.e., Equations 5.8-5.10 and 5.12-5.16), will yield the values of the 8 unknowns (namely, K_2, $[RR_2^{/}N]$, $[H^+]$, $[RR_2^{/}NH^+]$, $[HCO_3^-]$, $[CO_2]$, $[OH^-]$, and $[CO_3^{2-}]$). On the other hand, $[RR_2^{/}N]_0$, α, and P_{CO_2} can be obtained from the experiment involving the measurement of equilibrium solubility of CO_2 as mentioned in Section 3.5. He_{CO_2} can be estimated using the polynomial model provided in Chapter 4 (Equation 4.10). The chemical equilibrium constants K_3, K_4, and K_6 are calculated using the correlations mentioned in Austgen et al. (1989 and 1991).

The simultaneous solution of the 8 coupled nonlinear algebraic equations (i.e., Equations 5.8-5.10 and 5.12-5.16) was achieved with the use of a finite element method (FEM) based on COMSOL 4.1 software with 0D stationary solver mode. In this case, an initial guess for each unknown is required. After the software is operated with the first set of initial guess,,values of the unknowns are obtained. Then, these new values are subsequently used as the initial guesses for solving the 8 unknowns. This process is

repeated until the percentage deviation of the results of each unknown for successive attempts is less than 0.01%.

At this point, the values of the 8 unknowns, K_2, $[RR_2'N]$, $[H^+]$, $[RR_2'NH^+]$, $[HCO_3^-]$, $[CO_2]$, $[OH^-]$, and $[CO_3^{2-}]$, are obtained. The values of K_2 at various operating conditions, including initial DEAB concentration, temperature, CO_2 loading, and CO_2 partial pressure, were collected and then correlated (using a non-linear regression package called NLREG program) with several existing models in the literature, namely the Kent-Eisenberg model (Kent and Eisenberg, 1987), Austgen model (Austgen et al., 1989 and 1991), Li-Shen model (Li and Shen, 1993), and Hu-Chakma model (Hu and Chakma, 1990a).

5.2.2 Calculating the equilibrium solubility of CO_2 in aqueous solutions of DEAB

At this point, the equilibrium solubility of CO_2 or α is considered as the unknown instead of K_2 (since K_2 is known through a previous set of calculations). By solving the 8 coupled nonlinear algebraic equations (Equations 5.8-5.10 and 5.12-5.16), the 8 unknowns, namely, α, $[RR_2'N]$, $[H^+]$, $[RR_2'NH^+]$, $[HCO_3^-]$, $[CO_2]$, $[OH^-]$, and $[CO_3^{2-}]$ can be calculated. In this case, $[RR_2'N]_0$ and P_{CO_2} are considered as the operating conditions. The different calculated values of α are obtained for various values of $[RR_2'N]_0$ and P_{CO_2}.

The same procedure as in Section 5.2.1 was applied in order to simultaneously solve Equations 5.8-5.10 and 5.12-5.16 for the 8 unknowns (α, $[RR_2'N]$, $[H^+]$, $[RR_2'NH^+]$, $[HCO_3^-]$, $[CO_2]$, $[OH^-]$, and $[CO_3^{2-}]$). The calculated results of the

equilibrium solubility of CO_2 (α) were then compared with the experimental values in terms of absolute average deviation (AAD).

5.3 Heat of CO_2 absorption in aqueous DEAB solutions

The heat of acid gas absorption, mainly CO_2 and hydrogen sulfide (H_2S), is an important property required for an acid gas removal plant because it is directly related to the steam requirements for the amine regeneration stage. The heat of CO_2 absorption can be measured experimentally using a calorimeter. It can also be estimated based on the Gibbs-Helmholtz equation (Gabrielsen et al., 2005; Kim and Svendsen, 2007), as shown in Equation 5.17.

$$\frac{d\left(\ln K_2\right)}{d\left(\frac{1}{T}\right)} = -\frac{\Delta \mathrm{H}_{abs}}{R} \tag{5.17}$$

where $\Delta \mathrm{H}_{abs}$ is heat of CO_2 absorption (J/mol), R is universal gas constant (J/mol K), and K_2 is the chemical equilibrium constant, which governs CO_2-amine reaction, as given in Equation 5.2.

5.4 Results and discussion

5.4.1 Equilibrium solubility of CO_2 in aqueous DEAB solutions

The experimental determination of the equilibrium solubility of CO_2 in aqueous DEAB solutions was conducted over a temperature range of 298 K to 333 K, a CO_2 partial pressure range of 10 kPa to 100 kPa, and a DEAB concentration range of 1 M to 2.5 M (for 5 M DEAB, the experiment was conducted at 298 K and a partial pressure range of 9-30 kPa). Based on our previous study (Maneeintr et al., 2009), it was shown

that DEAB has a very high CO_2 absorption capacity compared with conventional amines such as monoethanolamine (MEA), even at practical partial pressures of CO_2 used in the CO_2 absorption process, as shown in Figure 5.1. Also, the molecular weight of DEAB is high, 145 g/mol. This also implies high viscosity at very high DEAB concentrations. Bearing in mind the viscosity limitation, and the fact that it does not need a high concentration of DEAB to achieve the same CO_2 recovery efficiency as conventional amines, we decided to work with DEAB concentrations in the range of 1 M-2.5 M. The experimental results are shown in Tables 5.1-5.4 and plotted in Figures 5.2 to 5.5. By comparing the equilibrium solubility of CO_2 in 2 M DEAB with those in 2 M MEA, 2 M diethanolamine (DEA), 2 M methyldiethanolamine (MDEA), 2 M 2-amino-2-methyl-1-propanol (AMP), 2 M piperazine (PZ), as shown in Figure 5.1, it was found that the equilibrium solubility of CO_2 in 2 M DEAB is the highest and is also comparable with those in 2 M PZ. The equilibrium solubility of CO_2 in 2 M DEAB is clearly higher than those in 2 M AMP, 2 M MDEA, 2 M MEA, and 2 M DEA, respectively. In addition, it can be observed from Figures 5.2-5.5 that the equilibrium solubility of CO_2 decreases as temperature increases and increases as CO_2 partial pressure increases, as expected. These results are similar to those of Tontiwachwuthikul et al. (1991), Baek et al. (2000), and Maneeintr et al. (2009), who used aqueous solutions of MEA, AMP, 2-amino-2-methyl-1,3-propanediol (AMPD), DEAB, 4-isopropylamino-2-butanol, 4-piperidino-2-butanol, 4-propylamino-2-butanol, and 4-(ethyl-methyl-amino)-2-butanol (for the effect of temperature on equilibrium solubility of CO_2, the results for 1 M and 2.5 M follow the same trend as those of 2 M). The experimental results for equilibrium solubility of CO_2 in aqueous DEAB solutions at 298 K, 313 K, and 333 K are given in Figures 5.2, 5.3, and

5.4, respectively. It was found that the equilibrium solubility of CO_2 in aqueous DEAB solutions increases as DEAB concentration increases within the DEAB concentration range of 1 M to 2.5 M., but the equilibrium solubility of CO_2 in 5 M aqueous DEAB solutions at 298 K was found to be lower than the equilibrium solubility of CO_2 in 1 M DEAB at 298 K.

The equilibrium solubility of CO_2 in aqueous DEAB solutions decreases as temperature increases because the solubility of CO_2 declines with increasing temperature; thus, the system tends toward CO_2 desorption rather than CO_2 absorption. For the effect of CO_2 partial pressure, the equilibrium solubility of CO_2 increases as CO_2 partial pressure increases due to the higher driving force for CO_2 absorption at higher CO_2 partial pressure. In the present study, it was observed that the equilibrium solubility of CO_2 increases as DEAB concentration increases over the concentration range of 1 M to 2.5 M. This could be because at 1 M DEAB, the DEAB molecule is diluted by a water molecule, so there is ineffectiveness in the CO_2 molecule contacting the DEAB molecule. By increasing the concentration of DEAB, the probability of CO_2 molecules contacting DEAB molecules increases, resulting in an increase of the equilibrium solubility of CO_2 as DEAB concentration increases within a range of 1 M to 2.5 M. However, at a high DEAB concentration, e.g., 5 M, the equilibrium solubility of CO_2 decreases drastically and drops below the value for 1 M DEAB, as shown in Figure 5.2. This is because at this high of DEAB concentration, the solution is not only viscous (limiting mass transfer), but also saturated with DEAB molecules; thus, not all DEAB molecules can come into contact with CO_2, resulting in the observed drastic decrease in equilibrium solubility of CO_2 with an increasing in DEAB concentration at high DEAB concentrations.

Table 5.1 Equilibrium Solubility of CO_2 in 1 M aqueous DEAB solutions

298 K		313 K		333 K	
CO_2 partial pressure (kPa)	CO_2 loading	CO_2 partial pressure (kPa)	CO_2 loading	CO_2 partial pressure (kPa)	CO_2 loading
11	0.83	11	0.78	11	0.52
13	0.87	15	0.80	13	0.56
35	0.89	36	0.83	33	0.63
60	0.90	57	0.89	62	0.71
71	0.92	66	0.89	72	0.75
99	0.93	78	0.90	99	0.81
		100	0.91		

Table 5.2 Equilibrium Solubility of CO_2 in 2 M aqueous DEAB solutions[a]

298 K		313 K		333 K	
CO_2 partial pressure (kPa)	CO_2 loading	CO_2 partial pressure (kPa)	CO_2 loading	CO_2 partial pressure (kPa)	CO_2 loading
10	0.92	10	0.83	10	0.76
15	0.94	15	0.88	15	0.79
31	0.95	30	0.92	31	0.81
51	0.97	51	0.95	51	0.83
76	0.98	76	0.97	76	0.88
100	1.00	100	0.99	100	0.93

[a]the equilibrium solubility of CO_2 in 2 M DEAB results obtain from Maneeintr, 2010

Table 5.3 Equilibrium Solubility of CO_2 in 2.5 M aqueous DEAB solutions

298 K		313 K		333 K	
CO_2 partial pressure (kPa)	CO_2 loading	CO_2 partial pressure (kPa)	CO_2 loading	CO_2 partial pressure (kPa)	CO_2 loading
11	0.95	11	0.89	11	0.83
13	0.96	15	0.92	13	0.85
35	1.00	36	0.98	33	0.89
60	1.01	57	0.98	62	0.94
70	1.02	66	0.99	72	0.96
99	1.03	78	1.00	99	0.98
		100	1.02		

Table 5.4 Equilibrium Solubility of CO_2 in 5 M aqueous DEAB solutions

298 K	
CO_2 partial pressure (kPa)	CO_2 loading
9	0.59
16	0.61
21	0.62
30	0.64

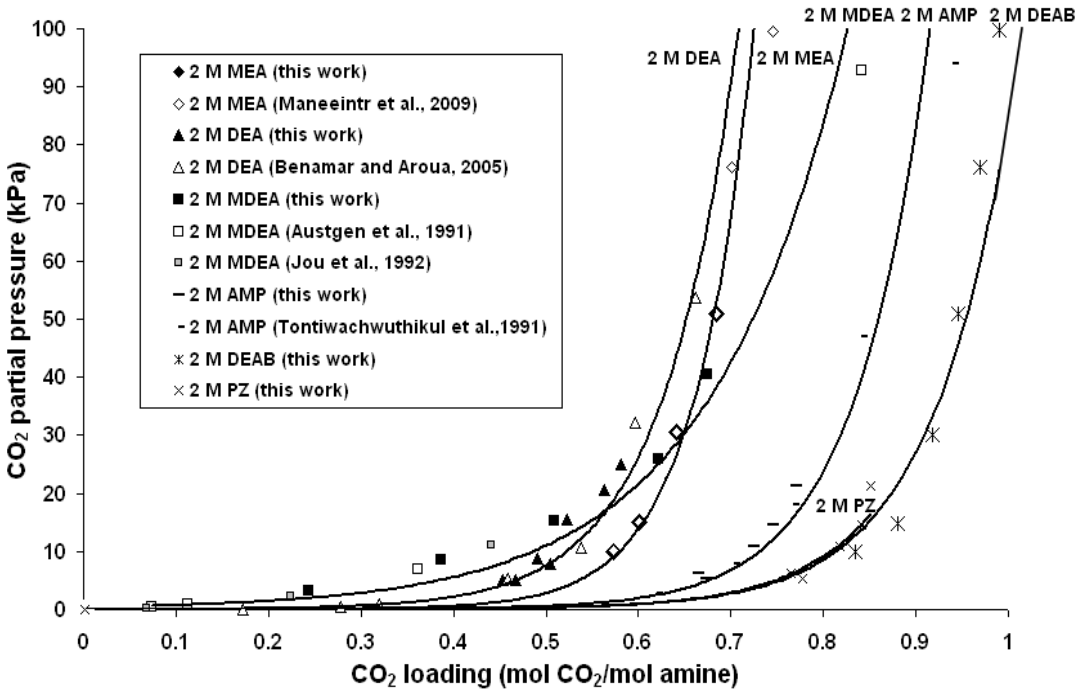

Figure 5.1 Equilibrium solubility of CO_2 in aqueous solutions of 2 M MEA, 2 M DEA, 2 M MDEA, 2 M AMP, 2 M DEAB, and 2 M PZ (lines are trend lines of the experimental results obtained from this study).

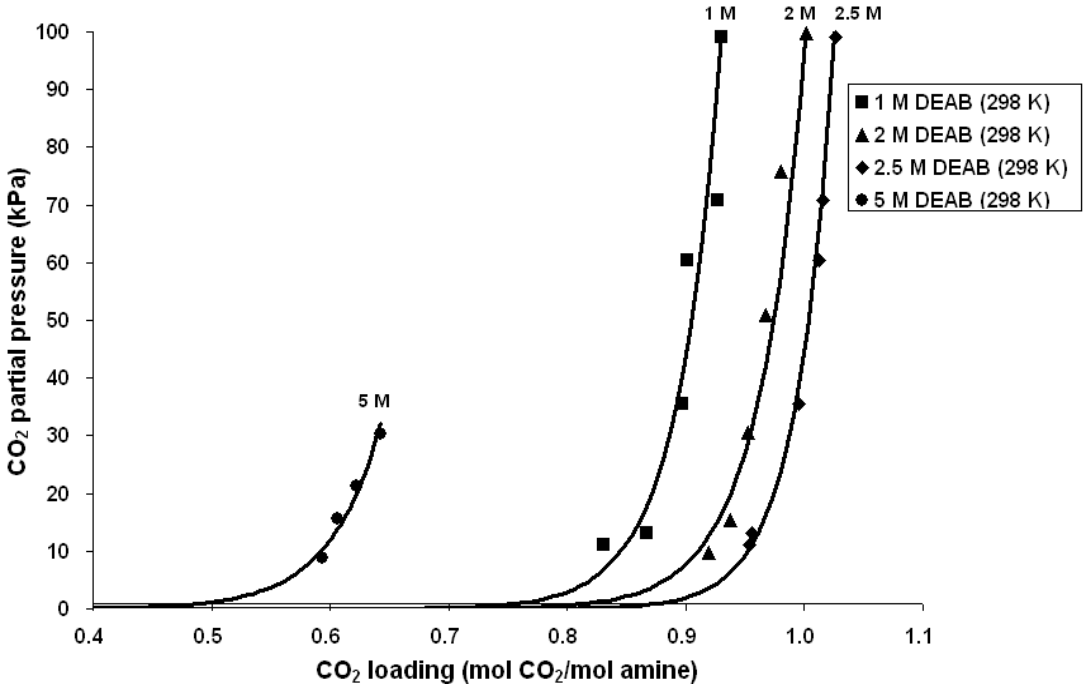

Figure 5.2 Equilibrium solubility of CO_2 in 1 M, 2 M, 2.5 M, and 5 M aqueous DEAB solutions at 298 K (solid lines are trend lines).

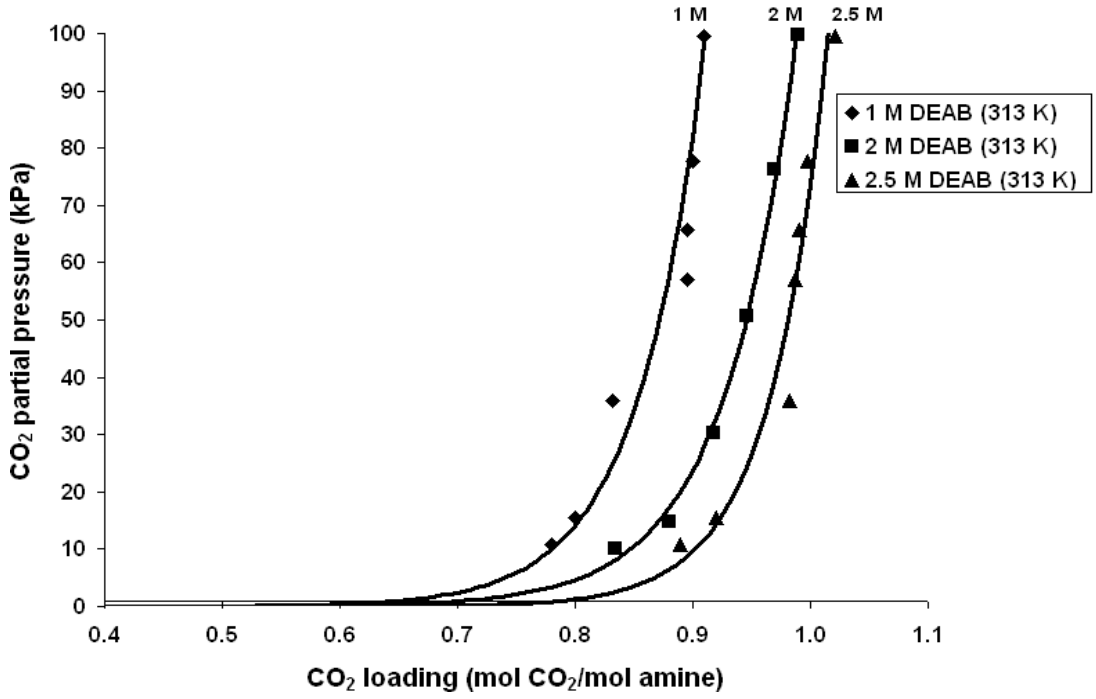

Figure 5.3 Equilibrium solubility of CO_2 in 1 M, 2 M, and 2.5 M aqueous DEAB solutions at 313 K (solid lines are trend lines).

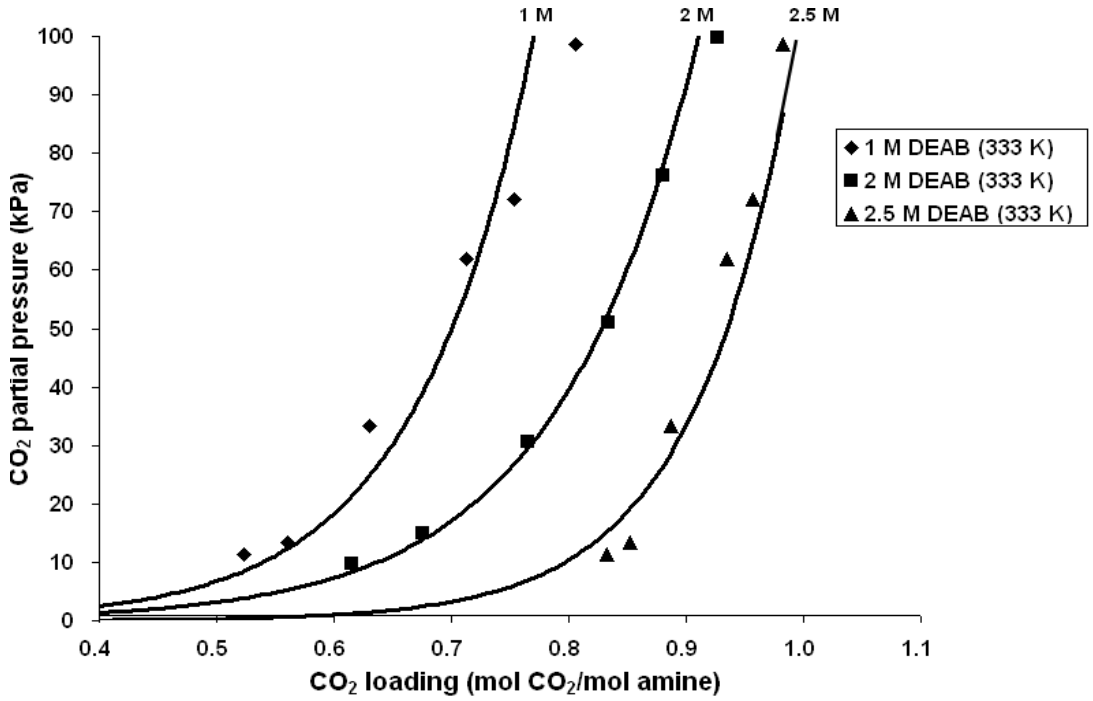

Figure 5.4 Equilibrium solubility of CO_2 in 1 M, 2 M, and 2.5 M aqueous DEAB solutions at 333 K (solid lines are trend lines).

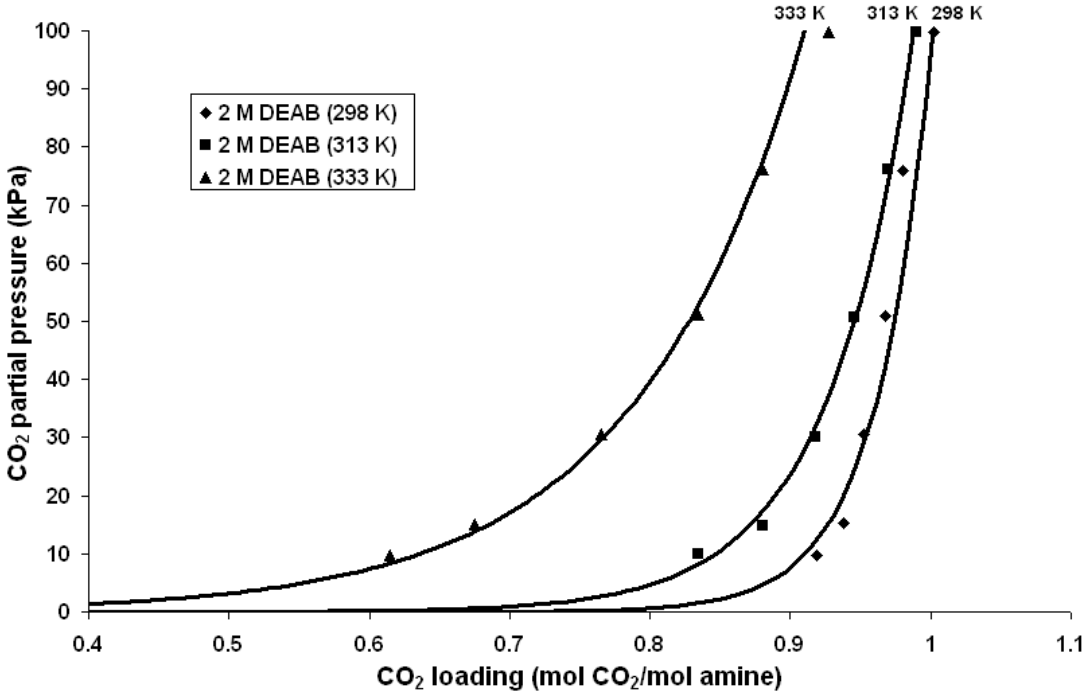

Figure 5.5 Equilibrium solubility of CO_2 in 2 M aqueous DEAB solutions at 298 K, 313 K, and 333 K (solid lines are trend lines).

5.4.2 Correlation of equilibrium solubility of CO_2 in aqueous DEAB solutions

In order to obtain the predicted equilibrium solubility of CO_2, a correlation for K_2 is required. By simultaneously solving the Equations 5.8-5.10 and 5.12-5.16, the 8 unknowns (which are K_2, $[RR_2'N]$, $[H^+]$, $[RR_2'NH^+]$, $[HCO_3^-]$, $[CO_2]$, $[OH^-]$, and $[CO_3^{2-}]$) are obtained. The K_2 values obtained at different conditions were then fitted to several models, namely, Kent-Eisenberg, Austgen, Li-Shen, and Hu-Chakma models, using a NLREG program. In this case, α was the unknown while K_2 was known, and all the unknowns are α, $[RR_2'N]$, $[H^+]$, $[RR_2'NH^+]$, $[HCO_3^-]$, $[CO_2]$, $[OH^-]$, and $[CO_3^{2-}]$. The values of these unknown variables were obtained by simultaneously solving Equations 5.8-5.10 and 5.12-5.16.

5.4.2.1 Kent-Eisenberg model

The Kent-Eisenberg model was proposed by Kent and Eisenberg (1976) as a predictive model for the equilibrium constant in order to represent the equilibrium solubility of CO_2 and H_2S over aqueous solutions of MEA and DEA by fitting the experimental solubility results with the predictive model. It is widely used due to the simplicity of the model (Li and Shen, 1993), which depends only on the temperature in Kelvin (T), as shown in Equation 5.18.

$$K_i = \exp\left[A + \frac{B}{T} + \frac{C}{T^2} + \frac{D}{T^3} + \frac{E}{T^4}\right] \tag{5.18}$$

This model was used for the CO_2-DEAB system. The values of the parameters (A, B, C, D, and E) for K_2 for this system, which were determined using the NLREG program, are given in Table 5.5.

The COMSOL software was applied for solving Equations 5.8-5.10 and 5.12-5.16 for α and bulk concentrations ($[RR_2'N]$, $[H^+]$, $[RR_2'NH^+]$, $[HCO_3^-]$, $[CO_2]$, $[OH^-]$, and $[CO_3^{2-}]$), while K_2 was calculated using the Kent-Eisenberg model. The predicted results of the equilibrium solubility of CO_2 in aqueous DEAB solutions (using K_2 from the Kent-Eisenberg model) are shown in Figures 5.6, 5.7, and 5.8 as lines. It was found that the predicted results fit moderately well with the experimental results with an AAD of 7.3%, which is in an acceptable range of AAD less than 10%.

5.4.2.2 Austgen model

Austgen et al. (1989 and 1991) proposed a thermodynamic model for prediction of H_2S and CO_2 solubility in aqueous solutions of MEA, DEA, blended MEA-MDEA, and blended DEA-MDEA using the electrolyte-NRTL equation. In this model, the activity coefficient was applied as a representative of long-range ion-ion interaction and short-range binary interaction. The Austgen model is also a function of only the temperature in Kelvin (T), as shown in Equation 5.19.

$$K_i = \exp\left[a + \frac{b}{T} + c\ln T + dT\right] \tag{5.19}$$

This model was also applied to the CO_2-DEAB system from which the values of K_2 were correlated with the Austgen model in Equation 5.19. The values of the parameters (a, b, c, and d) were determined using the NLREG program. The parameters (a, b, c, and d) are presented in Table 5.6.

In order to determine the equilibrium solubility of CO_2, COMSOL software was used to solve Equations 5.8-5.10 and 5.12-5.16 for α and bulk concentrations,

while K_2 was calculated using the Austgen model. The predicted results are plotted in Figures 5.6, 5.7, and 5.8, where it can be seen that the predicted results are almost the same as those using the Kent-Eisenberg model with an AAD of 7.3%.

Table 5.5 Parameters for the Kent-Eisenberg model for K_2 in Equation 5.18

Parameters	For K_2
A	-109.3
B	6.88×10^4
C	-1.008×10^7
D	1.0
E	1.0

Table 5.6 Parameters for the Austgen model for K_2 in Equation 5.19

Parameters	For K_2
a	-193
b	-1.685×10^4
c	67.85
d	-0.4325

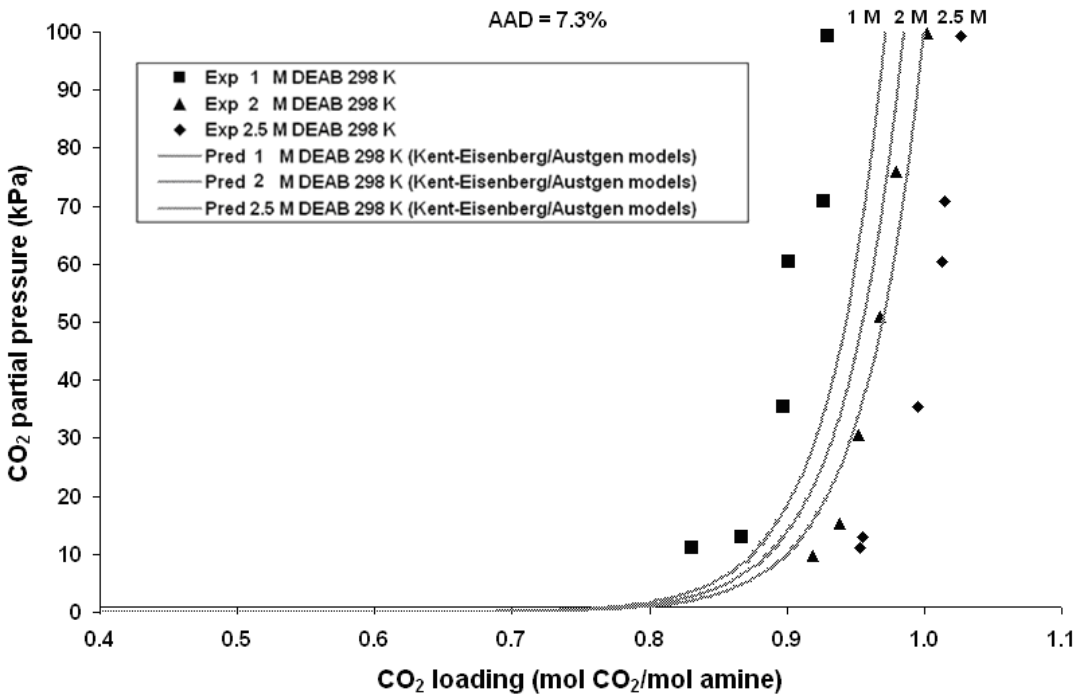

Figure 5.6 Equilibrium solubility of CO_2 in 1 M, 2 M, and 2.5 M aqueous DEAB solution at 298 K; lines are calculated using the Kent-Eisenberg model and Austgen model in Equations 5.18 and 5.19, respectively.

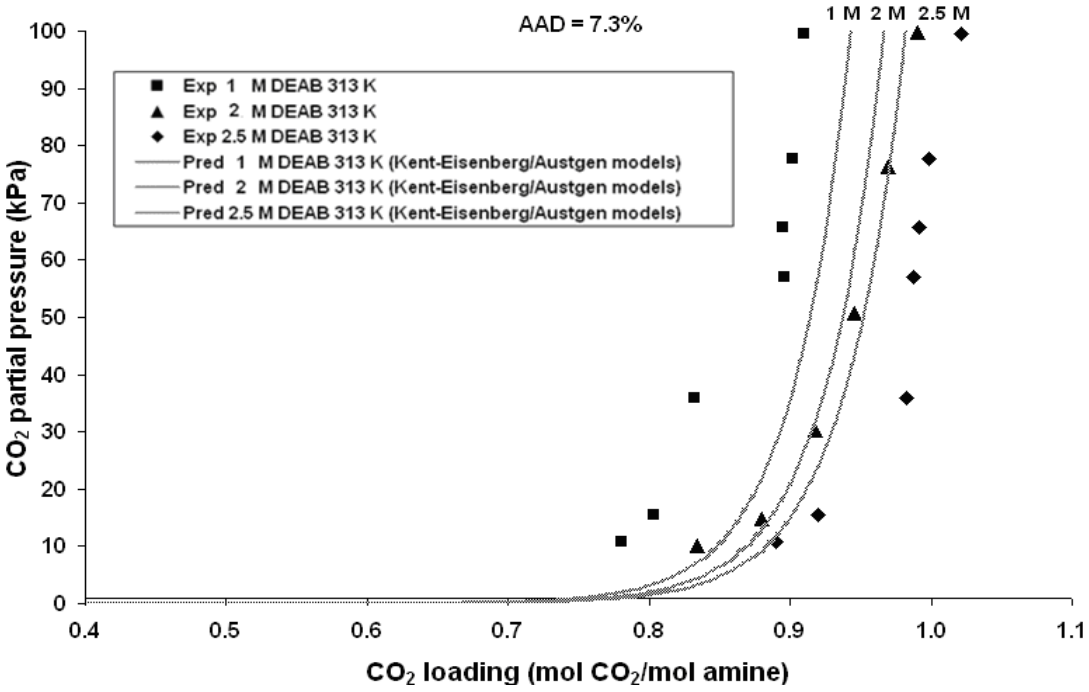

Figure 5.7 Equilibrium solubility of CO_2 in 1 M, 2 M, and 2.5 M aqueous DEAB solution at 313 K; lines are calculated using the Kent-Eisenberg model and Austgen model in Equations 5.18 and 5.19, respectively.

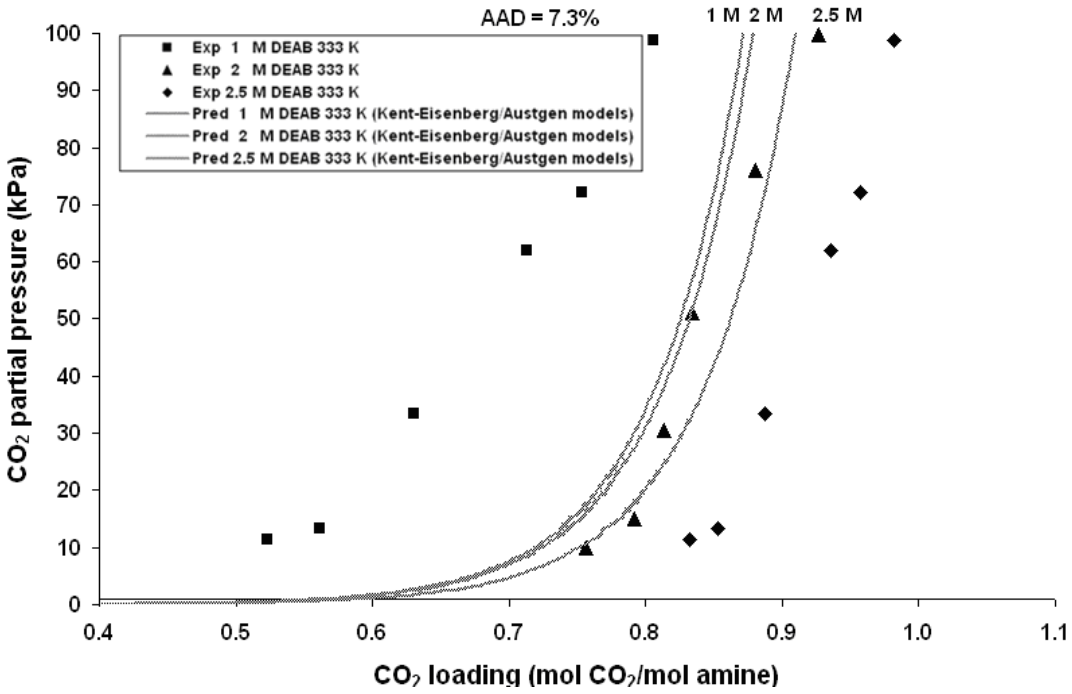

Figure 5.8 Equilibrium solubility of CO_2 in 1 M, 2 M, and 2.5 M aqueous DEAB solution at 333 K; lines are calculated using the Kent-Eisenberg model and Austgen model in Equations 5.18 and 5.19, respectively.

5.4.2.3 Li-Shen model

The Li-Shen model was proposed by Li and Shen (1993) in order to predict the equilibrium solubility of CO_2 in aqueous solutions of blended MEA-MDEA. This model takes not only temperature into account, but also considers the effects of CO_2 loading and free amine concentration as presented in Equation 5.20.

$$K_i = \exp\left[A_1 + \frac{A_2}{T} + \frac{A_3}{T^2} + B_1\alpha + \frac{B_2}{\alpha} + \frac{B_3}{\alpha^2} + B_4 \ln[R_3N] \right] \quad (5.20)$$

where α and $[R_3N]$ are equilibrium solubility of CO_2 (or CO_2 loading) and free DEAB concentration, respectively.

The parameters (A_1, A_2, A_3, B_1, B_2, B_3, and B_4) for K_2 in Equation 5.20 for the CO_2-DEAB system were determined using the NLREG program. The parameters are presented in Table 5.7. Equations 5.8-5.10 and 5.12-5.16 were simultaneously solved using COMSOL software (using the K_2 from Li-Shen model) for α and bulk concentrations. The predicted results are shown in Figures 5.9, 5.10, and 5.11. It can be seen that the predicted values fit moderately well with the experimental values with an AAD of 7.1%.

Table 5.7 Parameters for the Li-Shen model for K_2 in Equation 5.20

Parameters	For K_2
A_1	188.7
A_2	-581
A_3	0.916
B_1	-81.5
B_2	-132.4
B_3	31.05
B_4	-1.314

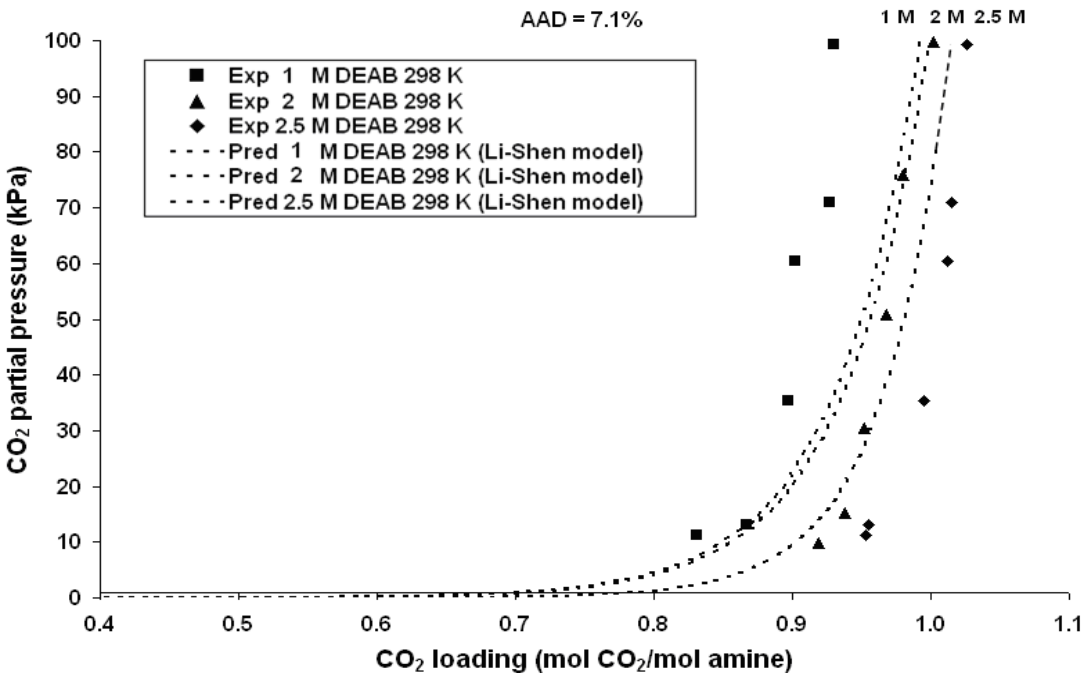

Figure 5.9 Equilibrium solubility of CO_2 in 1 M, 2 M, and 2.5 M aqueous DEAB solution at 298 K; lines are calculated using the Li-Shen model in Equation 5.20.

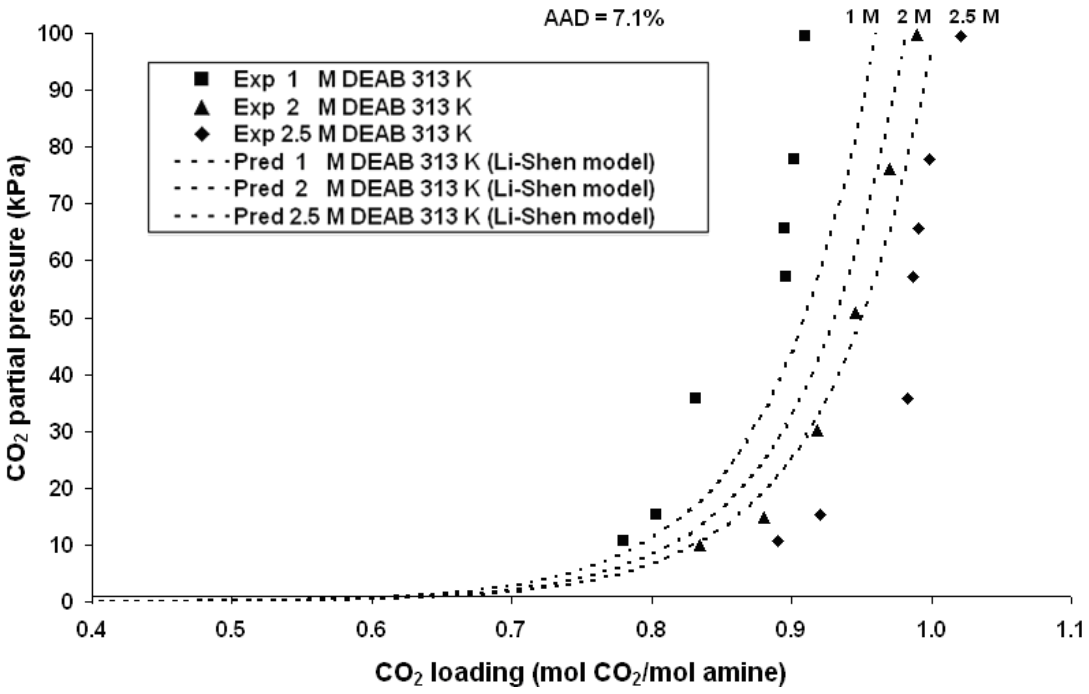

Figure 5.10 Equilibrium solubility of CO_2 in 1 M, 2 M, and 2.5 M aqueous DEAB solution at 313 K; lines are calculated using the Li-Shen model in Equation 5.20.

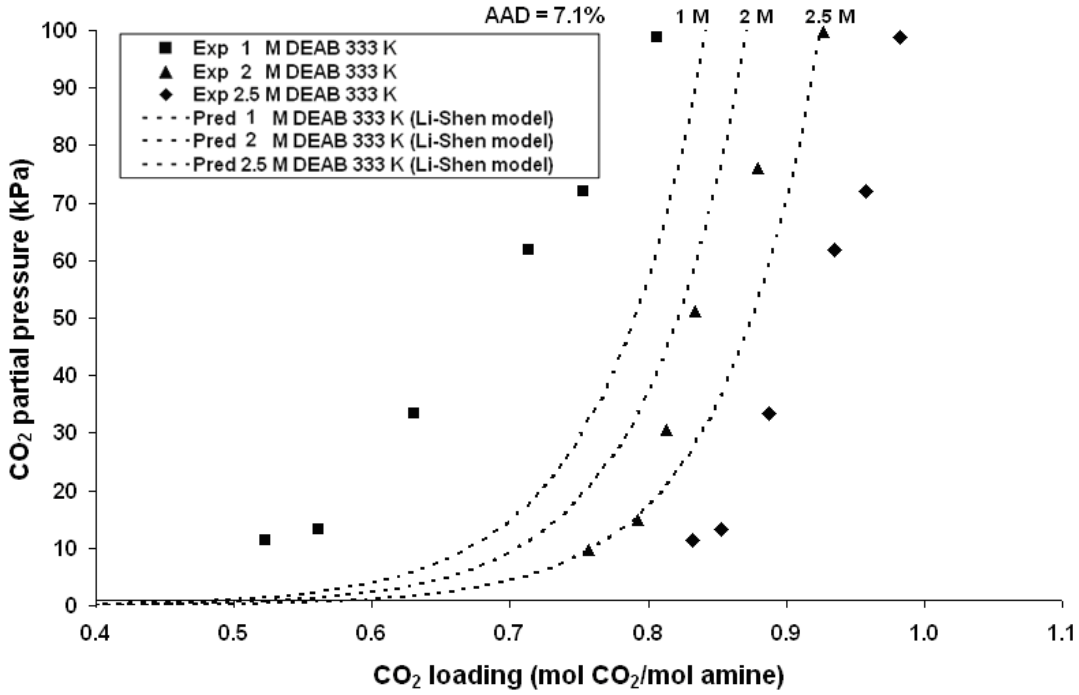

Figure 5.11 Equilibrium solubility of CO_2 in 1 M, 2 M, and 2.5 M aqueous DEAB solution at 333 K; lines are calculated using the Li-Shen model in Equation 5.20.

5.4.2.4 Hu-Chakma model

Hu and Chakma (1990a) proposed a mathematical model for predicting the CO_2 and H_2S equilibrium solubility in aqueous solutions of diglycolamine (DGA). The model represents the equilibrium constant in terms of temperature, physically dissolved H_2S (or CO_2) concentration, and free amine concentration. For the present study, the physically dissolved CO_2 concentration in aqueous DEAB solutions can be calculated using Equation 5.16. The authors concluded that the predicted results from their model are in good agreement with the experimental results. The Hu-Chakma model is shown in Equation 5.21.

$$K_i = \exp\left[D_1 + D_2 T + D_3 \frac{P_{CO_2}}{He_{CO_2}} + D_4 \ln[R_3 N]\right] \tag{5.21}$$

where $\frac{P_{CO_2}}{He_{CO_2}}$ represents $[CO_2]$, which is the physically dissolved CO_2 concentration in aqueous DEAB solutions. He_{CO_2} can be calculated from Equation 4.10 in Chapter 4.

By correlating the values of K_2 with the Hu-Chakma model of Equation 5.21 using the NLREG program, the parameters (D_1, D_2, D_3, and D_4) were determined and are presented in Table 5.8.

In order to determine the equilibrium solubility of CO_2, COMSOL software was used to solve Equations 5.8-5.10 and 5.12-5.16 for α and bulk concentrations while K_2 was calculated with the Hu-Chakma model. The predicted results are plotted in Figures 5.12, 5.13, and 5.14. It was found that the predicted results fit moderately well with the experimental results with an AAD of 8.3%, which is in an acceptable range of

AAD less than 10%. The parity chart that compares the experimental and predicted results is shown in Figure 5.15.

Table 5.8 Parameters for the Hu-Chakma model for K_2 in Equation 5.21

Parameters	For K_2
D_1	-6.903
D_2	3.56×10^{-2}
D_3	-84.8
D_4	-1.92

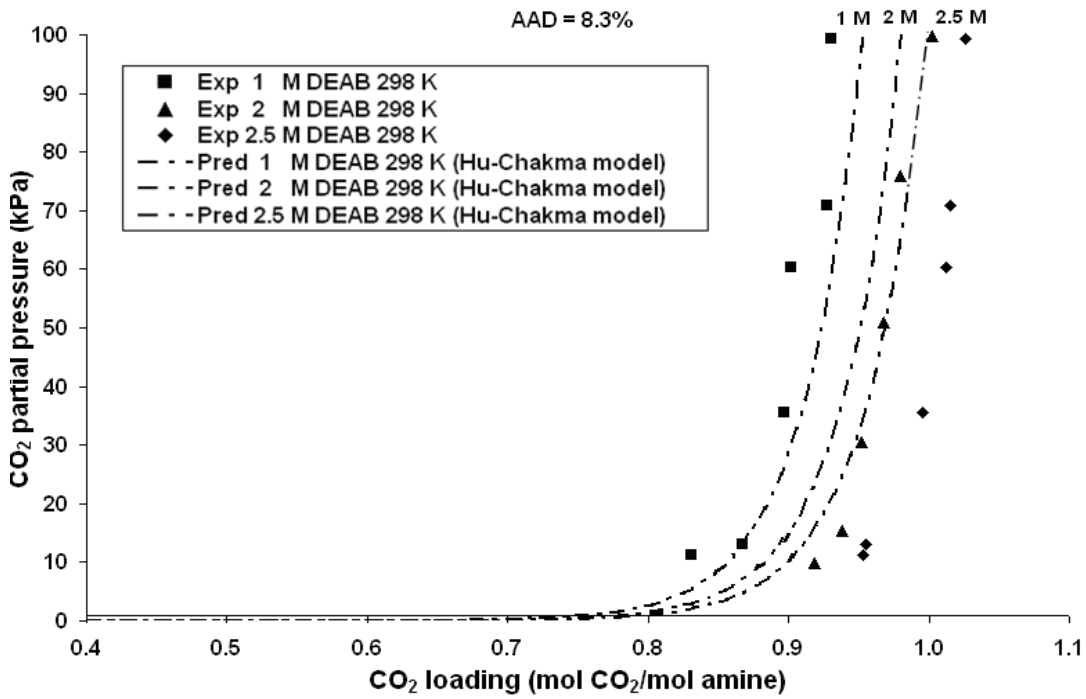

Figure 5.12 Equilibrium solubility of CO_2 in 1 M, 2 M, and 2.5 M aqueous DEAB solution at 298 K; lines are calculated using the Hu-Chakma model in Equation 5.21.

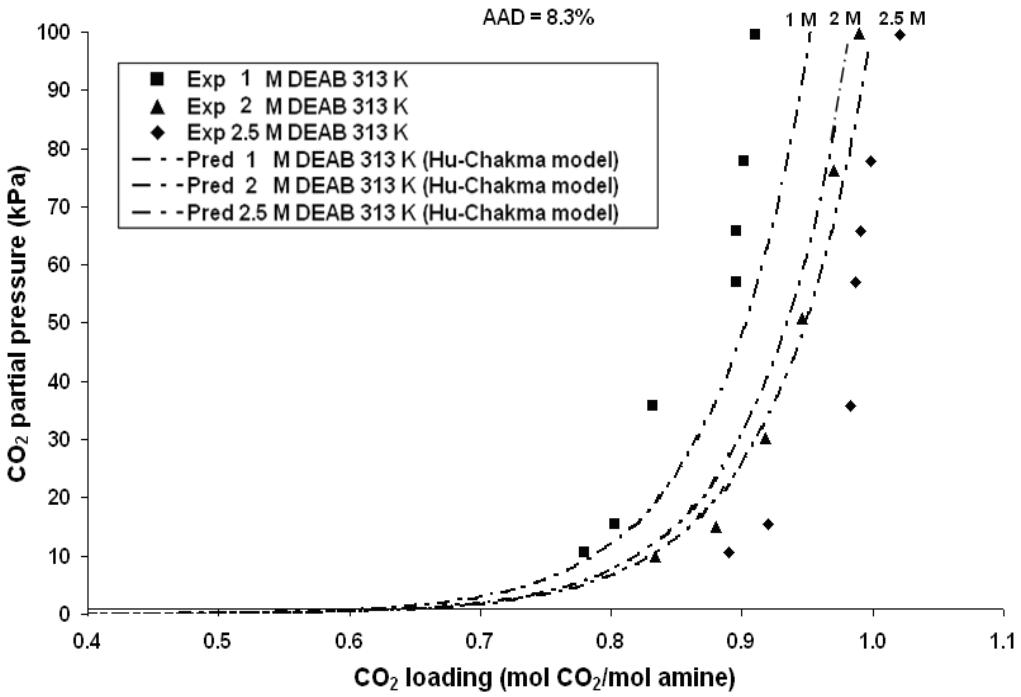

Figure 5.13 Equilibrium solubility of CO_2 in 1 M, 2 M, and 2.5 M aqueous DEAB solution at 313 K; lines are calculated using the Hu-Chakma model in Equation 5.21.

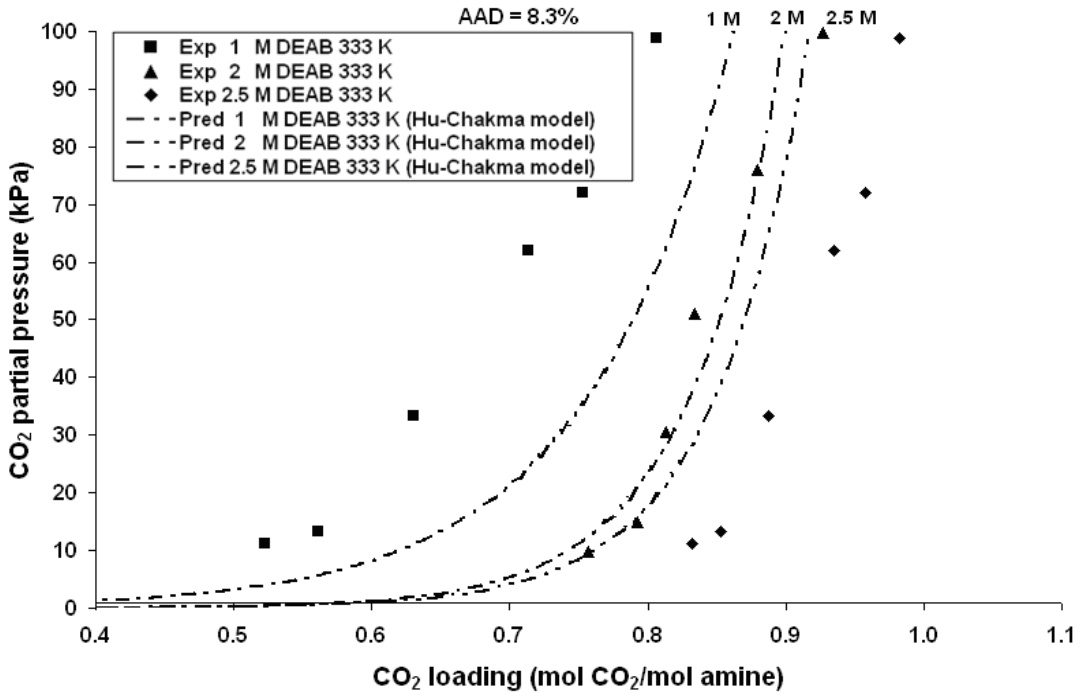

Figure 5.14 Equilibrium solubility of CO_2 in 1 M, 2 M, and 2.5 M aqueous DEAB solution at 333 K; lines are calculated using the Hu-Chakma model in Equation 5.21.

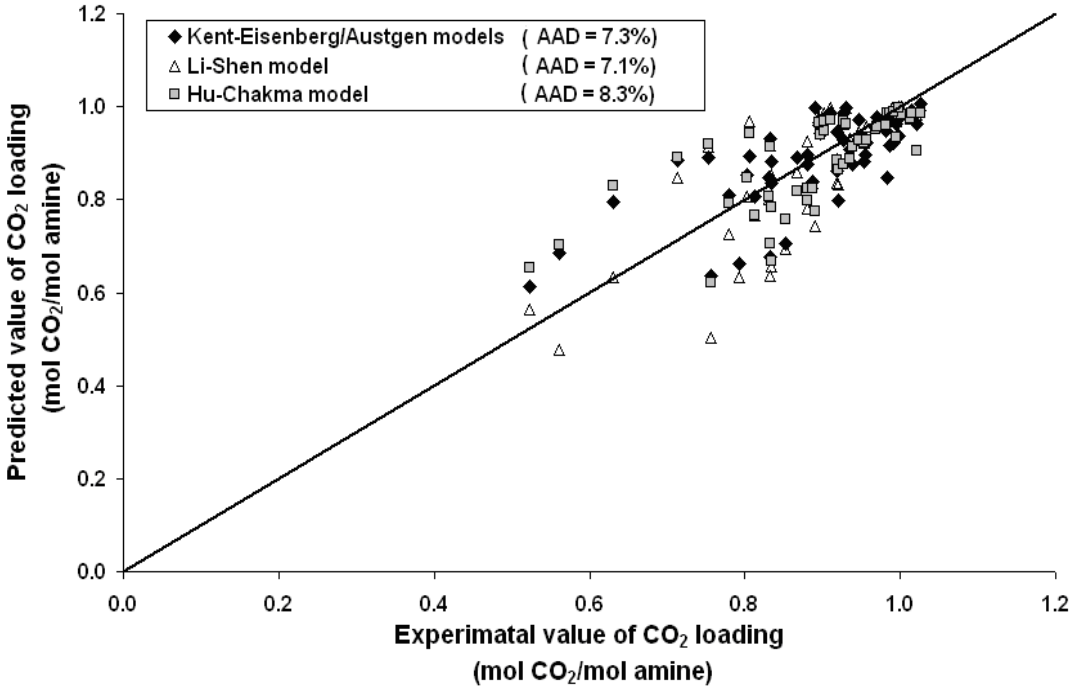

Figure 5.15 Parity chart comparing experimental and predicted results of CO_2 equilibrium solubility of aqueous DEAB solutions.

Several predictive models for K_2 (the Kent-Eisenberg, Austgen, Li-Shen, and Hu-Chakma models) were applied separately for the prediction of equilibrium solubility of CO_2 in aqueous solutions of DEAB. By comparing the predicted results of CO_2 equilibrium solubility, it can be said that the Li-Shen model seems to provide the best predicted results among the four at an AAD of 7.1%. The others models also provide good predicted results. For example, for Kent-Eisenberg/Austgen models, the AAD is 7.3%, and for the Hu-Chakma model, the AAD is 8.3%, as shown in Figure 5.15.

As can be seen in Figures 5.6, 5.7, and 5.8, the Kent-Eisenberg model and the Austgen model provide almost the same predicted results for the equilibrium solubility of CO_2 in aqueous DEAB solutions, which corroborates the assertion by Hu and Chakma (1990b) that there is no significant difference in using the Kent-Eisenberg model and the Austgen model because both models consider that the chemical equilibrium constant (K_i) depends only on temperature in Kelvin.

However, it has been mentioned by various researchers (Hu and Chakma, 1990a; Tontiwachwuthikul et al., 1991; Li and Shen, 1993; Beak and Yoon, 1998; Beak et al., 2000) that in order to predict the equilibrium solubility of acid gas in an aqueous amine solution, the equilibrium constant, which governs amine reaction, should not only be considered as a function of temperature, but also as a function of other parameters such as acid gas loading, free amine concentration, and physically dissolved CO_2 concentration. The Li-Shen model and the Hu-Chakma model take these parameters into consideration. The Li-Shen model correlates K_i with temperature, CO_2 loading, and free DEAB concentration, as shown in Equation 5.20. The results from this study have shown that the

predicted CO_2 equilibrium solubility results using K_2 calculated from the Li-Shen model provides the best agreement with the experimental results with an AAD of 7.1%.

Even though the Hu-Chakma model considers K_i as a function of temperature, physically dissolved CO_2 concentration, and free DEAB concentration, as shown in Equation 5.21, the predicted CO_2 equilibrium solubility results using K_2 calculated from the Hu-Chakma model provide the highest deviation from the experimental results at an AAD of 8.3%. One parameter that makes the Hu-Chakma model different from the Li-Shen model is the dependency on physically dissolved CO_2 concentration (which is CO_2 loading in the case of the Li-Shen model). CO_2 loading represents the capacity of amine to react with CO_2 in terms of moles of absorbed CO_2 per mole of amine. It is clear that CO_2 loading is directly related to the CO_2-amine reaction. This shows that the physically dissolved CO_2 concentration might not be a very good parameter for correlating K_i. It is generally accepted that the chemical equilibrium constant is strongly related to chemical reaction and equilibrium concentration of the involved species. Thus, using physically dissolved CO_2 concentration instead of CO_2 loading results in a bigger deviation in the predicted CO_2 equilibrium solubility.

After comparing the predicted CO_2 equilibrium solubility results using several predictive models for K_2 (the Kent-Eisenberg, Austgen, Li-Shen, and Hu-Chakma models), it can be seen that all models provide good agreement with the experimental results with acceptable AAD of less than 10 %. Small deviations between each model can be observed, as presented in Figure 5.15. This study shows, for the first time, that either model of the four can be use as a predictive correlation for chemical equilibrium constant, which is K_2 for the solubility of CO_2 in aqueous DEAB solution. Even though the Li-

Shen model provides the best correlation, the Kent-Eisenberg and Austgen models would be recommended for use due to their simplicity and convenience and because they are relatively as accurate as the Li-Shen model.

5.4.3 Heat of CO_2 absorption in aqueous DEAB solutions

Gabrielsen et al. (2005) estimated the heat of CO_2 absorption in MEA, DEA, and MDEA using the derived Gibbs-Helmholtz equation (Equation 5.17). They observed that the estimated results were close to the experimental results obtained from the calorimeter in the work of Carson et al. (2000). In the present study, the heat of CO_2 absorption in aqueous DEAB solution (ΔH_{abs}) was calculated using Equation 5.17. The equilibrium constant that governs the CO_2-DEAB reaction (K_2) was calculated using the Austgen model, Equation 5.19. The estimated heat of CO_2 absorption in aqueous DEAB solution was found to be -39.2 kJ/mol, as presented in Table 5.9 together with the experimental and the estimated results for MEA, DEA, and MDEA obtained from the works of Carson et al. (2000) and Gabrielsen et al. (2005). The minus symbol indicates that the reaction of CO_2 with MEA, DEA, MDEA, and DEAB is exothermic. By comparing the heat of CO_2 absorption in aqueous DEAB with that in aqueous MEA, DEA, and MDEA, it was found that the heat of CO_2 absorption in aqueous DEAB solution is lower than that in MDEA, DEA, and MEA, respectively. On the other hand, it can be said that the heat of desorption or regeneration for DEAB is 39.2 kJ/mol. Conversely, the regeneration energy for DEAB is lower than that for MDEA, DEA, and MEA, respectively, which corresponds well with the work of Maneeintr et al. (2009) who compared the regeneration energy of MEA and

DEAB in terms of cyclic capacity at different temperature ranges. They found that DEAB requires lower regeneration energy than MEA.

Table 5.9 Heat of CO_2 absorption in aqueous solutions of MEA, DEA, MDEA, and DEAB

Amine	Estimated Heat of CO_2 absorption; ΔH_{abs} (kJ/mol)	Experimental Heat of CO_2 absorption; ΔH_{abs} (kJ/mol)
MEA	-87.9[b]	-82[c]
DEA	-73.5[b]	-69[c]
MDEA	-48.8[b]	-49[c]
DEAB	-39.2	N/A

[b]Esimated values are obtained from Gabrielsen et al. (2005)

[c] Experimental values are obtained from Carson et al. (2000)

5.5 Summaries

1. The equilibrium solubility of CO_2 in aqueous DEAB solutions decreases as temperature increases but increases as CO_2 partial pressure and DEAB concentration increase over a temperature range of 298 K to 333 K, a CO_2 partial pressure range of 10 kPa to 100 kPa, and a DEAB concentration range of 1 M to 2.5 M.

2. The equilibrium solubility of CO_2 in aqueous DEAB solution is found to be very high (comparable with PZ) and higher than that in AMP, MDEA, MEA, and DEA, respectively.

3. The predicted CO_2 equilibrium solubility results using several predictive models for K_2 (the Kent-Eisenberg, Austgen, Li-Shen, and Hu-Chakma models) provide good agreement with the experimental results within the acceptable range of less than 10 % AAD.

4. Small deviations of the predicted CO_2 equilibrium solubility results were be observed while the different predictive models for K_2 were applied (Kent-Eisenberg/Austgen model had an AAD of 7.3%, Li-Shen model had an AAD of 7.1%, and Hu-Chakma model had an AAD of 8.3%).

5. The chemical equilibrium constant that governs the CO_2-DEAB-water reaction (K_2 of Equation 5.2) can be calculated by either the Kent-Eisenberg, Austgen, Li-Shen, or Hu-Chakma models. However, the Kent-Eisenberg and Austgen models are recommended for use due to their simplicity and convenience and because they are relatively as accurate as the Li-Shen model.

6. The estimated heat of CO_2 absorption in aqueous DEAB solution using the derived Gibbs-Helmholtz equation was found to be -39.2 kJ/mol, which is lower than that in MDEA, DEA, and MEA, respectively. Therefore, the regeneration energy for DEAB is lower than that for MDEA, DEA, and MEA, respectively.

5.6 References

1. Austgen, D.M.; Rochelle, G.T.; Peng, W.; Chen, C.C. Model of vapor-liquid equilibria for aqueous acid gas-alkanolamine systems using the electrolyte-NRTL equation. Ind. Eng. Chem. Res. 1989, 26, 1060-1073.

2. Austgen, D.M.; Rochelle, G.T.; Chen, C.C. Model of vapor-liquid equilibria for aqueous acid gas-alkanolamine system. 2. Representation of H_2S and CO_2 solubility in aqueous MDEA and CO_2 solubility in aqueous mixtures of MDEA with MEA or DEA. Ind. Eng. Chem. Res. 1991, 30, 543-555.

3. Beak, J.I.; Yoon, J.I. Solubility of carbon dioxide in aqueous solutions of 2-amino-2-methyl-1,3-propanediol. J. Chem. Eng. Data 1998, 43, 635-637.

4. Baek, J.I.; Yoon, J.H.; Eum, H.M. Prediction of equilibrium solubility of carbon dioxide in aqueous 2-amino-2-methyl-1,3-propanediol solutions. Korean J. Chem. Eng. 2000, 17, 484-487.

5. Benamar, A.; Aroua, M.K. Modeling of CO_2 solubility and carbamate concentration in DEA, MDEA and their mixtures using the Deshmukh-Mather model. Fluid Phase Equilibria 2005, 231, 150-162.

6. Carson, J.K.; Marsh, K.N.; Mather, A.E. Enthalpy of solution of carbon dioxide in (water+monoethanolamnine, or diethanolamine, or N-methylidiethanolamine) and (water+monoethanolamine + N-methylidiethanolamine) at T = 298.15 K[a]. J. Chem Thermodyn. 2000, 32, 1285-1296.

7. Gabrielsen, J.; Michelsen, M.L.; Stenby, E.H.; Kontogeorgis, G.M. A model for estimating CO_2 solubility in aqueous alkanolamines. Ind. Eng. Chem. Res. 2005, 44, 3348-3354.

8. Hu, W.; Chakma, A. Modelling of equilibrium solubility of CO_2 and H_2S in aqueous diglycolamine (DGA) solutions. The Canadian Journal of Chemical Engineering 1990a, 68, 523-525.

9. Hu, W.; Chakma, A. Modelling of equilibrium solubility of CO_2 and H_2S in aqueous amino methyl propanol (AMP) solutions. Chem. Eng. Commun. 1990b, 94, 53-61.

10. Jou, F.Y.; Mather, A.E.; Otto, F.D. Solubility of H_2S and CO_2 in aqueous methyldiethanolamine solutions. Ind. Eng. Chem. Process Des. Dev. 1992, 21, 539-544.

11. Kent, R.L.; Eisenberg, B. Better data for amine treating. Hydrocarbon Process 1976, 55, 87-90.

12. Kim, I.; Svendsen, H.F. Heat of absorption of carbon dioxide (CO_2) in monoethanolamine (MEA) and in 2-(aminoethyl)-ethanolamine (AEEA) solutions. Ind. Eng. Chem. Res. 2007, 46, 5803-5809.

13. Kohl, A.; Nielsen, R.B., Gas purification; Gulf Publishing Company: Houston, Texas, USA, 1997.

14. Li, M.H.; Shen, K.P. Calculation of equilibrium solubility of carbon dioxide in aqueous mixtures of monoethanolamine and methyldiethanolamine. Fluid Phase Equilibria 1993, 85, 129-140.

15. Maneeintr, K. New solvents for acid gas treating; Ph.D. thesis, University of Regina: Regina, Canada, 2010.

16. Maneeintr, K.; Idem, R. O.; Tontiwachwuthikul, P.; Wee, A. G. H. Synthesis, solubilities, and cyclic capacity of amino alcohols for CO_2 Capture from flue gas streams. Energy procedia 2009, 1, 1327-1334.

17. Rochelle, G.T. Research needs for acids gas kinetics and equilibria in alkanolamine systems. 70th GPA annual convention 1991, 66-82.

18. Tontiwachwuthikul, P.; Meisen, A.; Lim, J.C. Solubility of CO_2 in 2-amino-2methyl-1-propanol solutions. J. Chem. Eng. Data 1991, 36, 130-133.

19. Tontiwachwuthikul, P.; Wee, A. G. H.; Idem, R. O.; Maneeintr, K.; Fan, G. J.; Veawab, A.; Aroonwilas, A.; Chakma, A. Method for capturing carbon dioxide from gas streams. US Patent Application. US Patent Application, No. US 2008/0050296 A1, 2008.

Chapter 6 Kinetics of CO_2 Absorption into Aqueous Solutions of 4-(Diethylamino)-2-Butanol

6.1 Introduction

A wide variety of amines such as monoethanolamine (MEA), diethanolamine (DEA), and methyldiethanolamine (MDEA) have been used in industrial carbon dioxide (CO_2) capturing processes for a number of years (Kohl and Nielsen, 1997). Recently, Tontiwachwuthikul et al. (2008); Maneeintr et al. (2009), and this work in Chapter 5 have developed and investigated the performance of a newly developed amino alcohol solvent, 4-diethylamino-2-butanol (DEAB). These studies have found that the absorption capacity of DEAB is comparable with piperazine (PZ) and higher than that of 2-amino-2-methyl-1-propanol (AMP), MDEA, DEA, and MEA. Moreover, they also found that the regeneration energy requirement of DEAB is lower than that of MDEA, DEA, and MEA, respectively. Regarding these outstanding performances, DEAB is now being considered as a promising alternative solvent for capturing CO_2. However, a better solvent for capturing CO_2 should not only provide high absorption capacity and low regeneration energy, but should also have a fast reaction rate (reaction kinetics), low solvent degradation, and low corrosiveness. More importantly, more effective design of the absorber for amine-based CO_2 treating plants requires an increased understanding of the reaction kinetics between CO_2 and amine (Rochelle, 1991).

A laminar jet absorber is one of the apparatuses that provide very accurate and reliable kinetics data because the interfacial area is known accurately and the physical absorption rates have been shown to agree with the Higbie's penetration theory prediction

(Astarita et al., 1983; Aboudheir et al., 2003 and 2004). One of the very first numerical comprehensive reaction rate/kinetics models of CO_2 absorption in aqueous amine solutions was developed by Hagewiesche et al. (1995). They studied the absorption of CO_2 in aqueous solutions of blended MEA-MDEA using a laminar jet absorber and based on Higbie's penetration theory. However, the experiments were performed at only 313 K. Recently, a more comprehensive kinetics models for CO_2 absorption into loaded aqueous amine solutions of MEA, blended MEA-MDEA, and blended MDEA-PZ were developed by Idem et al. (2009); Edali et al. (2009 and 2010); Edali (2010). In their studies, the experimental kinetics data were obtained from a laminar jet absorber at various temperatures, amine concentrations, CO_2 loadings, and contact times. Moreover, the chemical equilibrium, the mass transfer, and the chemical kinetics of all possible reactions were taken into account in their comprehensive models. Two numerical techniques, which are the finite difference method (FDM) based on the Barakat-Clark scheme and the finite element method (FEM) based on COMSOL software, were used for solving the reaction rate/kinetics model. They found that both FDM and FEM provide very accurate predicted CO_2 absorption rates. Also, no significant difference between the results obtained from FDM and FEM were observed.

In this chapter, the experimental kinetics data of CO_2 absorption in aqueous DEAB solutions were measured using the laminar jet absorber over ranges of temperatures, DEAB concentrations, CO_2 loadings, and contact times. The obtained experimental data were then used to develop the comprehensive numerical reaction rate/kinetics model (using FEM based on COMSOL software) for the absorption of CO_2 in aqueous solutions of DEAB. The chemical equilibrium, the mass transfer, and the

chemical kinetics of all possible reactions were also taken into account in this comprehensive model.

6.2 Theory

Based on the proposed mechanism for the reaction between CO_2 and DEAB, a vapour-liquid equilibrium (VLE) model and an absorption rate/kinetics model for predicting the kinetics data were developed.

6.2.1 Chemical reaction scheme for CO_2-DEAB aqueous system

The chemical reactions in CO_2-DEAB aqueous system are governed by the following equations:

$$RR_2^{/}N + H^+ \xleftrightarrow{K_1} RR_2^{/}NH^+ \tag{6.1}$$

$$CO_2 + RR_2^{/}N + H_2O \xleftrightarrow{K_2, k_{22}, -k_{22}} RR_2^{/}NH^+ + HCO_3^- \tag{6.2}$$

$$H_2O + CO_2 \xleftrightarrow{K_3} H^+ + HCO_3^- \tag{6.3}$$

$$CO_2 + OH^- \xleftrightarrow{K_4, k_{24}, -k_{24}} HCO_3^- \tag{6.4}$$

$$HCO_3^- \xleftrightarrow{K_5} H^+ + CO_3^{2-} \tag{6.5}$$

$$H_2O \xleftrightarrow{K_6} H^+ + OH^- \tag{6.6}$$

$RR_2^{/}N$ represents DEAB where R is $(CH_2)_2CH(CH_3)OH$ and R' is CH_2CH_3. K_i is the chemical equilibrium constant for reaction i. k_{2i} is the second order forward rate coefficient for reaction i, DEAB is considered to be a tertiary amine, since it has 3 carbon atoms attached to the nitrogen atom. In this case, DEAB does not react directly with CO_2 but acts as a base, which catalyzed the hydration of CO_2 (Hagewiesche et al.,

1995; Kohl and Nielsen, 1997), as presented in Equation 6.2. Reactions 6.2 and 6.4 are considered to be reversible with finite reaction rates, whereas reactions 6.1, 6.3, 6.5, and 6.6 are considered to be reversible and instantaneous with respect to mass transfer and at equilibrium, since they involve only proton transfer (Hagewiesche et al., 1995).

Based on Equations 6.1-6.6, it can be seen that not all of the chemical equilibrium constants are independent. Only 4 chemical equilibrium constants (K_2, K_3, K_4, and K_6) are independent. The remaining two (K_1 and K_5) can be obtained by the combination of independent chemical equilibrium constants, as shown in Equations 6.7 and 6.8. Also, water concentration is considered to be constant due to the presence of an excess amount of water in the solution (the water concentration is much higher than DEAB concentration).

$$K_1 = \frac{\left[RR_2^{/}NH^+\right]}{\left[H^+\right]\left[RR_2^{/}N\right]} = \frac{K_2}{K_3} \tag{6.7}$$

$$K_5 = \frac{\left[H^+\right]\left[CO_3^{2-}\right]}{\left[HCO_3^-\right]} = \frac{K_2}{K_1 K_6} \tag{6.8}$$

The chemical species in Equations 6.1-6.6 have been renamed for convenience in the numerical treatment as $C_1 = \left[CO_2\right], C_2 = \left[HCO_3^-\right]$, $C_3 = \left[OH^-\right]$, $C_4 = \left[CO_3^{2-}\right]$, $C_5 = \left[H^+\right]$, $C_6 = \left[RR_2^{/}N\right]$, $C_7 = \left[RR_2^{/}NH^+\right]$. Also, subscripts 1-7 represent the chemical species of $CO_2, HCO_3^-, OH^-, CO_3^{2-}$, $H^+, RR_2^{/}N$, and $RR_2^{/}NH^+$, respectively.

6.2.2 Vapour-liquid equilibrium (VLE) model

The bulk concentrations of all chemical species in liquid phase at equilibrium ($C_1 - C_7$), which are required for the kinetics study, can be estimated using the VLE

model. The input parameters for this model are the initial concentration of DEAB in the solution ($[DEAB]_0$; kmol/m^3), equilibrium CO_2 solubility in aqueous solutions of DEAB or CO_2 loading (α ; mol CO_2/mol DEAB), equilibrium constants of involved reactions (K_i), and physical solubility of CO_2 in the solution or Henry's constant (He ; kPa m^3/kmol). The concentrations of $C_1 - C_7$ can be obtained by simultaneously solving the mass balance equations, the equilibrium constant equations, and the Henry's law relationship as shown below:

Total DEAB balance:

$$[DEAB]_0 = C_6 + C_7 \tag{6.9}$$

Total carbon balance:

$$\alpha[DEAB]_0 = C_1 + C_2 + C_4 \tag{6.10}$$

Charge balance:

$$C_5 + C_7 = C_2 + C_3 + 2C_4 \tag{6.11}$$

Independent equilibrium constants:

$$K_2 = \frac{C_2 C_7}{C_1 C_6} \tag{6.12}$$

$$K_3 = \frac{C_2 C_5}{C_1} \tag{6.13}$$

$$K_4 = \frac{C_2}{C_1 C_3} \tag{6.14}$$

$$K_6 = C_3 C_5 \tag{6.15}$$

Henry's law relationship:

$$He_{CO_2} = P_{co_2} \Big/ C^*_{CO_2} \tag{6.16}$$

The chemical equilibrium constant K_2 is given in Equation 5.19 (in Chapter 5), and K_3, K_4, and K_6 can be found in the works of Austgen et al. (1991). The physical solubility of CO_2 into aqueous DEAB solutions or He_{CO_2} can be estimated using Equation 4.10 via the N_2O analogy as described in Chapter 4.

The 8 coupled nonlinear algebraic equations (i.e., Equations 6.9-6.16) were then simultaneously solved for the 8 unknowns, which are $C_1 - C_7$ and equilibrium partial pressure of CO_2 (P_{co_2}), by inputting the initial guess for each unknown. In the present study, the FEM based on COMSOL 4.1 software with 0D stationary solver mode was applied. After the software had been operated with the first set of initial guesses, values of the unknowns were obtained. Then, these new values were subsequently used as the initial guesses for solving the 8 unknowns. This process was repeated until the percentage deviation of the results of each unknown for successive attempts was less than 0.01%.

6.2.3 CO_2 absorption rate/kinetics model

A comprehensive CO_2 absorption rate/kinetics model was developed in order to interpret the absorption rate data of CO_2 in aqueous DEAB solutions, from which the kinetics data were extracted. This model takes into account the coupling between chemical equilibrium, mass transfer, and chemical kinetics of all possible chemical reactions. Also, the model is capable of predicting the CO_2 absorption rate and enhancement factor from the physiochemical properties, as well as predicting the kinetics

of reaction (which is the second order forward rate coefficient for reaction 6.2 or k_{22} or k_{DEAB}) from the experimental CO_2 absorption rate data.

The model was derived from a full 3D cylindrical coordinate system, which is the shape of the cylindrical liquid jet generated in the laminar jet absorber, as shown in Figure 6.1. The gas-liquid interface is considered as an outer boundary. Also, the diffusion in radial direction is taken into account. Therefore, the absorption of CO_2 into the cylindrical liquid jet, with constant density and diffusivity, is governed by Equation 6.17 (Astarita et al., 1983).

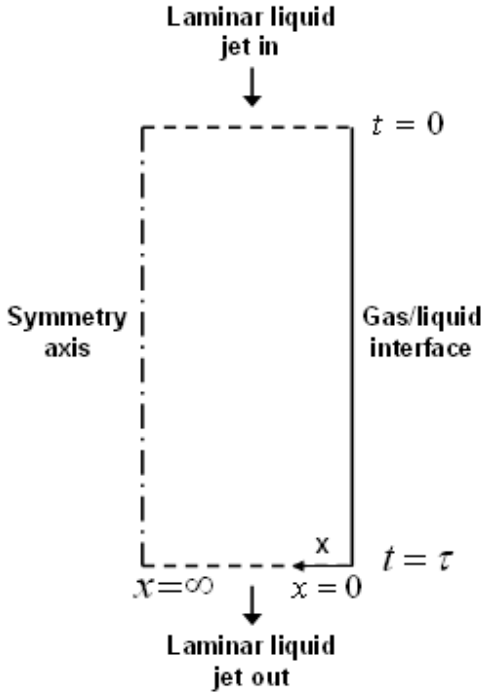

Figure 6.1 Schematic diagram of the liquid jet in the laminar jet absorber.

Equation 6.17 indicates that the molecular transport is equal to the sum total of the convection term, accumulation term ($\partial C / \partial t$), and reaction rate (R).

$$D\nabla^2 C = u \cdot \nabla C + \frac{\partial C}{\partial t} + R \tag{6.17}$$

The assumption of constant density and diffusivity is valid in the laminar jet absorber because the change of concentration does not represent a substantial variation in the mole fraction of the diffusant due to the short contact time (Aboudheir et al., 2003). Equation 6.17 can be simplified by following assumptions: (a) the penetration theory is applicable for the transport of the gas into liquid, in which the reaction takes place by unsteady state molecular diffusion in the liquid; (b) the penetration depth of the absorbed molecule is much smaller than the jet diameter due to the short contact time (created in the laminar jet absorber) between the absorbed gas and the liquid jet. Therefore, there is no curvature effect. The absorption of gas into liquid is then considered to be an infinite depth with flat surface; (c) the diffusion in the flow direction is negligible; (d) the liquid jet is quiescent so that no convection movements affect the transport of the absorbed gas. Regarding these conditions, Equation 6.17 can be simplified to the diffusion equation of Equation 6.18. This equation governs the variation of time and space of the concentration of all reactants and products in the liquid phase (one equation for each component or material balance).

$$D\frac{\partial^2 C}{\partial x^2} = \frac{\partial C}{\partial t} + R \tag{6.18}$$

Thus, the partial differential equations (PDEs) and the nonlinear algebraic equations governing the diffusion-reaction process of Equations 6.1-6.6 can be described as follows:

CO_2 balance:

$$\frac{\partial C_1}{\partial t} = D_1 \frac{\partial^2 C_1}{\partial x^2} + R_2 + R_4 \tag{6.19}$$

Total carbon balance:

$$\frac{\partial C_1}{\partial t} + \frac{\partial C_2}{\partial t} + \frac{\partial C_4}{\partial t} = D_1 \frac{\partial^2 C_1}{\partial x^2} + D_2 \frac{\partial^2 C_2}{\partial x^2} + D_4 \frac{\partial^2 C_4}{\partial x^2} \tag{6.20}$$

Total DEAB balance:

$$\frac{\partial C_6}{\partial t} + \frac{\partial C_7}{\partial t} = D_6 \frac{\partial^2 C_6}{\partial x^2} + D_7 \frac{\partial^2 C_7}{\partial x^2} \tag{6.21}$$

Total charge balance:

$$\frac{\partial C_2}{\partial t} + \frac{\partial C_3}{\partial t} + 2\frac{\partial C_4}{\partial t} - \frac{\partial C_5}{\partial t} - \frac{\partial C_7}{\partial t} = D_2 \frac{\partial^2 C_2}{\partial x^2} + D_3 \frac{\partial^2 C_3}{\partial x^2} + 2D_4 \frac{\partial^2 C_4}{\partial x^2} - D_5 \frac{\partial^2 C_5}{\partial x^2} - D_7 \frac{\partial^2 C_7}{\partial x^2} \tag{6.22}$$

All reactions at equilibrium (only the independent equilibrium constants), including K_2, K_3, and K_6, are given in Equations 6.12, 6.13, and 6.15, respectively.

R_2 and R_4, which are the reaction rate expressions for reactions 6.2 and 6.4, respectively, can be presented as follows:

$$R_2 = -k_{DEAB} C_1 C_6 + \left(\frac{k_{DEAB}}{K_2} \right) C_2 C_7 \tag{6.23}$$

$$R_4 = -k_{24} C_1 C_3 + \left(\frac{k_{24}}{K_4} \right) C_2 \tag{6.24}$$

D_i is the diffusivity of chemical species i into the solution (m^2/s). The diffusivity of CO_2 in aqueous solution of DEAB (D_1) can be calculated from the predictive

correlation via the N_2O analogy given in Equation 4.14 (in Chapter 4). Hikita et al. (1980) measured the diffusivity of MEA, DEA, and triethanolamine (TEA) in aqueous solution. They reported that the diffusivity was affected by the group complexity. Since DEAB is a tertiary amine, the as same as TEA, it is reasonable to estimate the diffusivity of DEAB from that of TEA (the same assumption has also been made in the case of MDEA by Hagewiesche et al. (1995)). Thus, The diffusivity of DEAB (D_6 ; cm^2/s) can be estimated by:

$$D_6 = \left(1.739 \times 10^{-9}\right)\mu^{-0.569842} T \tag{6.25}$$

where μ is solution viscosity (g/cm s) and T is temperature in K. Also, the diffusivity of $HCO_3^-, OH^-, CO_3^{2-}, H^+$, and $RR_2^{'}NH^+$ were assumed to be equal to that of DEAB, which is the most abundant species in the solution (Hagewiesche et al., 1995).

The forward rate coefficient of Equation 6.4 (k_{24} ; $m^3/kmol\ s$) was calculated from the correlation developed by Pinsent et al. (1956) as follows:

$$\log\left(k_{24}\right) = 13.635 - \frac{2895}{T} \tag{6.26}$$

Thus, there are 7 partial differential-nonlinear algebraic equations (Equations 6.12, 6.13, 6.15, and 6.19-6.22), which can be solved for the concentration of chemical species $C_1 - C_7$.

Initial conditions:

for all chemical species, j = 1, 2, 3,…,7

$$C_j(x,0) = C_j^0 \text{ at } t = 0 \text{ and } 0 \le x \ge \infty \tag{6.27}$$

Boundary conditions:

for all chemical species, j = 1, 2, 3,…,7

$$C_j(\infty,t) = C_j^0 \text{ at } x = \infty \text{ and } 0 \le t \ge \tau \tag{6.28}$$

for volatile chemical species, j = 1

$$C_j(0,t) = C_j^* = {P_j}/{He_j} \text{ at } x = 0 \text{ and } 0 \le t \ge \tau \tag{6.29}$$

for non-volatile chemical species, j = 2, 3, 4,…,7

$$\frac{\partial C_j}{\partial t}(0,t) = 0 \text{ at } x = 0 \text{ and } 0 \le t \ge \tau \tag{6.30}$$

where C_1^* is the interfacial concentration of CO_2 in the solution (kmol/m^3), which is defined as the partial pressure of CO_2 in the gas (P_1; kPa) divided by the physical solubility of CO_2 in the solution or Henry's law constant (He_1; kPa m^3/kmol). C_j^0 is the bulk concentration of species j in liquid phase (kmol/m^3), which can be obtained by the vapour-liquid equilibrium model.

For the laminar jet absorber, the contact time (τ) is found to be:

$$\tau = \frac{\pi d^2 h}{4L} \tag{6.31}$$

where d is jet diameter (m), h is jet height (m), and L is volumetric liquid flow rate (m^3/s).

From the Higbie's penetration theory, the liquid phase mass transfer coefficient for physical absorption of CO_2 (k_L^0; m/s) is defined as:

$$k_L^0 = 2\sqrt{\frac{D_1}{\pi\tau}} = \frac{4}{d\pi}\sqrt{\frac{D_1 L}{h}} \tag{6.32}$$

The local CO_2 absorption rateper unit area (N ; kmol/m^2 s) is given as:

$$N = -D_1\left(\frac{\partial C_j}{\partial t}\right)_{x=0} \tag{6.33}$$

Thus, the average CO_2 absorption rate per unit area (N_{ave}; kmol/m^2 s) is obtained by integrating Equation 6.33 over the contact time τ :

$$N_{ave} = -\frac{D_1}{\tau}\int_0^{\tau}\frac{\partial C_j}{\partial t}(0,t)dt \tag{6.34}$$

The effect of chemical reaction in terms of the enhancement factor, E, which is defined as the ratio of the absorption rate of CO_2 into a reacting liquid to that if there was no reaction, is given by:

$$E = \frac{N_{ave}}{k_L^0\left(C_1^* - C_1^0\right)} \tag{6.35}$$

For each absorption rate experiment, Equations 6.12, 6.13, 6.15, and 6.19-6.22 were solved using FEM based on COMSOL 4.1 software with 1D time-dependent mode by considering the forward reaction rate constant of Equation 6.4 (k_{DEAB}) as an adjustable parameter. The experimental enhancement factor ($E_{\exp}$) can be obtained directly from the experiment using Equation 6.35 (while the N_{ave} was measured experimentally). Also, the predicted enhancement factor (E_{pred}) can be obtained numerically by integrating the local CO_2 absorption rate per unit area (N) over contact time τ , as shown in Equation 6.34. $\left(\frac{\partial C_1}{\partial t}\right)_{x=0}$ can be acquired as the result of solving Equations 6.12, 6.13, 6.15, and 6.19-6.22 using COMSOL software. Also, the integration over contact time τ was done by using the integration function in the COMSOL software. For each experiment (at

different initial DEAB concentrations, temperatures, initial CO_2 loadings, and contact times), the parameter k_{DEAB} was adjusted until $\left|\frac{E_{\exp} - E_{pred}}{E_{\exp}}\right| \leq 1\%$ (Hagewiesche et al., 1995). Then, the forward reaction rate constant, k_{DEAB}, was correlated with the reaction rate constant expression as shown in Equation 6.36.

$$k_{DEAB} = A \cdot \exp\left(-\frac{B}{T}\right) \tag{6.36}$$

6.3 Results and discussion

6.3.1 Vapour-liquid equilibrium model

The VLE model for aqueous DEAB solution was developed in order to obtain the bulk concentrations of all chemical species ($C_1 - C_7$), which are required for the CO_2 absorption rate/kinetic model. Some results for the bulk concentrations obtained by the VLE model are shown in Figure 6.2. This figure shows the species concentrations at 0 to 1 CO_2 loading for 2 M of aqueous DEAB solution at 313 K. It can be observed from Figure 6.2 that the DEAB concentration decreases as CO_2 loading increases. This is due to the DEAB protonation and the CO_2-DEAB-water reaction, as shown in Equations 6.1 and 6.2, respectively. As a result, the protonated DEAB concentration, $DEABH^+$, increases as CO_2 loading increases. One of the major products, which is HCO_3^-, is found to increase as CO_2 loading increases. As CO_2 loading increases (which means more CO_2 is introduced to the system), HCO_3^- is formed due to CO_2 reacting with DEAB-water, water, and OH^-, as shown in Equations 6.2, 6.3, and 6.4, respectively. At CO_2 loading less than 0.4, $\left[CO_3^{2-}\right]$ is found to increase due to the CO_3^{2-} formation by HCO_3^-, as

shown in Equation 6.5. However, $\left[CO_3^{2-}\right]$ decreases when CO_2 loading is higher than 0.4. This is because the acidity of the solution increases as CO_2 loading increases. Then, Equation 6.5 is reversed to form HCO_3^- from CO_3^{2-}.

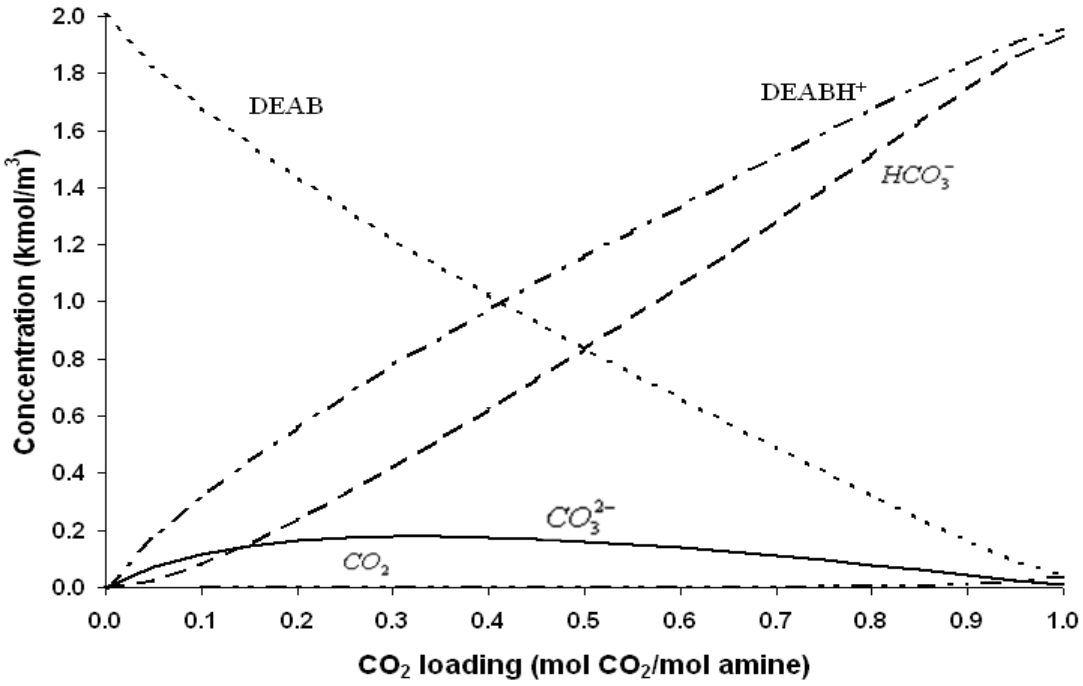

Figure 6.2 Liquid phase speciation and concentration in aqueous DEAB solutions as a function of CO_2 loading (α) at initial DEAB concentration of 2 kmol/m^3 and 313 K (data obtained by vapour-liquid equilibrium model developed in this study).

6.3.2 CO_2 absorption rate/kinetics model

The CO_2 absorption rate in aqueous DEAB solutions was measured using a laminar jet absorber at atmospheric pressure over a temperature range of 298 K to 318 K, DEAB concentration range of 1 M to 2 M, CO_2 loading range of 0.001 mol CO_2/mol amine to 0.18 mol CO_2/mol amine, and contact time range of 0.0044 s to 0.018 s. These operating conditions were selected because (1) DEAB was found to have lower heat of absorption than MDEA, DEA, and MEA, as mention in Chapter 5; thus, lower absorption temperature is applicable in the case of DEAB; (2) DEAB provides very high CO_2 absorption capacity (comparable with PZ) as mentioned in Chapter 5 and also Tontiwachwuthukul et al. (2008) and Maneeintr et al. (2009); thus, low DEAB concentration can achieve satisfactory CO_2 absorption capacity; (3) the ideal solution assumption is applicable at low CO_2 loading (Edali, 2010). The experimental results for CO_2 absorption rate in aqueous DEAB solutions are presented in Table B1 (in Appendix B).

The experimental absorption rate data were then interpreted by the numerical solved CO_2 absorption rate/kinetics model using FEM based on COMSOL 4.1 software with 1D time-dependent mode by considering k_{DEAB} as an adjustable parameter. The k_{DEAB} results were correlated with the reaction rate constant expression of Equation 6.36 as:

$$k_{DEAB} = \left(4.01\times10^{13}\right)\exp\left(-\frac{7527.7}{T}\right) \tag{6.37}$$

The predicted k_{DEAB} at 313 K compared with that of MDEA, AMP, DEA, MEA, and PZ are shown in Table 6.1. By comparing k_{DEAB} and k_{MDEA} (both DEAB and MDEA

are considered as tertiary amines), it can be seen that the k_{DEAB} is much higher than k_{MDEA}, which means that the absorption reaction of CO_2 with DEAB is much faster than that with MDEA. Moreover, it can also be observed that the k_{DEAB} is comparable with k_{AMP} and k_{DEA}. It is generally accepted that AMP and DEA are considered to be reactive with CO_2 since they are a primary sterically hindered amine and secondary amine, respectively (Sartori and Savage, 1983; Kohl and Nielsen, 1997). However, the k_{DEAB} is much smaller than k_{MEA} and k_{PZ}, since MEA is a primary amine, which is very reactive with CO_2, and PZ is a very fast accelerator. It was reasoned by Tontiwachwuthikul et al. (2008), who worked on the rational molecular deign and placement of functional groups of amino alcohol compounds, that there is a structure-performance relationship between amino alcohols and CO_2. Since DEAB is also considered an amino alcohol compound, this might be one of the reasons why DEAB is reactive with CO_2 and reacts faster than a conventional tertiary amine such as MDEA. Therefore, it can be summarized that the CO_2 absorption reaction with DEAB is faster than that with MDEA and is also comparable with that of AMP and DEA but slower than that of MEA and PZ, respectively.

The experimental enhancement factors, which represent the ratio of the absorption rate of CO_2 into a reacting liquid to that of if there were no reaction, for CO_2 absorption in aqueous DEAB solutions at 308 K over a DEAB concentration range of 1 M to 2 M are shown in Table 6.2. The results show that the enhancement factor increases as DEAB concentration increases over the range of 1 M to 2 M because there are more DEAB molecules, which are chemically reactive with CO_2, introduced to the solutions.

In addition, the reaction rate/kinetics model developed in this study is also able to predict the CO_2 absorption rate in aqueous DEAB solutions at various temperatures,

initial DEAB concentrations, initial CO_2 loadings, and contact times. The CO_2 absorption rate can be obtained numerically by integrating the local CO_2 absorption rate per unit area (N) over contact time τ as shown in Equation 6.34. $\left(\frac{\partial C_1}{\partial t}\right)_{x=0}$ can be acquired as the results of solving partial differential-nonlinear algebraic equations of Equations 6.12, 6.13, 6.15, and 6.19-6.22 by COMSOL software. Also, the integration over contact time τ was done using the integration function in the COMSOL software. The predicted CO_2 absorption rates compared with the experimental values are shown in Figure 6.3 as a parity chart with an AAD of 6.5%, which is favourably acceptable. Thus, it can be said that the numerical comprehensive reaction rate/kinetics model for CO_2 absorption into aqueous DEAB solution developed in this work is adequate and provides accurate results.

Table 6.1 Forward reaction rate constant (k) of MDEA, AMP, DEA, DEAB, MEA, and PZ at 313 K

	k (m^3/kmol s)		References
k_{MDEA}	12.9	13.0	Rinker et al. (1995) and Kierzkowska and Chacuk (2010)
k_{AMP}	1,276	1,393	Saha and Bandyopadhyay (1995) and Choi et al. (2007)
k_{DEA}	1,375	1,520	Zhang et al. (2002) and Blanc and Demarais (1984)
k_{DEAB}	1,440		This work
k_{MEA}	10,090	10,681	Hagewiesche et al. (1995) and Edali et al. (2007)
k_{PZ}	93,230	103,000	Dang and Rochelle (2003) and Zhang et al. (2001)

Table 6.2 Enhancement factor of 1 M, 1.5 M, and 2 M DEAB at 308 K

Concentration of DEAB (M)	Enhancement factor
1.0	3.81
1.5	4.47
2.0	5.07

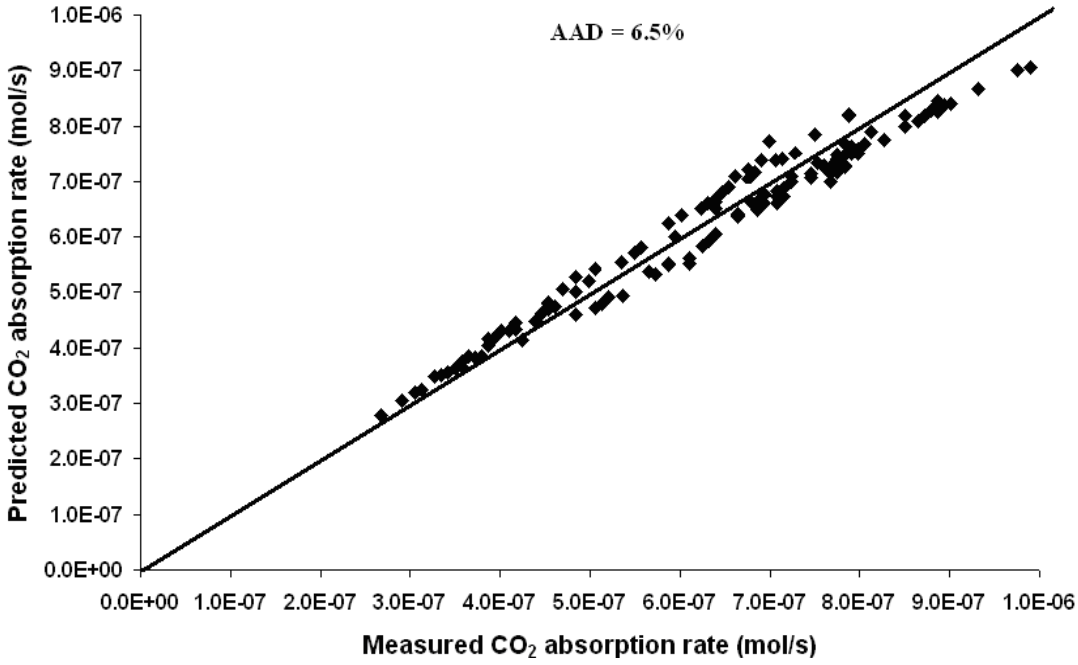

Figure 6.3 Parity chart comparing experimental and predicted CO_2 absorption rate in aqueous DEAB solution.

6.4 Summaries

1. A comprehensive numerically solved reaction rate/kinetics model for CO_2 absorption into aqueous DEAB solutions was successfully developed. The rate constant for CO_2 absorption reaction with DEAB, k_{DEAB}, was obtained over a temperature range of 298 K to 318 K is $k_{DEAB} = \left(4.01 \times 10^{13}\right) \exp\left(-\frac{7527.7}{T}\right)$

2. Regarding the reaction rate constant (k), it can be summarized that the CO_2 absorption reaction with DEAB is faster than that with MDEA and is comparable with that with AMP and DEA but slower than that with MEA and PZ, respectively.

3. The predicted CO_2 absorption rates obtained for the developed reaction rate/kinetics model are fit favourably with the experimental results with an AAD of 6.5%.

6.5 References

1. Aboudheir, A.; Tontiwachwuthikul, P.; Chakma, A.; Idem, R. Kinetics of reactive absorption of carbon dioxide in high CO_2-loaded concentrated aqueous MEA solutions. Chem. Eng. Sci. 2003, 58, 5195-5210.

2. Aboudheir, A.; Tontiwachwuthikul, P.; Chakma, A.; Idem, R. Novel design for the nozzle of a laminar jet absorber. Ind. Eng. Chem. Res. 2004, 43, 2568-2574.

3. Al-Ghawas, H. A.; Ruiz-Ibanez, G.; Sandall, O. C. Absorption of carbonyl sulphide in aqueous methyldiethanolamine. Chem. Eng. Sci. 1989, 44, 631-639.

4. Astarita, G.; Savage, D.; Bisio, A. Gas treating with chemical solvents; Wiley, New York, 1983.

5. Austgen, D.M.; Rochelle, G.T.; Chen, C.C. Model of vapor-liquid equilibria for aqueous acid gas-alkanolamine system. 2. Representation of H_2S and CO_2 solubility in aqueous MDEA and CO_2 solubility in aqueous mixtures of MDEA with MEA or DEA. Ind. Eng. Chem. Res. 1991, 30, 543-555.

6. Blanc, C.; Demarais, G. The reaction rate of CO_2 with diethanolamine. Int. Chem. Eng. 1984, 24, 43-51.

7. Choi, W.J.; Cho, K.C.; Lee, S.S.; Shim, J.G.; Hwang, H.R., Park, S.W.; Oh, K.J. Removal of carbon dioxide by absorption into blended amines: kinetics of absorption into aqueous AMP/HMDA, AMP/MDEA, and AMP/piperazine solutions. Green Chem. 2007, 9, 594-598.

8. Dang, H.; Rochelle, G.T. CO_2 absorption rate and solubility on monoethanolamine/piperazine/water. Seperation Science and Technology 2003, 38, 337-357.

9. Edali, M. Kinetics, modeling, and simulation of carbon dioxide absorption into mixed aqueous loaded solution blendes of methyldiethanolamine with monoethanolamine and with piperazine; Ph.D. thesis, University of Regina, Regina, Canada, 2010.

10. Edali, M.; Aboudheir, A.; Idem, R. Kinetics of carbon dioxide absorption into mixed aqueous solutions of MDEA and MEA using laminar jet apparatus and numerically solved absorption-rate/kinetic model. The COMSOL Conference, Boston, 2007.

11. Edali, M.; Aboudheir, A.; Idem, R. Kinetics of carbon dioxide absorption into mixed aqueous solutions of MDEA and MEA using a laminar jet apparatus and a numerically solved 2D absorption rate/kinetics model. International Journal of Greenhouse Gas Control 2009, 3, 550-560.

12. Edali, M.; Aboudheir, A.; Idem, R. 1D and 2D absorption-rate/kinetic modeling and simulation of carbon dioxide absorption into mixed aqueous solutions of MDEA and PZ in a laminar jet apparatus. International Journal of Greenhouse Gas Control 2010, 4, 143-151.

13. Hagewiesche, D.P.; Ashour, S.S.; Al-Ghawas, H.A.; Sandall, O.C. Absorption of carbon dioxide into aqueous blends of monoethanolamine and N-methyldiethanolamine. Chem Eng. Sci. 1995, 50, 1071-1079.

14. Hikita, H.; Ishikawa, H.; Uke, K.; Murakami, T. Diffusivities of mono-, di-, and tri-ethanolamine in aqueous solutions. J. Chem. Eng. Data 1980, 25, 324-325.

15. Idem, R.; Edali, M.; Aboudheir, A. Kinetics, modeling, and simulation of the experimental kinetics data of carbon dioxide absorption into mixed aqueous solutions of MDEA and PZ using laminar jet apparatus with a numerically solved absorption-rate/kinetic model. Energy procedia 2009, 1, 1343-1350.

16. Kierzkowska, P.H.; Chacuk, A. Kinetics of carbon dioxide absorption into aqueous MDEA solutions. Ecological Chemistry and Engineering S 2010, 17, 463-475.

17. Kohl, A.L.; Nielsen, R.B. Gas Purification: 5th Edition; Gulf Publishing Company: Houston, Texas, USA, 1997.

18. Maneeintr, K.; Idem, R. O.; Tontiwachwuthikul, P.; Wee, A. G. H. Synthesis, solubilities, and cyclic capacity of amino alcohols for CO_2 Capture from flue gas streams. Energy procedia 2009, 1, 1327-1334.

19. Pinsent, B.R.W.; Pearson, L.; Roughton, F.J.W. The kinetics of combination of carbon dioxide with hydroxide ions. Trans. Faraday Soc. 1956, 52, 1512-1520.

20. Rinker, E.B.; Ashour, S.S.; Sandall, O.C. Kinetics and modeling of carbon dioxide absorption into aqueous solutions of N-methyldiethanolamine. Chemical Engineering Science 1995, 50, 755-768.

21. Rochelle, G.T. Research needs for acids gas kinetics and equilibria in alkanolamine systems. 70th GPA annual convention 1991, 66-82.

22. Saha, A.K.; Bandyopadhyay, S.S. Kinetics of absorption of CO_2 into aqueous solutions of 2-amino-2-methyl-1-propanol. Chemical Engineering Science 1995, 50, 3587-3598.

23. Sartori, G.; Savage, D.W. Sterically hindered amines for CO_2 removal from gases. Ind. Eng. Chem. Fundam. 1983, 22, 239-249.

24. Tontiwachwuthikul, P.; Wee, A. G. H.; Idem, R. O.; Maneeintr, K.; Fan, G. J.; Veawab, A.; Aroonwilas, A.; Chakma, A. Method for capturing carbon dioxide from gas streams. US Patent Application. US Patent Application, No. US 2008/0050296 A1, 2008.

25. Zhang, X.; Zhang, C.F.; Qin, S.J.; Zheng, Z.S. A kinetics study on the absorption of carbon dioxide into a mixed aqueous solution of methyldiethanolamine and piperazine. Ind. Eng. Chem. Res. 2001, 40, 3785-3791.

26. Zhang, X.; Zhang, C.F.; Liu, Y. Kinetics of absorption of CO_2 into aqueous solution of MDEA blended with DEA. Ind. Eng. Chem. Res. 2002, 41, 1135-1141.

Chapter 7 Solubility and Diffusivity of N_2O and Equilibrium Solubility of CO_2 in Aqueous Solutions of Blended Monoethanolamine and 4-(Diethylamino)-2-Butanol

7.1 Introduction

Monoethanolamine (MEA), diethanolamine (DEA), methyldiethanolamine (MDEA) have been industrially used for capturing carbon dioxide (CO_2) for a number of years (Kohl and Nielsen, 1997). Primary and secondary amines, which are MEA and DEA, respectively, are reactive with CO_2. However, limitations of CO_2 absorption capacity and high regeneration energy (associated with carbamate formation) are observed. On the other hand, tertiary amines, such as MDEA, have lower reactivity but higher CO_2 absorption capacity and lower regeneration energy (due to carbonate and bicarbonate formation). It has been found that the absorption of CO_2 using blended amines have several advantages over the use of single amines. Mixing primary or secondary amines with tertiary amines can enhance the CO_2 absorption rate and reduce the energy requirement for the regeneration process (Chakravarty et al., 1985; Kohl and Nielsen, 1997). Example of blended of primary or secondary amines with tertiary amine are MEA-MDEA and DEA-MDEA. However, MEA has been selected to be mixed with MDEA rather than DEA due to the higher reactivity of MEA over DEA.

Recently, it has been observed by various researchers (Chapters 5 and 6; Tontiwachwuthikul et al., 2008; Manneintr et al., 2009) that 4-diethylamino-2-butanol (DEAB) has higher absorption capacity and lower regeneration energy compared with the conventional amines such as MDEA, DEA, and MEA. Moreover, the CO_2 absorption

reaction in DEAB has been found to be faster than that in MDEA, as well as comparable with that in 2-amino-2-methyl-1-propanol (AMP) and DEA but lower than that in MEA and piperazine (PZ), respectively. Regarding these outstanding properties, DEAB is now being considered to be mixed with MEA in order to enhance the reaction rate of DEAB and counter the high energy requirement of MEA. Therefore, this blended MEA-DEAB solvent required preliminary study for its potential as a promising alternative solvent for capturing CO_2 in terms of CO_2 absorption capacity, CO_2 absorption rate (reaction kinetics data), and mass transfer coefficient.

In order to develop the kinetics model for CO_2 absorption, physical solubility and physical diffusivity of CO_2 in amine solutions at various temperatures and amine concentrations are required. It is generally understood that CO_2 reacts chemically with amine, so physical solubility and physical diffusivity of CO_2 into amine solutions cannot be measured directly. Thus, the measurements of nitrous oxide (N_2O) solubility and diffusivity through the N_2O analogy can be used to determine the solubility and the diffusivity of CO_2 in aqueous amine solutions (Clarke, 1963; Sada et al., 1977 and 1978). This is due to the similarity of molecular weight, chemical configuration, volume, and electronic structure between CO_2 and N_2O (Liu et al., 1999). Not only the kinetics model of CO_2 absorption, but also the CO_2 absorption capacity is important for designing a CO_2 treating plant. Generally, CO_2 absorption capacity is considered in terms of equilibrium CO_2 solubility or CO_2 loading in mol CO_2 per mol amine.

The MEA concentration used industrially in the CO_2 treating process is found to be in a range of 5 M - 7 M, especially 5 M. Therefore, the concentration of the blended MEA-DEAB solutions was limited to be in the range of 5 M to 7 M for this study. The

MEA concentration in the solution was kept constant at 5 M. However, the DEAB concentration was varied from 0.25 M, 0.5 M. 1.0 M, 1.5 M, and 2 M. Thus, the total amine concentrations are found to be 5.25 M to 7 M, respectively.

In this chapter, the experimental results of the N_2O solubility and N_2O diffusivity in aqueous solutions of blended MEA-DEAB are reported over ranges of temperatures and amine concentrations. These experimental data were then used to develop predictive correlations for the N_2O solubility and N_2O diffusivity in aqueous solutions of blended MEA-DEAB. In addition, the equilibrium solubility of CO_2 was measured and predicted over ranges of temperatures, amine concentrations, and CO_2 partial pressures.

7.2 Theory: calculating equilibrium solubility of CO_2 in aqueous solutions of blended MEA-DEAB

The chemical equilibrium for a CO_2/MEA-DEAB aqueous system is governed by the following equations:

$$RR_2'N + H^+ \overset{K_1}{\longleftrightarrow} RR_2'NH^+ \tag{7.1}$$

$$CO_2 + RR_2'N + H_2O \overset{K_2}{\longleftrightarrow} RR_2'NH^+ + HCO_3^- \tag{7.2}$$

$$R''NH_2 + H^+ \overset{K_3}{\longleftrightarrow} R''NH_3^+ \tag{7.3}$$

$$R''NH_2 + CO_2 \overset{K_4}{\longleftrightarrow} R''NHCOO^- + H^+ \tag{7.4}$$

$$H_2O + CO_2 \overset{K_5}{\longleftrightarrow} H^+ + HCO_3^- \tag{7.5}$$

$$CO_2 + OH^- \overset{K_6}{\longleftrightarrow} HCO_3^- \tag{7.6}$$

$$HCO_3^- \overset{K_7}{\longleftrightarrow} H^+ + CO_3^{2-} \tag{7.7}$$

$$H_2O \overset{K_8}{\longleftrightarrow} H^+ + OH^- \tag{7.8}$$

$RR_2^{/}N$ represents DEAB where R is $(CH_2)_2CH(CH_3)OH$ and R' is CH_2CH_3. $R''NH_2$ represents MEA where R'' is $(CH_2)_2OH$. K_i is the chemical equilibrium constant for reaction i. MEA is a primary amine, which reacts directly with CO_2 to form carbamate, as shown in Equation 7.4. DEAB is considered to be a tertiary amine, since it has 3 carbon atoms attached to the nitrogen atom. In this case, DEAB does not react directly with CO_2, but it acts as a base that catalyzes the hydration of CO_2 (Kohl and Nielsen, 1997), as presented in Equation 7.2.

The expressions for the chemical equilibrium constants can be described as:

$$K_1 = \frac{\left[RR_2^{/}NH^+\right]}{\left[H^+\right]\left[RR_2^{/}N\right]} = \frac{K_2}{K_5} \tag{7.9}$$

$$K_2 = \frac{\left[RR_2^{/}NH^+\right]\left[HCO_3^-\right]}{\left[CO_2\right]\left[RR_2^{/}N\right]} \tag{7.10}$$

$$K_3 = \frac{\left[R''NH_3^+\right]}{\left[R''NH_2\right]\left[H^+\right]} \tag{7.11}$$

$$K_4 = \frac{\left[R''NHCOO^-\right]\left[H^+\right]}{\left[R''NH_2\right]\left[CO_2\right]} \tag{7.12}$$

$$K_5 = \frac{\left[H^+\right]\left[HCO_3^-\right]}{\left[CO_2\right]} \tag{7.13}$$

$$K_6 = \frac{\left[HCO_3^-\right]}{\left[CO_2\right]\left[OH^-\right]} \tag{7.14}$$

$$K_7 = \frac{\left[H^+\right]\left[CO_3^{2-}\right]}{\left[HCO_3^-\right]} = \frac{K_2}{K_1K_8} \tag{7.15}$$

$$K_8 = \left[H^+\right]\left[OH^-\right] \tag{7.16}$$

Based on Equations 7.9-7.16, it can be seen that not all of the chemical equilibrium constants are independent. Only 6 chemical equilibrium constants ($K_2 - K_6$, and K_8) are independent. The remaining two (K_1 and K_7) can be obtained by the combination of independent chemical equilibrium constants, as shown in Equations 7.9 and 7.15. Also, water concentration is considered to be constant due to the fact that the water concentration is much higher than the amine concentration.

The total DEAB balance, total MEA balance, total carbon balance, and the charge balance according to the chemical equilibrium equations (Equations 7.1-7.8) can be expressed as:

$$\left[RR_2^{/}N\right]_0 = \left[RR_2^{/}NH^+\right] + \left[RR_2^{/}N\right] \tag{7.17}$$

$$\left[R''NH_2\right]_0 = \left[R''NH_3^+\right] + \left[R''NH_2\right] + \left[R''NHCOO^-\right] \tag{7.18}$$

$$\alpha\left(\left[RR_2^{/}N\right]_0 + \left[R''NH_2\right]_0\right) = \left[CO_2\right] + \left[HCO_3^-\right] + \left[CO_3^{2-}\right] + \left[R''NHCOO^-\right] \tag{7.19}$$

$$\left[RR_2^{/}NH^+\right] + \left[R''NH_3^+\right] + \left[H^+\right] = \left[R''NHCOO^-\right] + \left[OH^-\right] + \left[HCO_3^-\right] + 2\left[CO_3^{2-}\right] \tag{7.20}$$

where $\left[RR_2^{/}N\right]_0$, $\left[R''NH_2\right]_0$, and α are the initial DEAB concentration, initial MEA concentration, and CO_2 loading (or equilibrium solubility of CO_2), respectively.

In addition, the physical solubility of CO_2 in aqueous solutions of blended MEA-DEAB, which will also be determined in this chapter, can be related by Henry's law relationship as:

$$P_{CO_2} = He_{CO_2}\left[CO_2\right] \tag{7.21}$$

where P_{CO_2} and He_{CO_2} represent partial pressure of CO_2 in gas phase and Henry's constant of CO_2 in aqueous solutions of blended MEA-DEAB, respectively.

A solution of the 11 coupled nonlinear algebraic equations (i.e. Equations 7.10-7.14 and 7.16-7.21), will yield the values of the 11 unknowns, which are α, $\left[RR_2'N\right]$, $\left[R''NH_2\right]$, $\left[H^+\right]$, $\left[RR_2'NH^+\right]$, $\left[RR_2'NH^+\right]$, $\left[R''NHCOO^-\right]$, $\left[HCO_3^-\right]$, $\left[CO_2\right]$, $\left[OH^-\right]$, and $\left[CO_3^{2-}\right]$. On the other hand, $\left[RR_2'N\right]_0$, $\left[R''NH_2\right]_0$, and P_{CO_2} can be obtained from an experiment involving the measurement of equilibrium solubility of CO_2, as mentioned in Section 3.5. He_{CO_2} will also be determined in this chapter. The chemical equilibrium constant K_2 can be calculated by the correlation given in Chapter 5 (Equation 5.19) and $K_3 - K_6$, and K_8 can be predicted by the correlations mentioned in Austgen et al. (1991).

The simultaneous solution of the 11 coupled nonlinear algebraic equations (i.e. Equations 7.10-7.14 and 7.16-7.21) was achieved with the use of a finite element method (FEM) based on COMSOL 4.1 software with 0D stationary solver mode. In this case, an initial guess for each unknown is required. After the software was operated with the first set of initial guesses, values of the unknowns were obtained. Then, these new values were subsequently used as the initial guesses for solving the 11 unknowns. This process was repeated until the percentage deviation of the results of each unknown for successive attempts was less than 0.01%. The calculated results of the equilibrium solubility of CO_2 (α) were then compared with the experimental values in terms of absolute average deviation (AAD).

7.3 Results and Discussion

7.3.1 N_2O solubility in aqueous solutions of blended MEA-DEAB

The N_2O solubility measurements of aqueous solutions of blended MEA-DEAB were conducted over a temperature range of 298 K to 343 K and concentration range of 5 M MEA+0.25 M DEAB to 5 M MEA+2 M DEAB. The results are shown in Table 7.1 and plotted in Figure 7.1. It can be observed that the N_2O solubility increases as temperature increases and decreases as a DEAB concentration in the blended solution increases. In the present study, the N_2O solubility or He_{N_2O} is defined as a ratio of partial pressure of N_2O at equilibrium (P_{N_2O}) and concentration of dissolved N_2O at equilibrium (C_{N_2O}), as shown in Equation 3.6. As temperature increases, the concentration of dissolved N_2O (C_{N_2O}) tends to decrease, which leads to an increasing of N_2O solubility (He_{N_2O}), as can be seen in Figure 7.1 and Table 7.1. However, the N_2O solubility in aqueous solutions of blended MEA-DEAB (He_{N_2O}) decreases as DEAB concentration in the blended solution increases. This could be because of the effect of solution density. It was suggested by Hartono et al. (2008) that the N_2O solubility relates with the solution density. At low density, there are more free spaces for N_2O to be dissolved, which means that the C_{N_2O} would be high (in other words, N_2O solubility or He_{N_2O} would be low at low solution density). In the case of blended MEA-DEAB aqueous solution, it was found by Naami et al. (in press) that the solution density decreases as DEAB concentration in the blended solution increases. Therefore, the N_2O solubility in aqueous solutions of blended MEA-DEAB (He_{N_2O}) decreases as DEAB concentration in the blended solution increases, as shown in Figure 7.1 and Table 7.1.

In order to establish the predictive correlation for N_2O solubility in aqueous solutions of blended MEA-DEAB at various concentrations and temperatures, several predictive models have been applied, such as the semiempirical model (Wang et al., 1992), polynomial model (Versteeg and van Swaaij, 1988), and Redlich-Kister equation (Redlich and Kister, 1948). These three different models were then used to establish the predictive correlations for the N_2O solubility in aqueous solutions of blended MEA-DEAB.

7.3.1.1 Semiempirical model

Wang et al. (1992) reported that the semiempirical model provides good predictive results for N_2O solubility in aqueous amine solutions for both single amine (MEA, DEA, MDEA, di-isopropanolamine (DIPA), and AMP) and blended amine systems (AMP-MDEA, AMP-tetramethylene sulphone (TMS), and DEA-ethylene glycol (EG)). The semiempirical model can be written as:

$$\ln He_{N_2O-Solution} = \phi_{H_2O}\phi_{MEA}\left(k_1 + k_2 t + k_3 t^2 + k_4 \phi_{H_2O}\right) + \phi_{MEA}\phi_{DEAB}\left(k_5 + k_6 t + k_7 t^2 + k_8 \phi_{H_2O}\right)$$

$$+ \phi_{H_2O}\phi_{DEAB}\left(k_9 + k_{10} t + k_{11} t^2 + k_{12} \phi_{H_2O}\right) + \phi_{H_2O}\phi_{MEA}\phi_{DEAB} k_{13} + \phi_{MEA} \ln He_{N_2O-MEA}$$

$$+ \phi_{H_2O} \ln He_{N_2O-H_2O} + \phi_{DEAB} \ln He_{N_2O-DEAB} \qquad (7.22)$$

where ϕ_i is the volume fraction of species i, t is temperature in degrees centigrade, and $He_{N_2O-Solution}$, $He_{N_2O-H_2O}$, He_{N_2O-MEA}, and $He_{N_2O-DEAB}$ are N_2O solubility in aqueous solutions of blended MEA-DEAB, water, MEA, and DEAB, respectively. The $He_{N_2O-DEAB}$

is given in Equation 4.5 (in Chapter 4) and the $He_{N_2O-H_2O}$ and He_{N_2O-MEA} are given in the work of Versteeg and van Swaaij (1988) and Wang et al. (1992), respectively.

The experimental data for N_2O solubility in aqueous solutions of blended MEA-DEAB, which are shown in Table 7.1, were used to correlate with the semiempirical model of Equation 7.22 using a non-linear regression package (NLREG program). The unknown parameters (k_1-k_{13}) were determined and are listed in Table 7.2. The predicted results using the semiempirical model are plotted and compared with the experimental results in Figure 7.1. It can be observed that the predicted results are in good agreement with the experimental results with an AAD of 2.7%.

Table 7.1 Solubility of N_2O in aqueous solutions of blended MEA-DEAB

Concentration (M)	Total amine concentration (M)	N_2O solubility (10^3 kPa m^3/kmol)				
		298 K	313 K	323 K	333 K	343 K
5 M MEA+0.25 M DEAB	5.25	6.21	7.71	9.16	9.47	11.17
5 M MEA+0.5 M DEAB	5.5	6.37	7.40	8.26	8.80	9.36
5 M MEA+0.8 M DEAB	5.8	6.19	7.32	7.96	8.47	8.88
5 M MEA+1 M DEAB	6	5.79	6.75	7.45	7.79	8.06
5 M MEA+1.5 M DEAB	6.5	5.48	5.74	5.86	5.88	6.47
5 M MEA+2 M DEAB	7	5.24	5.41	5.48	5.60	6.15

Table 7.2 Parameters for the semiempirical model in Equation 7.22

Parameters	Value	Parameters	Value
k1	706.64	k8	-1.3275×10^3
k2	-2.3×10^{-2}	k9	-651.2
k3	2.7×10^{-5}	k10	3.45×10^{-1}
k4	-1×10^3	k11	-4.44×10^{-3}
k5	968.10	k12	-28
k6	-8.07×10^{-1}	k13	-163.6
k7	7.9×10^{-3}		

7.3.1.2 Polynomial model

The polynomial model is an empirical model that was applied for predicting the N_2O solubility in aqueous solution of dimethylmonoethanolamine (DMMEA), DEA, triethanolamine (TEA), monoisopropanolamine (MIPA), and DIPA, as presented by Versteeg and van Swaaij (1988). However, this is the first time that the polynomial model was applied to correlate the N_2O solubility in aqueous solution of blended amine. The polynomial model can be defined as:

$$He_{N_2O-Solution} = A_0 + A_1C + A_2C^2 + A_3C^3 \qquad (7.23)$$

where C is total molar amine concentration.

The unknown parameters (A_0-A_3) for a specific temperature can be determined using the regression analysis via the NLREG program. The parameters are shown in Table 7.3.

The predicted N_2O solubility results using the polynomial model are plotted and compared with the experimental results as shown in Figure 7.1 where it can be seen that the predicted results fit well with the experimental results with an AAD of 2.5%.

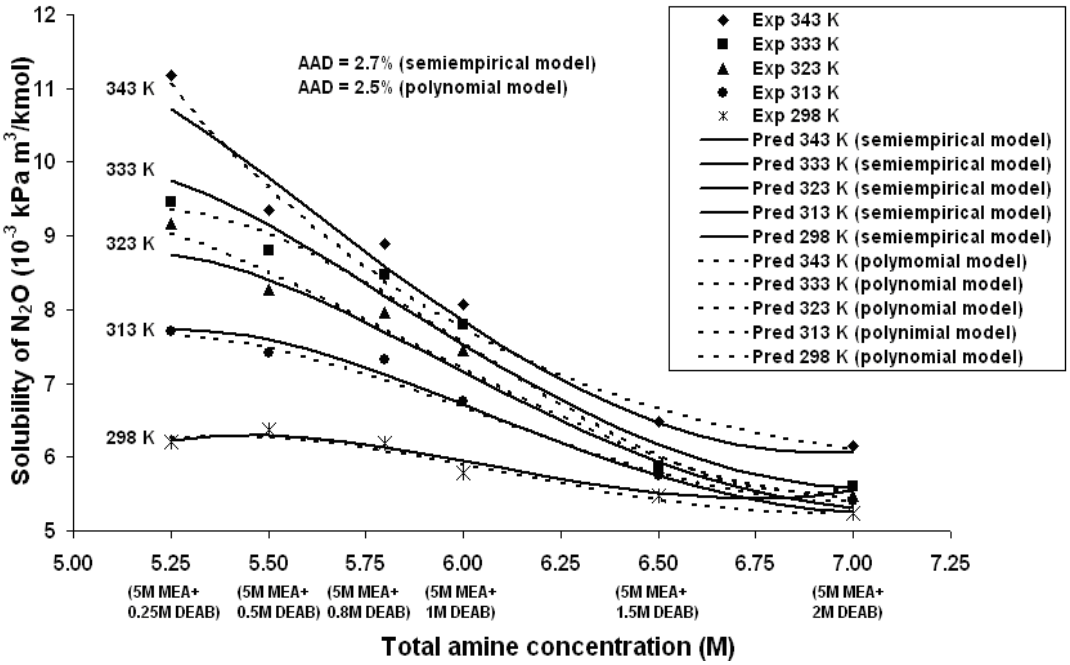

Figure 7.1 Solubility of N_2O in aqueous solution of blended MEA-DEAB; solid lines are calculated from the semiempirical model in Equation 7.22 and dashed lines are calculated from polynomial model in Equation 7.23.

7.3.1.3 Redlich-Kister equation

The Redlich-Kister equation was proposed by Redlich and Kister (1948). It has been widely used to correlate physical properties for binary and ternary solutions. In the present study, the Redlich-Kister equation was used to correlate the N_2O solubility in aqueous solutions of blended MEA-DEAB. The Redlich-Kister equation can be written as:

$$\ln He_{N_2O-Solution} = x_{H_2O} \ln He_{N_2O-H_2O} + x_{MEA} \ln He_{N_2O-MEA} + x_{DEAB} \ln He_{N_2O-DEAB}$$
$$+ \left[x_{H_2O} x_{MEA} \left(B_0 + B_1 (x_{H_2O} - x_{MEA})\right)\right] + \left[x_{H_2O} x_{DEAB} \left(B_2 + B_3 (x_{H_2O} - x_{DEAB})\right)\right] \quad (7.24)$$
$$+ \left[x_{MEA} x_{DEAB} \left(B_4 + B_5 (x_{MEA} - x_{DEAB})\right)\right]$$

where x_i is mole fraction of species i.

At a specific temperature, the unknown parameters (i.e. B_0-B_5) can be determined using regression analysis via NLREG program. The regression results are shown in Table 7.4.

The predicted N_2O solubility results calculated from the Redlich-Kister equation do not correlate well with the experimental results, as can be seen in Figure 7.2, which gives an AAD of 138.2%.

Table 7.3 Parameters for the polynomial model of Equation 7.23

Temperature (K)	A_0	A_1	A_2	A_3
298	-1.2532×10^5	6.614×10^4	-1.0950×10^4	5.9453×10^2
313	-1.5296×10^5	8.2633×10^4	-1.3928×10^4	7.6496×10^2
323	-1.1666×10^5	6.8582×10^4	-1.21×10^4	6.847×10^2
333	-3.203×10^5	1.6975×10^5	-2.8694×10^4	1.5849×10^3
343	1.6871×10^5	-6.4736×10^4	8.651×10^3	-3.888×10^2

Table 7.4 Parameters for the Redlich-Kister equation of Equation 7.24

Temperature (K)	B_0	B_1	B_2	B_3	B_4	B_5
298	48.56	-46.36	-768.37	672.1	-1279.9	2.25×10^4
313	30.21	-24.16	-615.63	569	1914.99	-9359.34
323	4.62	9.19	-670.51	574.19	-1413.32	2.3410^4
333	-26.41	46.89	-964.1	865.66	165.1	1.35×10^4
343	8.12	3.28	-58.64	30.14	585.34	-4141

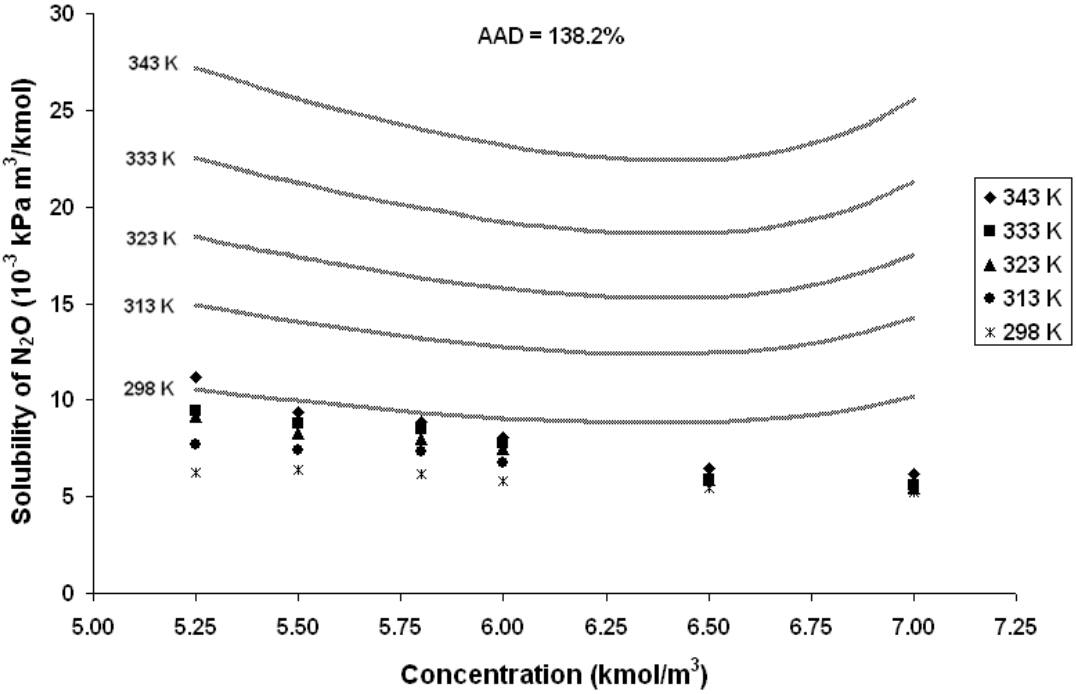

Figure 7.2 Solubility of N_2O in aqueous solution of blended MEA-DEAB; solids lines are calculated from the Redlich-Kister equation in Equation 7.24.

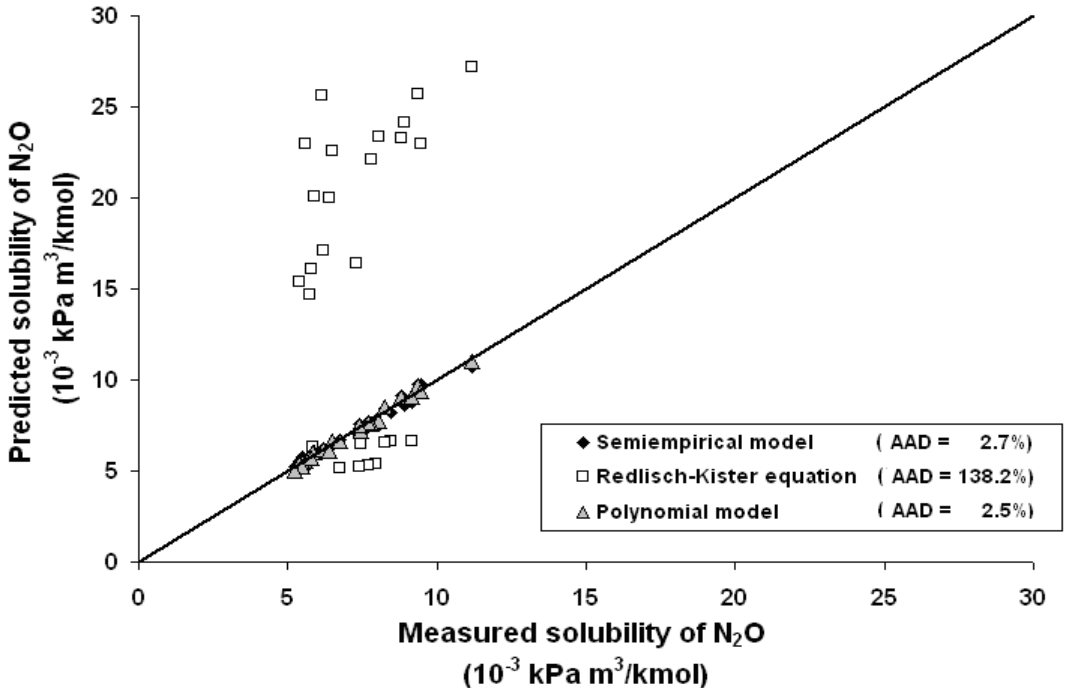

Figure 7.3 Parity chart comparing experimental and predicted results of N_2O solubility in aqueous solutions of blended MEA-DEAB.

Several predictive models (the semiempirical model, polynomial model, and Redlich-Kister equation) for the N_2O solubility in aqueous solutions of blended MEA-DEAB were developed, as shown in Equations 7.22, 7.23, and 7.24, respectively. By comparing the predicted results with the experimental results, as shown in Figure 7.3, it can be observed that the polynomial model provided the best predicted results among the three at an AAD of 2.5%. However, the semiempirical model also provided good predicted results with only small difference compared with the polynomial model at an AAD of 2.7%. It was also found that the Redlich-Kister equation is the only model that does not correlate well with the experimental results with an AAD of 138.2%.

The Redlich-Kister equation considers the N_2O solubility in aqueous solutions of blended MEA-DEAB at a specific temperature in terms of mole fraction of each species in the solution and N_2O solubility in the individual species in the solution, which are water, MEA, and DEAB, as shown in Equation 7.24. Theoretically, the Redlich-Kister should have correlated well with the experimental results. However, in the present study, the Redlich-Kister equation can only be used as a first order Redlich-Kister equation (since n = 1 for $(x_i - x_i^{/})^n$, as can be seen in Equation 7.24) due to the limitation of experimental data. Since the first order Redlich-Kister equation was applied, a large deviation of the predicted results from the experimental results (an AAD of 138.2%) was observed, as shown in Figures 7.2 and 7.3. Better predicted results for N_2O solubility could have been expected if a higher order Redich-Kister equation were applied.

Similar to the Redlich-Kister equation, the polynomial model also correlates N_2O solubility at a specific temperature. However, the polynomial model considers N_2O solubility to be a polynomial function with respect to total amine concentration (including

both MEA and DEAB), as shown in Equation 7.23. Figures 7.1 and 7.3 show that the predicted results obtained from the polynomial model provide the best fit with the experimental results with an AAD of 2.5%. However, the polynomial model, which is the empirical model, does not represent the blended amine system well, since the polynomial model considers N_2O solubility to be a function of total amine concentration instead of individual amine concentration (the semiempirical model and Redlich-Kister equation consider the N_2O solubility as a function of individual amine concentration). Therefore, the polynomial model might not be adequate for correlating the N_2O solubility in aqueous solutions of blended MEA-DEAB.

The semiempirical model correlates N_2O solubility with volume fraction of each species in the solution, temperature, and also N_2O solubility in the individual species in the solution, which are water, MEA, and DEAB, as shown in Equation 7.22. It was found that the predicted results obtained from the semiempirical model fit well with the experimental results with an AAD of 2.7%, which is comparable with that obtained from the polynomial model. Moreover, the semiempirical model represents the blended amine system better than the polynomial model since it takes both MEA and DEAB concentrations in terms of volume fractions into account. Thus, the semiempirical model is recommended for use due to its good representation of blended aqueous amine solutions and because it is relatively as accurate as the polynomial model.

7.3.2 N_2O diffusivity in aqueous solutions of blended MEA-DEAB

The N_2O diffusivity measurements of aqueous solutions of blended MEA-DEAB were determined using a laminar jet absorber over the temperature range of 298 K to 323

K and concentration range of 5 M MEA+0.25 M DEAB to 5 M MEA+2 M DEAB. The experimental results of N_2O diffusivity of aqueous solutions of blended MEA-DEAB are shown in Table 7.5 and plotted in Figure 7.4. The results show that the N_2O diffusivity increases as temperature increases but decreases as amine concentration increases. It is generally accepted that both temperature and viscosity play an important role in N_2O diffusivity (Li and Lee, 1996). As temperature increases, the N_2O molecule gains more energy, which leads to higher diffusivity of N_2O. For viscosity, there will be a higher resistivity of N_2O to diffusing into the high viscosity solution than the low viscosity solution; thus, the N_2O diffusivity decreases as viscosity increases. In the case of aqueous solutions of blended MEA-DEAB, it was observed by Naami et al. (in press) that the viscosity of the blended solutions increases as DEAB concentration in the blended solution increases but decreases as temperature increases. Therefore, the N_2O diffusivity in aqueous solutions of blended MEA-DEAB decreases as DEAB concentration in the blended solution increases and increases as temperature increases, as can be found in Figure 7.4 and Table 7.5.

Two predictive models, the semiempirical model (Li and Lee, 1996) and modified Stokes-Einstein model (Versteeg and van Swaaij, 1988; Xu et al., 1996), were applied in order to establish a predictive correlation for the N_2O diffusivity in aqueous solutions of blended MEA-DEAB at various temperatures and amine concentrations.

7.3.2.1 Semiempirical model

The semiempirical model is widely used to correlate N_2O diffusivity in aqueous amine solutions for both single and blended amine systems, such as MEA, DEA, DIPA,

MDEA, TEA, AMP, blended DEA-AMP, and blended DEA-MDEA (Li and Lee, 1996; Ko et al., 2001). The semiempirical model can be defined as:

$$D_{N_2O} = \left(a + bC_{MEA} + cC_{MEA}^2 + dC_{DEAB} + eC_{DEAB}^2 + fC_{MEA}C_{DEAB}\right)\exp\left(\frac{g + hC_{MEA} + iC_{DEAB}}{T}\right) \tag{7.25}$$

where C_{MEA} and C_{DEAB} are the molar concentration of MEA and DEAB, respectively, and T is temperature in Kelvin.

The parameters of a to i were determined using the NLREG package. Therefore, the semiempirical model for the N_2O diffusivity in aqueous solutions of blended MEA-DEAB can be written as:

$$D_{N_2O} = [\left(-3.57x10^{-4}\right) + \left(2.34x10^{-4}C_{MEA}\right) + \left(-2.94x10^{-5}C_{MEA}^2\right) + \left(-1x10^{-4}C_{DEAB}\right)$$

$$+ \left(-2.412x10^{-4}C_{DEAB}^2\right) + \left(1.38x10^{-4}C_{MEA}C_{DEAB}\right)] \tag{7.26}$$

$$\exp\left(\frac{\left(-1.952x10^{3}\right) + \left(-4.38x10^{2}C_{MEA}\right) + \left(-5.06x10^{2}\right)}{T}\right)$$

The predicted results obtained from the semiempirical model of Equation 7.26 are plotted as solid lines in Figure 7.4. It can be seen from Figures 7.4 and 7.5 that the semiempirical model provides good predicted results compared with the experimental results with an AAD of 3.6%.

7.3.2.2 Modified Stokes-Einstein model

As mentioned above, the solution viscosity plays an important role in N_2O diffusivity. Therefore, the modified Stokes-Einstein model considers the N_2O diffusivity

to be a function of viscosity $(\eta; Pa \cdot s)$. Versteeg and van Swaaij (1988) applied the modified Stokes-Einstein model for various amines, such as MEA, DEA, TEA, MDEA, monoisopropanolamine (MIPA), and DIPA. The modified Stokes-Einstein model was proposed as shown below:

$$D_{N_2O} \cdot \eta^{0.8} = \text{Constant} \tag{7.27}$$

The viscosity of the aqueous solutions of blended MEA-DEAB can be found in the work of Naami et al. (in press). The constants in Equation 7.27 were determined using NLREG program, so the modified Stokes-Einstein model can be written as:

$$D_{N_2O} \cdot \eta^{0.8} = 4.3x10^{-3} \tag{7.28}$$

The predicted N_2O diffusivity results are plotted as dashed lines in Figure 7.4. It was found that the modified Stokes-Einstein model does not correlate well with the experimental results with an AAD of 56.2%, as shown in Figures 7.4 and 7.5.

Table 7.5 Diffusivity of N_2O in aqueous solutions of blended MEA-DEAB

Concentration (M)	Total amine concentration (M)	N_2O diffusivity (10^{10} m^2/s)		
		298 K	313 K	323 K
5 M MEA+0.25 M DEAB	5.25	1.26	2.72	3.87
5 M MEA+1 M DEAB	6	0.63	1.63	2.37
5 M MEA+1.5 M DEAB	6.5	0.36	0.68	1.08
5 M MEA+2 M DEAB	7	0.09	0.20	0.34

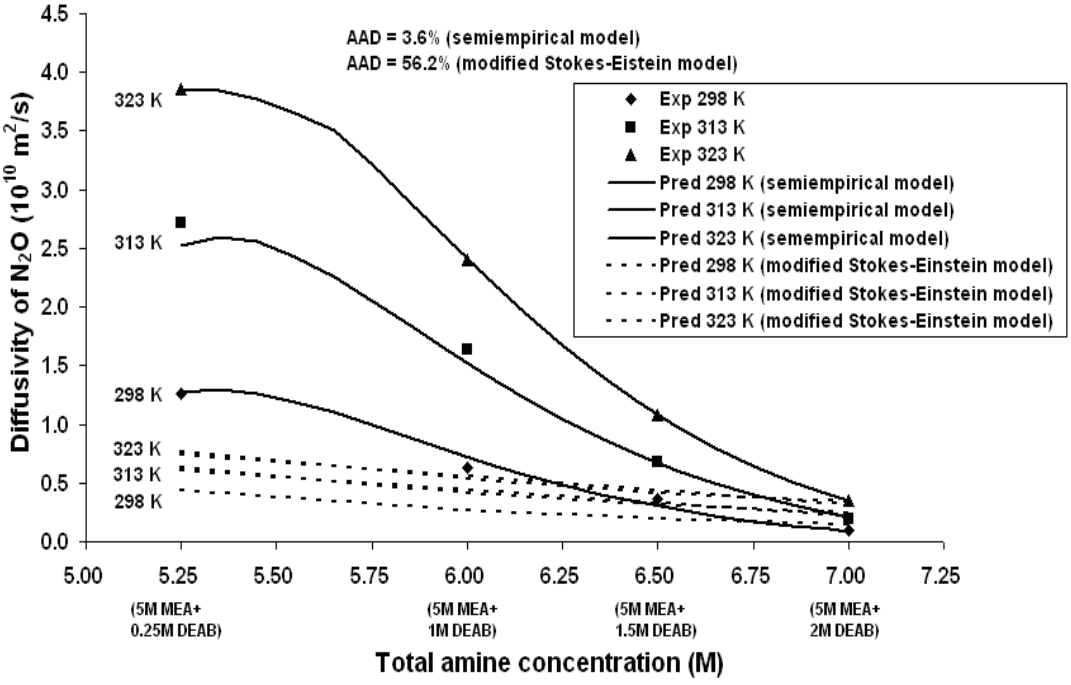

Figure 7.4 Diffusivity of N_2O in aqueous solutions of blended MEA-DEAB at various concentrations and temperatures; the solid lines are predicted from the semiempirical model in Equation 7.26 and the dashed lines are predicted from the modified Stokes-Einstein model in Equation 7.28.

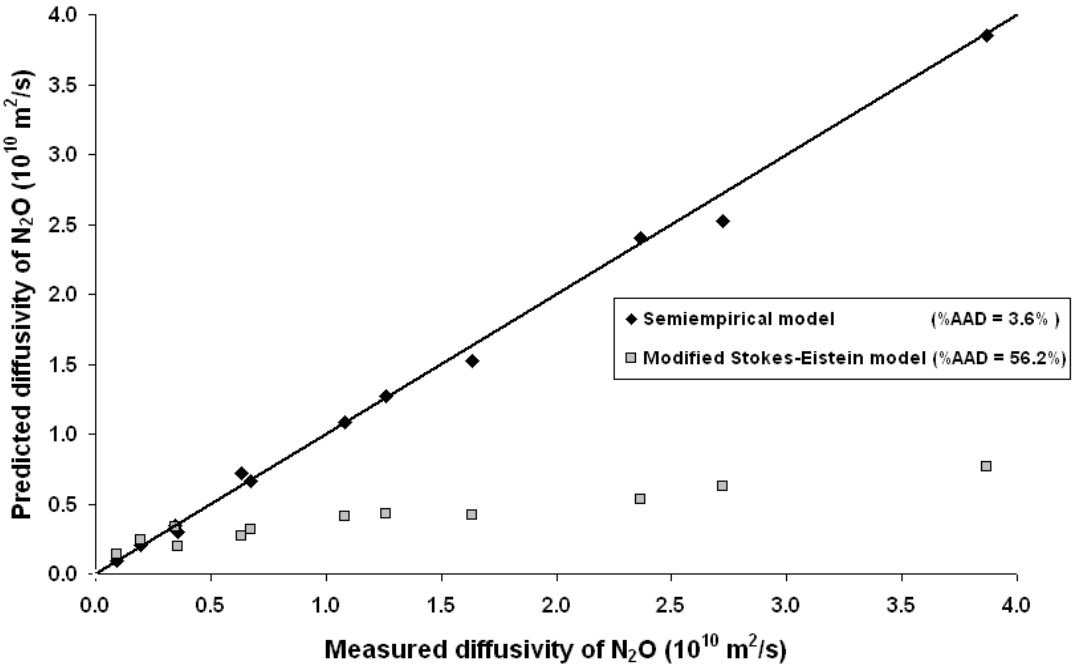

Figure 7.5 Parity chart comparing the experimental and predicted results of diffusivity of N_2O in aqueous solutions of blended MEA-DEAB.

By comparing the semiempirical and the modified Stokes-Einstein models, it is clear that the semiempirical model provides better predicted results for the N_2O diffusivity in aqueous solutions of blended MEA-DEAB, as shown in Figures 7.4 and 7.5. This is because the semiempirical model takes both temperature and amine concentration into account. Since both temperature and amine concentration directly control the solution viscosity (it was mentioned by Li and Lee (1996) that the temperature and viscosity play an important role in N_2O diffusivity), the semiempirical model seems to be adequate for predicting N_2O diffusivity in aqueous solutions of blended MEA-DEAB. On the other hand, the modified Stokes-Einstein model, which correlated the N_2O diffusivity directly with viscosity, does not work well for the prediction of N_2O diffusivity, as shown in Figures 7.4 and 7.5. It was reported by Xu et al. (1991), who used the modified Stokes-Einstein model shown in Equation 7.27 to correlate the N_2O diffusivity in 9.7 M and 10.1 M aqueous TMS solution, that the predicted results obtained from the modified Stokes-Einstein model do not fit well with the experimental results, with an AAD of 46%. We also found that the modified Stokes-Einstein model does not work well, with an AAD of 56.2% (at total amine concentration rage of 5.25 M to 7 M). However, the modified Stokes-Einstein model works fairly well for the prediction of N_2O diffusivity in aqueous solutions of 1 M to 2.5 M DEAB at an AAD of 10.2%, as can be seen in Chapter 4. These results confirm that the modified Stokes-Einstein model is not applicable at high amine concentrations because the solution tends to be a non-ideal solution at high amine concentration, as it behaves differently from the modified Stokes-Einstein relation.

7.3.3 Equilibrium solubility of CO_2 in aqueous solutions of blended MEA-DEAB

The equilibrium solubility of CO_2 in aqueous solution of blended MEA-DEAB was measured over a temperature range of 298 K to 333 K, a CO_2 partial pressure range of 10 kPa to 100 kPa, and a concentration range of 5 M MEA+0.25 M DEAB to 5 M MEA+2 M DEAB. The results are shown in Tables 7.6-7.10 and plotted in Figures 7.6, 7.7, and 7.8. As expected, equilibrium solubility of CO_2 decreases as temperature increases and increases as CO_2 partial pressure increases, which corresponds well with the results in Chapter 5 and those of Austgen et al. (1991); Li and Shen (1993); Maneeintr et al. (2009), who used aqueous solutions of DEAB and blended MEA-MDEA. In addition, the equilibrium solubility of CO_2 also increases as DEAB concentration increases over a concentration range of 5 M MEA+0.25 M DEAB to 5 M MEA+2 M DEAB.

The equilibrium solubility of CO_2 in aqueous solutions of blended MEA-DEAB decreases as temperature increases because the solubility of CO_2 declines with increasing temperature; thus, the system tends toward CO_2 desorption rather than CO_2 absorption. For the effects of CO_2 partial pressure, the equilibrium solubility of CO_2 increases as CO_2 partial pressure increases due to the higher driving force for CO_2 absorption at higher CO_2 partial pressure. In the present study, it was observed that the equilibrium solubility of CO_2 increases as DEAB concentration in the blended solution increases over a concentration range of 5 M MEA+0.25 M DEAB to 5 M MEA+2 M DEAB. Furthermore, the blended solutions of 5 M MEA and 0.25 M to 2 M DEAB provide higher equilibrium solubility of CO_2 than that from 5 M MEA, as can be seen in Figure 7.7. This is due to the very high CO_2 equilibrium solubility of DEAB, which is

comparable with piperazine (PZ), as mentioned in Chapter 5. Therefore, the addition of DEAB into MEA, which has lower equilibrium solubility of CO_2, results in the increase of equilibrium solubility of CO_2 in the blended solution, as suggested by Chakravarty et al. (1985). Moreover, there might be a structural interaction between MEA and DEAB that allows CO_2 to react with amine easily; thus, the equilibrium solubility of the blended MEA-DEAB solution increases as DEAB concentration in the blended solution increases. However, the increment of equilibrium CO_2 solubility at 313 K tends to decline at DEAB concentrations higher than 1.5 M (i.e., at 2 M), as can be seen in Figure 7.9 (the results at 298 K and 313 K follow the same trend as those at 313 K). This is because at amine concentrations of 5 M MEA+0.25 M DEAB to 5 M MEA+1.5 M DEAB, the solutions are not saturated yet. Therefore, the addition of DEAB, which has very high CO_2 equilibrium solubility, can enhance the CO_2 equilibrium solubility of the blended solutions. On the other hand, at high amine concentrations of 5 M MEA+2 M DEAB, the solutions approach saturation with the both MEA and DEAB molecules; thus, not all of the MEA and DEAB molecules can react with CO_2. Therefore, the increment of CO_2 equilibrium solubility declines. In addition, it can be observed from Figure 7.9 that the formulation of 5 M MEA+1.5 M DEAB seems to be the best MEA-DEAB combination over a concentration range of 5 M MEA+0.25 M DEAB to 5 M MEA+2 M DEAB in terms of the equilibrium solubility of CO_2.

This study not only considers the experimental results for equilibrium solubility of CO_2 in aqueous solutions of blended MEA-DEAB, but also has attempted to calculate the equilibrium solubility of CO_2 at various temperatures, concentrations, and CO_2 partial

pressures because experimental measurements are not only costly, but also time consuming.

In order to obtain the predicted equilibrium solubility of CO_2 (α), the 11 coupled nonlinear algebraic equations (i.e., Equations 7.10-7.14 and 7.16-7.21) need to be simultaneously solved for the 11 unknowns, which are α, $[RR_2'N]$, $[R''NH_2]$, $[H^+]$, $[RR_2'NH^+]$, $[RR_2'NH^+]$, $[R''NHCOO^-]$, $[HCO_3^-]$, $[CO_2]$, $[OH^-]$, and $[CO_3^{2-}]$. In this case, FEM based on COMSOL 4.1 software with 0D stationary solver mode was applied. The predicted equilibrium solubility of CO_2 in aqueous solutions of blended MEA-DEAB are plotted in Figures 7.6, 7.7, and 7.8 as solid lines. The results show that the predicted results fit moderately well with the experimental results with an AAD of 6.3%, which is in an acceptable range of AAD less than 10%. The parity chart that compares the experimental and predicted results is shown in Figure 7.10.

Even though the predicted results for equilibrium solubility of CO_2 fit moderately well with the experimental results, most of the predicted results are under predicted, as can be seen in the parity chart in Figure 7.10. In particular, the predicted results at 333 K show the most deviation from the experimental results compared with those at 298 K and 313 K, as shown in Figure 7.8. This is because of the non-ideality of the solutions at high concentration and temperature. Note that the concentrations of blended MEA-DEAB range from 5 M MEA+0.25 M DEAB and 5 M MEA+2 M DEAB (total amine concentration of 5.25 M to 7 M), which are considered as high amine concentrations.

Table 7.6 Equilibrium solubility of CO_2 in aqueous solution of blended 5 M MEA and 0.25 M DEAB

298 K		313 K		333 K	
CO_2 partial pressure (kPa)	CO_2 loading	CO_2 partial pressure (kPa)	CO_2 loading	CO_2 partial pressure (kPa)	CO_2 loading
10	0.532	10	0.496	10	0.453
16	0.552	15	0.517	16	0.495
31	0.580	35	0.564	32	0.530
60	0.587	60	0.578	61	0.544
71	0.591	71	0.584	72	0.557
100	0.597	100	0.595	100	0.562

Table 7.7 Equilibrium solubility of CO_2 in aqueous solution of blended 5 M MEA and 0.5 M DEAB

298 K		313 K		333 K	
CO_2 partial pressure (kPa)	CO_2 loading	CO_2 partial pressure (kPa)	CO_2 loading	CO_2 partial pressure (kPa)	CO_2 loading
10	0.542	10	0.510	10	0.486
16	0.559	15	0.537	16	0.504
31	0.590	35	0.575	32	0.533
60	0.593	60	0.580	61	0.550
71	0.598	71	0.587	72	0.559
100	0.601	100	0.596	100	0.567

Table 7.8 Equilibrium solubility of CO_2 in aqueous solution of blended 5 M MEA and 1 M DEAB

298 K		313 K		333 K	
CO_2 partial pressure (kPa)	CO_2 loading	CO_2 partial pressure (kPa)	CO_2 loading	CO_2 partial pressure (kPa)	CO_2 loading
10	0.549	11	0.506	11	0.498
15	0.563	16	0.536	15	0.517
30	0.590	32	0.579	31	0.542
62	0.602	61	0.586	59	0.559
72	0.610	72	0.595	70	0.565
100	0.610	99	0.605	99	0.572

Table 7.9 Equilibrium solubility of CO_2 in aqueous solution of blended 5 M MEA and 1.5 M DEAB

298 K		313 K		333 K	
CO_2 partial pressure (kPa)	CO_2 loading	CO_2 partial pressure (kPa)	CO_2 loading	CO_2 partial pressure (kPa)	CO_2 loading
10	0.548	11	0.517	11	0.504
15	0.568	16	0.554	15	0.524
30	0.591	32	0.581	31	0.547
62	0.608	61	0.589	59	0.570
72	0.609	72	0.600	70	0.568
100	0.612	99	0.610	99	0.578

Table 7.10 Equilibrium solubility of CO_2 in aqueous solution of blended 5 M MEA and 2 M DEAB

298 K		313 K		333 K	
CO_2 partial pressure (kPa)	CO_2 loading	CO_2 partial pressure (kPa)	CO_2 loading	CO_2 partial pressure (kPa)	CO_2 loading
11	0.549	10	0.515	10	0.512
16	0.571	15	0.555	16	0.531
31	0.591	31	0.581	32	0.549
61	0.610	60	0.588	60	0.572
75	0.613	76	0.607	76	0.575
100	0.615	99	0.610	99	0.579

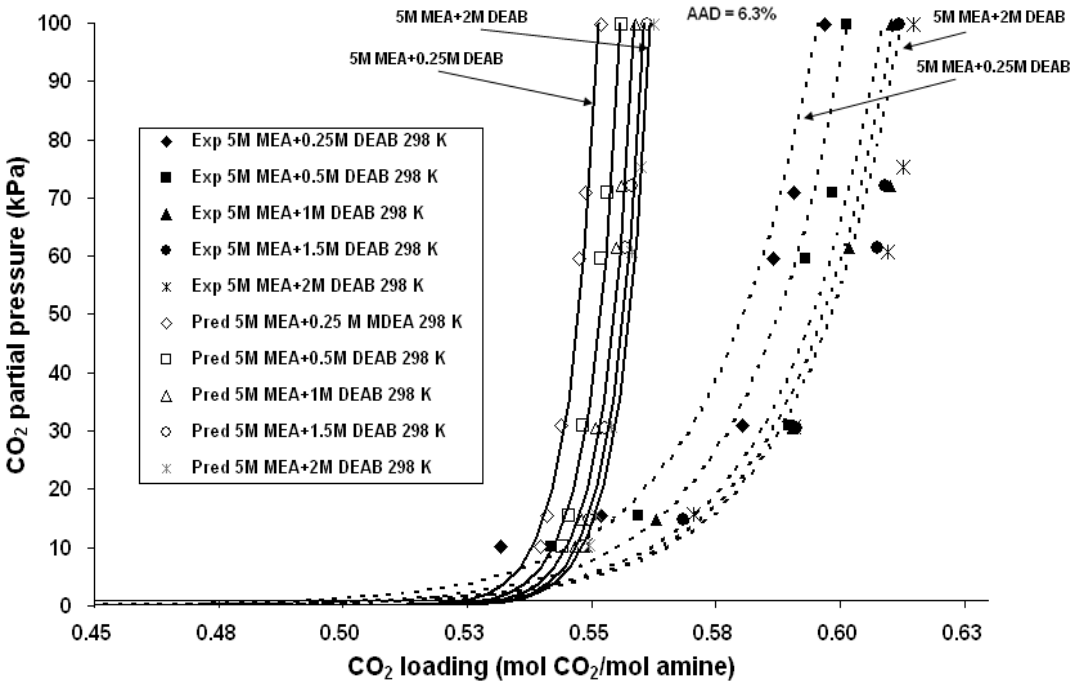

Figure 7.6 Equilibrium solubility of CO_2 in aqueous solution of blended 5 M MEA and 0.25 M, 0.5 M, 1 M, 1.5 M, and 2 M DEAB at 298 K; the dashed lines are the experimental results' trend lines and the solid lines are the predicted results.

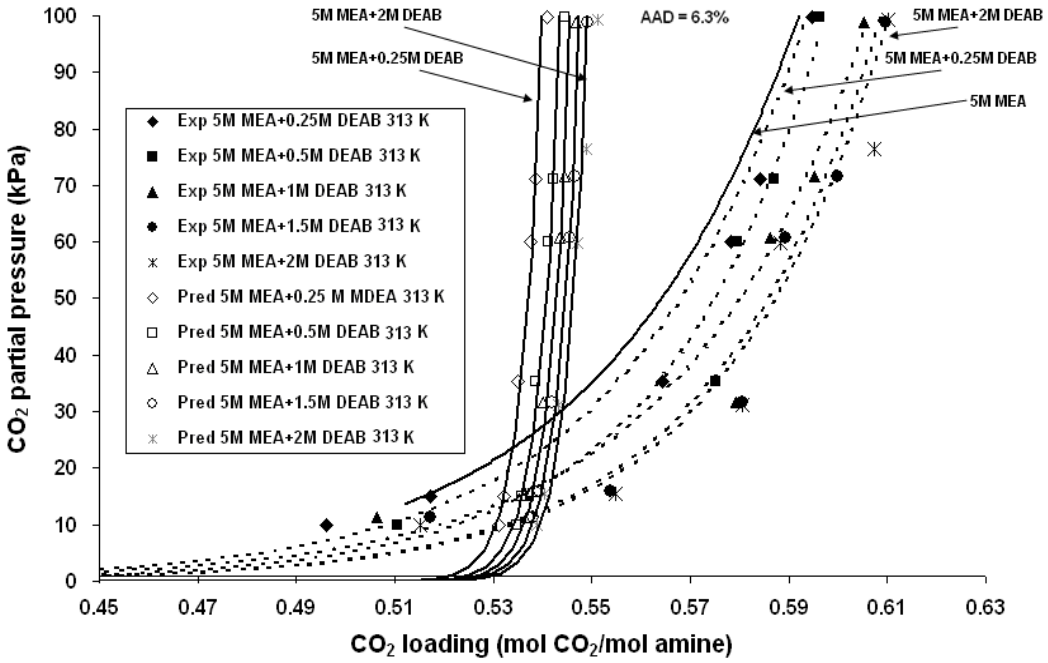

Figure 7.7 Equilibrium solubility of CO_2 in aqueous solution of blended 5 M MEA and 0.25 M, 0.5 M, 1 M, 1.5 M, and 2 M DEAB at 313 K; the dashed lines are the experimental results' trend lines and the solid lines are the predicted results.

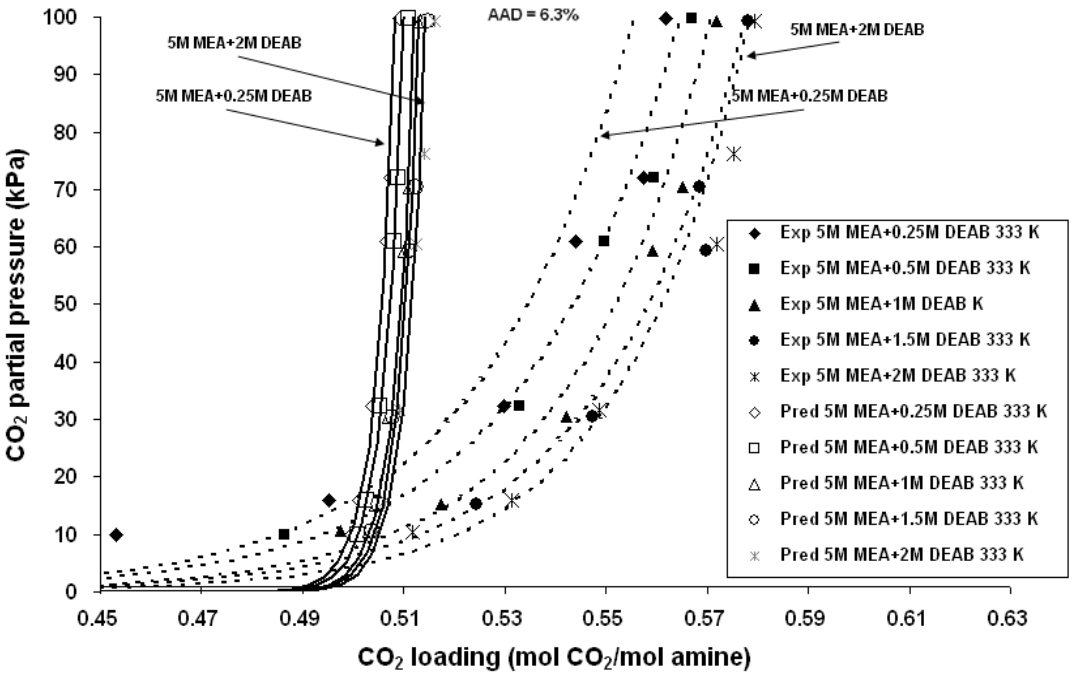

Figure 7.8 Equilibrium solubility of CO_2 in aqueous solution of blended 5 M MEA and 0.25 M, 0.5 M, 1 M, 1.5 M, and 2 M DEAB at 333 K; the dashed lines are the experimental results' trend lines and the solid lines are the predicted results.

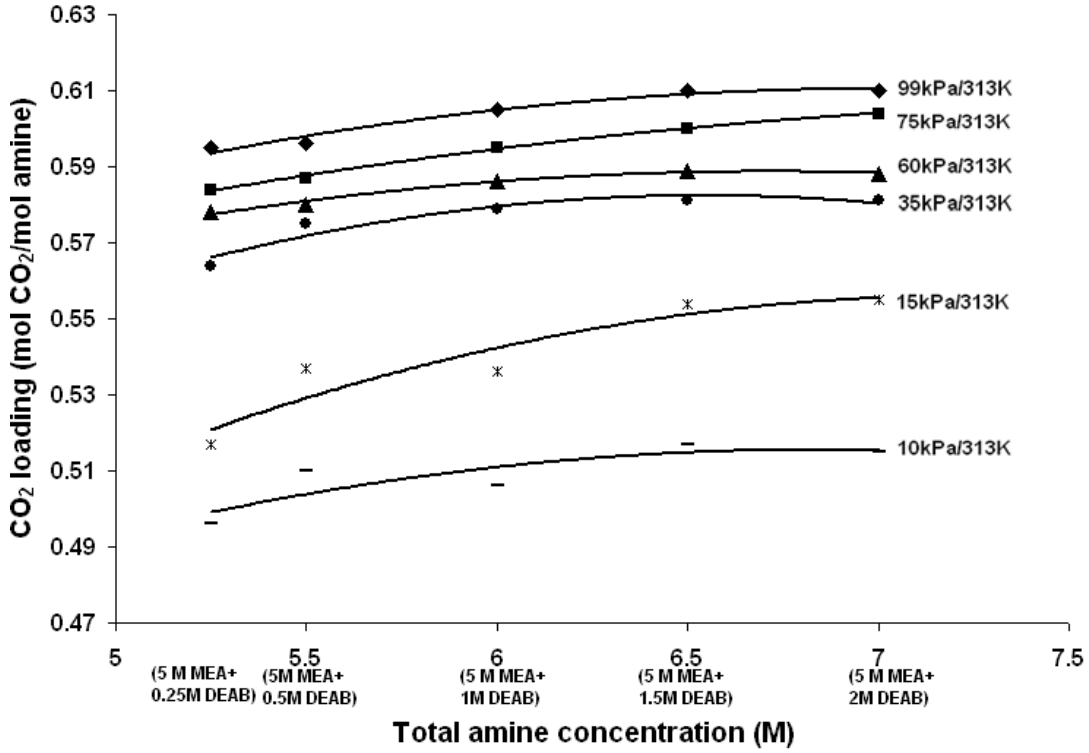

Figure 7.9 Equilibrium solubility of CO_2 in aqueous solutions of blended MEA-DEAB at 313 K and CO_2 partial pressure of 10 kPa to 99 kPa; the solid lines are trend lines.

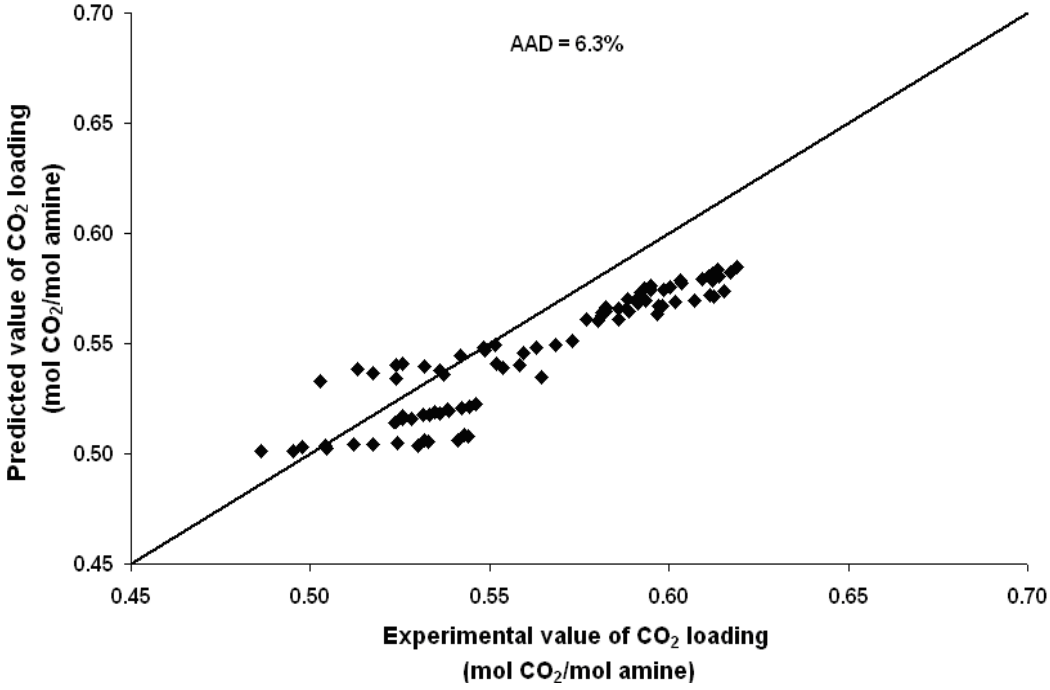

Figure 7.10 Parity chart comparing the experimental and predicted results of CO_2 equilibrium solubility in aqueous solutions of blended MEA-DEAB.

7.4 Summaries

1. The solubility of N_2O in aqueous solutions of blended MEA-DEAB increases as temperature increases and decreases as DEAB concentration in the blended solution increases over a temperature range of 298 K to 343 K and a concentration range of 5 M MEA+0.25 M DEAB to 5 M MEA+2 M DEAB. The predicted N_2O solubility obtained from the semiempirical model of Equation 7.22 is in good agreement with the experimental results with an AAD of 2.7%.

2. The diffusivity of N_2O in aqueous solutions of blended MEA-DEAB increases as temperature increases and decreases as DEAB concentration in the blended solution increases over a temperature range of 298 K to 323 K and a concentration range of 5 M MEA+0.25 M DEAB to 5 M MEA+2 M DEAB. The predicted N_2O diffusivity results obtained from the semiempirical model of Equation 7.26 fit well with the experimental results with an AAD of 3.6%.

3. The physical solubility and physical diffusivity of CO_2 in aqueous solutions of blended MEA-DEAB can then be estimated using the N_2O analogy.

4. The equilibrium solubility of CO_2 in aqueous solutions of blended MEA-DEAB decreases as temperature increases and increases as CO_2 partial pressure increases. Also, the equilibrium solubility of CO_2 increases as the DEAB concentration increases in the blended solution over a temperature range of 298 K to 333 K, a CO_2 partial pressure range of 10 kPa to 100 kPa, and a concentration range of 5 M MEA+0.25 M DEAB to 5 M MEA+2 M DEAB. Moreover, the equilibrium solubility of CO_2 in the blended solutions of MEA-DEAB was found to be higher than that in 5 M MEA.

5. Based on the equilibrium solubility of CO_2 in aqueous solutions of blended MEA-DEAB, it was found that the 5 M MEA+1.5 M DEAB is the best MEA-DEAB formulation over a concentration range of 5 M MEA+0.25 M DEAB to 5 M MEA+2 M DEAB.

6. The predicted equilibrium solubility of CO_2 in aqueous solutions of blended MEA-DEAB obtained from the mathematical modeling fit moderately well with the experimental results with an AAD of 6.3%.

7.5 References

1. Austgen, D.M.; Rochelle, G.T.; Chen, C.C. Model of vapor-liquid equilibria for aqueous acid gas-alkanolamine system. 2. Representation of H_2S and CO_2 solubility in aqueous MDEA and CO_2 solubility in aqueous mixtures of MDEA with MEA or DEA. Ind. Eng. Chem. Res. 1991, 30, 543-555.

2. Chakravarty, T.; Phukan, U.K.; Weiland, R.H. Reaction of acid gases with mixtures of amines. Chem. Eng. Prog. 1985, 81, 32-36.

3. Clarke, J. K. A. Kinetics of absorption of carbon dioxide in monoethanolamine solutions at short contact times. Ind. Eng. Chem. Fundam. 1963, 3, 239-245.

4. Hartono, A.; Juliussen, O.; Svendsen, F.H. Solubility of N_2O in aqueous solution of diethylenetriamine. J. Chem. Eng. Data 2008, 53, 2696-2700.

5. Ko, J.; Tsai, T.; Lin, C.; Wang, H.; Li, M. Diffusivity of nitrous oxide in aqueous alkanolamine solutions. J. Chem. Eng. Data 2001, 46, 160-165.

6. Kohl, A.L.; Nielsen, R.B. Gas Purification: 5th Edition; Gulf Publishing Company: Houston, Texas, USA, 1997.

7. Li, M.H.; Lee, W.C. Solubility and diffusivity of N_2O and CO_2 in (diethanolamine+N-methyldiethanolamine+water) and in (diethanolamine+2-amino-2-methyl-1-propanol+water). J. Chem. Eng. Data 1996, 41, 551-556.

8. Li, M.H., Shen, K.P. Calculation of equilibrium solubility of carbon dioxide in aqueous mixtures of monoethanolamine and methyldiethanolamine. Fluid Phase Equilibria 1993, 55, 87-90.

9. Liu, Y.; Zhang, L.; Watanasiri, S. Representing vapor-liquid equilibrium for an aqueous MEA-CO_2 system using the electrolyte nonrandom-two-liquid model. Ind. Eng. Chem. Res. 1999, 38, 2080-2090.

10. Maneeintr, K.; Idem, R. O.; Tontiwachwuthikul, P.; Wee, A. G. H. Synthesis, solubilities, and cyclic capacity of amino alcohols for CO_2 Capture from flue gas streams. Energy procedia 2009, 1, 1327-1334.

11. Naami, A.Edali., M.; Sema, T.; Idem, R.; Tontiwachwuthikul, P. Density and viscosity of aqueous solutions of blended monoethanolamine and 4-(Diethylamino)-2-Butanol Solutions. In Press.

12. Redlich, O.; Kister, A.T. Algebraic representation of thermodynamic properties and the classification of solutions. Ind. Eng. Chem. 1948, 40, 345-348.

13. Sada, E.; Kumazawa, H.; Butt M.A. Solubilities of gases in aqueous solutions of amine. J. Chem. Eng. Data 1977, 22, 277-278.

14. Sada, E.; Kumazawa; H.; Butt M.A. Solubilities of gases in aqueous solutions of amine. J. Chem. Eng. Data 1978, 23, 161-163.

15. Tontiwachwuthikul, P.; Wee, A. G. H.; Idem, R. O.; Maneeintr, K.; Fan, G. J.; Veawab, A.; Aroonwilas, A.; Chakma, A. Method for capturing carbon dioxide from gas streams. US Patent Application. US Patent Application, No. US 2008/0050296 A1, 2008.

16. Versteeg, G. F.; van Swaaij W.P.M. Solubility and diffusivity of acid gases (CO_2, N_2O) in aqueous alkanolamine solutions. J. Chem. Eng. Data 1988, 33, 29-34.

17. Wang, Y. W.; Xu, S.; Otto, F. D.; Mather, A. E. Solubility of N_2O in alkanolamines and in mixed solvents. The Chemical Engineering Journal 1992, 48, 31-40.

18. Xu, S.; Wang, Y.; Otto, F.D.; Mather, A. Solubilities and diffusivities of N_2O and CO_2 in aqueous sulfolane solutions. J. Chem. Tech. Biotechnl. 1991, 51, 197-208.

Chapter 8 Kinetics of CO_2 Absorption into Aqueous Solutions of Blended Monoethanolamine and 4-(Diethylamino)-2-Butanol

8.1 Introduction

The most commonly used amines for capturing carbon dioxide (CO_2) are primary amine; monoethanolamine (MEA), secondary amine; diethanolamine (DEA), tertiary amine; methyldiethanolamine (MDEA), and primary sterically hindered amine; 2-amino-2-methyl-1-propanol (AMP) (Sartori and Savage, 1983; Tontiwachwuthikul et al., 1991; Kohl and Nielsen, 1997). MEA and DEA react rapidly with CO_2 to form carbamates (Kohl and Nielsen, 1997). However, because there is a relatively high heat of CO_2 absorption associated with carbamate formation, the cost of regenerating MEA and DEA is high. In addition, the CO_2 absorption capacity for MEA and DEA are limited at 0.5 mol of CO_2 per mol of amine. On the other hand, MDEA lacks the N-H bond required for carbamate formation. Therefore, MDEA does not react with CO_2 directly. It promotes the hydrolysis of CO_2 to form protonated MDEA and bicarbonate. The MDEA-promoted hydrolysis of the CO_2 reaction is much slower than the carbamate formation with MEA and DEA, but MDEA requires lower regeneration energy due to the fact that the heat of absorption of bicarbonate formation reaction is lower than that of the carbamate formation reaction. MDEA also has an advantage over MEA and DEA in that its CO_2 absorption capacity is limited at 1 mol of CO_2 per mol of amine. The primary sterically hindered amine, AMP, is found to be reactive with CO_2. Since AMP is a highly branched primary amine, an instable hindered carbamate is formed by the AMP-CO_2 reaction. This instable species is easily hydrolyzed to form bicarbonate and free AMP. The released free

AMP can then react with CO_2 again, which leads to the CO_2 absorption capacity of 1 mol of CO_2 per mol of amine (Sartori and Savage, 1983).

Recently, a newly developed amino alcohol solvent, 4-diethylamino-2-butanol (DEAB), has been investigated in terms of its performance by various researchers (Tontiwachwuthikul et al. (2008); Maneeintr et al. (2009); this work in Chapters 5 and 6). They have found that the absorption capacity of DEAB is comparable with piperazine (PZ) and higher than AMP, MDEA, DEA, and MEA. Also, it has been found that the regeneration energy of DEAB is lower than that of MDEA, DEA, and MEA, respectively. Moreover, they have observed that DEAB, which is considered to be a tertiary amine, since it has three carbon atoms attached to the nitrogen atom, reacts with CO_2 faster than MDEA and is also comparable with AMP and DEA and slower than MEA and PZ, respectively. Regarding its outstanding performance, DEAB is now being considered as a promising alternative solvent for capturing CO_2.

Chakravarty et al. (1985) first suggested a mixing of primary or secondary amines with tertiary amines to take advantage of each amine's high-performing components. This means the disadvantages of one amine are compensated by another amine. The benefits of blended amine systems have been proven widely in the literature (Critchfield and Rochelle, 1987; Kohl and Nielsen, 1997; Zhang et al., 2002; Choi et al., 2007; Edali et al., 2007). Examples of blended amine systems are MEA-MDEA, DEA-MDEA, and AMP-MDEA. In the present study, two amines, which are MEA and DEAB, are considered. Mixing MEA with DEAB was proposed in order to (1) counter the high regeneration energy of MEA, (2) compensate for the low CO_2 absorption capacity of MEA, and (3) enhance the CO_2 absorption rate of DEAB. The regeneration energy

performance of blended MEA-DEAB aqueous solutions over a concentration range of 5 M MEA+0.25 M DEAB to 5 M MEA+2 M DEAB was investigated by Naami et al. (in press) in terms of cyclic capacity. They found that the regeneration energy for the blended MEA-DEAB aqueous solutions is lower than that of single MEA aqueous solutions. The CO_2 absorption capacity of the blended solutions was measured in terms of equilibrium solubility of CO_2 over a concentration range of 5 M MEA+0.25 M DEAB to 5 M MEA+2 M DEAB, as describe in Chapter 7. It was observed that the addition of small amounts of DEAB into aqueous MEA solutions can enhance the CO_2 absorption capacity of the blended solutions. Lastly, the effect of adding DEAB into MEA aqueous solution on the CO_2 absorption rate will be investigated in this chapter.

In this study, the experimental kinetics data of CO_2 in aqueous solutions of blended MEA-DEAB were measured using a laminar jet absorber over ranges of temperatures, amine concentrations, CO_2 loadings, and contact times. The obtained experimental data were then used to develop a comprehensive numerical reaction rate/kinetics model (using the finite element method (FEM) based on COMSOL software) for the absorption of CO_2 in aqueous solutions of blended MEA-DEAB. The chemical equilibrium, the mass transfer, and the chemical kinetics of all possible reactions were taken into account in this comprehensive model.

8.2 Theory

Based on the proposed mechanism for the reaction between CO_2 and MEA-DEAB, a vapour-liquid equilibrium (VLE) model and an absorption rate/kinetics model for predicting the kinetics data were developed.

8.2.1 Chemical reaction scheme for CO_2-MEA-DEAB aqueous system

The chemical reactions in CO_2-MEA-DEAB aqueous system are governed by the following equations:

$$RR_2'N + H^+ \xleftrightarrow{K_1} RR_2'NH^+ \tag{8.1}$$

$$CO_2 + RR_2'N + H_2O \xleftrightarrow{K_2, k_{22}, -k_{22}} RR_2'NH^+ + HCO_3^- \tag{8.2}$$

$$H_2O + CO_2 \xleftrightarrow{K_3} H^+ + HCO_3^- \tag{8.3}$$

$$CO_2 + OH^- \xleftrightarrow{K_4, k_{24}, -k_{24}} HCO_3^- \tag{8.4}$$

$$HCO_3^- \xleftrightarrow{K_5} H^+ + CO_3^{2-} \tag{8.5}$$

$$H_2O \xleftrightarrow{K_6} H^+ + OH^- \tag{8.6}$$

$$R''NH_2 + H^+ \xleftrightarrow{K_7} R''NH_3^+ \tag{8.7}$$

$$R''NH_2 + CO_2 \xleftrightarrow{K_8, k_{28}, -k_{28}} R''NHCOO^- + H^+ \tag{8.8}$$

$$R''NHCOO^- + H_2O \xleftrightarrow{K_9} R''NH_2 + HCO_3^- \tag{8.9}$$

$RR_2'N$ represents DEAB where R is $(CH_2)_2CH(CH_3)OH$ and R' is CH_2CH_3. $R''NH_2$ represents MEA where R'' is $(CH_2)_2OH$. K_i is the chemical equilibrium constant for reaction i. k_{2i} is the second order forward rate coefficient for reaction i. DEAB is considered to be a tertiary amine, since it has 3 carbon atoms attached to the nitrogen atom. In this case, DEAB does not react directly with CO_2, but it acts as a base that catalyzes the hydration of CO_2 (Kohl and Nielsen, 1997), as presented in Equation 8.2. MEA is a primary amine that reacts directly with CO_2 to form carbamate, as shown in Equation 8.8. Reactions 8.2, 8.4, and 8.8 are considered to be reversible with finite reaction rates, whereas reactions 8.1, 8.3, 8.5-8.7, and 8.9 are considered to be reversible

and instantaneous with respect to mass transfer and at equilibrium, since they involve only proton transfer (Hagewiesche et al., 1995).

Based on Equation 8.1-8.9, it can be seen that not all of the chemical equilibrium constants are independent. Only 6 chemical equilibrium constants (K_2, K_3, K_4, K_6, K_8 and K_9) are independent. The remaining three (K_1, K_5, and K_7) can be obtained by the combination of independent chemical equilibrium constants as shown in Equations 8.10-8.12. Also, the water concentration is considered to be constant due to the fact that the water concentration is much higher than the amine concentration.

$$K_1 = \frac{\left[RR_2^{/}NH^+\right]}{\left[H^+\right]\left[RR_2^{/}N\right]} = \frac{K_2}{K_3} \tag{8.10}$$

$$K_5 = \frac{\left[H^+\right]\left[CO_3^{2-}\right]}{\left[HCO_3^-\right]} = \frac{K_2}{K_1 K_6} \tag{8.11}$$

$$K_7 = \frac{\left[H^+\right]\left[R''NHCOO^-\right]}{\left[CO_2\right]\left[R''NH_2\right]} = \frac{K_3}{K_9} \tag{8.12}$$

For the kinetics study, reaction 8.9 can be neglected because of the low reaction rate and short contact time typical of the laminar jet absorber (Hagewiesche et al., 1995; Edali et al., 2007). However, reaction 8.9 needs to be included for the calculation of the bulk concentration of all chemical species in the vapour-liquid equilibrium (VLE) model. This is because reaction 8.9 becomes more important when the initial CO_2 loading of MEA increases (Hagewiesche et al., 1995).

The chemical species in Equations 8.1-8.9 have been renamed for convenience in the numerical treatment as follows:

$$C_1 = [CO_2], C_2 = [HCO_3^-], C_3 = [OH^-], C_4 = [CO_3^{2-}], C_5 = [H^+], C_6 = [RR_2'N],$$

$$C_7 = [RR_2'NH^+], C_8 = [R''NH_2], C_9 = [R''NH_3^+],\ C_{10} = [R''NHCOO^-].$$

Also, subscripts 1-10 represent the chemical species CO_2, HCO_3^-, OH^-, CO_3^{2-}, H^+, $RR_2'N$, $RR_2'NH^+$, $R''NH_2$, $R''NH_3^+$ and $R''NHCOO^-$, respectively.

8.2.2 Vapour-liquid equilibrium (VLE) model

The bulk concentrations of all chemical species in liquid phase at equilibrium ($C_1 - C_{10}$), which are required for the kinetics study, can be estimated using the VLE model. The input parameters for this model are initial concentration of MEA in the solution ($[MEA]_0$; kmol/m^3), initial concentration of DEAB in the solution ($[DEAB]_0$; kmol/m^3), equilibrium CO_2 solubility in aqueous solutions of blended MEA-DEAB or CO_2 loading (α; mol CO_2/mol DEAB), equilibrium constants of involved reactions (K_i), and physical solubility of CO_2 in the solution or Henry's constant (He; kPa m^3/kmol). The concentrations of $C_1 - C_{10}$ can be obtained by simultaneously solving the mass balance equations, equilibrium constant equations, and Henry's law relationship as shown below:

Total DEAB balance:

$$[DEAB]_0 = C_6 + C_7 \tag{8.13}$$

Total MEA balance:

$$[MEA]_0 = C_8 + C_9 + C_{10} \tag{8.14}$$

Total carbon balance:

$$\alpha\left(\left[MEA\right]_0 + \left[DEAB\right]_0\right) = C_1 + C_2 + C_4 + C_{10} \tag{8.15}$$

Charge balance:

$$C_5 + C_7 + C_9 = C_2 + C_3 + 2C_4 + C_{10} \tag{8.16}$$

Independent equilibrium constants:

$$K_2 = \frac{C_2 C_7}{C_1 C_6} \tag{8.17}$$

$$K_3 = \frac{C_2 C_5}{C_1} \tag{8.18}$$

$$K_4 = \frac{C_2}{C_1 C_3} \tag{8.19}$$

$$K_6 = C_3 C_5 \tag{8.20}$$

$$K_7 = \frac{C_9}{C_5 C_8} \tag{8.21}$$

$$K_8 = \frac{C_5 C_{10}}{C_1 C_8} \tag{8.22}$$

Henry's law relationship:

$$He_{CO_2} = P_{co_2} \Big/ C^*_{CO_2} \tag{8.23}$$

The chemical equilibrium constant K_2 is given in Equation 5.19 (in Chapter 5), and K_3, K_4, K_6, K_7, and K_8 can be found in the work Austgen et al. (1991). The Henry's constant or He_{CO_2} can be estimated via N_2O analogy using Equation 7.22 as described in Chapter 7.

The 11 coupled nonlinear algebraic equations (i.e. Equations 8.13-8.23) were then simultaneously solved for the 11 unknowns, which are $C_1 - C_{10}$ and equilibrium partial pressure of CO_2 (P_{co_2}), by inputting the initial guess for each unknown. In the present study, FEM based on COMSOL 4.1 software with 0D stationary solver mode was applied. After the software had been operated with the first set of initial guesses, values of the unknowns were obtained. Then, these new values were subsequently used as the second set of initial guesses for solving the 11 unknowns. This procedure was repeated until a different percentage deviation of the results of each unknown for successive attempts was less than 0.01%.

8.2.3 CO_2 absorption rate/kinetics model

A comprehensive CO_2 absorption rate/kinetics model was developed in order to interpret the absorption rate data of CO_2 in aqueous solutions of blended MEA-DEAB, from which the kinetics data were extracted. This model takes into account the coupling between chemical equilibrium, mass transfer, and chemical kinetics of all possible chemical reactions. Also, the model is capable of predicting the CO_2 absorption rate and enhancement factor, as well as predicting the kinetics of reaction (which is the second order forward rate coefficient for reaction 8.8 or k_{28} or k_{MEA}), from the experimental CO_2 absorption rate data.

The model was derived from a fully 3D cylindrical coordinate system, which is the shape of the cylindrical liquid jet generated in the laminar jet absorber, as shown in Figure 8.1. The gas-liquid interface is considered as an outer boundary. Also, the diffusion in radial direction is taken into account. Therefore, the absorption of CO_2 into

the cylindrical liquid jet, with constant density and diffusivity, is governed by Equation 8.24 (Astarita et al., 1983). This equation indicates that the molecular transport is equal to the sum total of the convection term, accumulation term ($\partial C/\partial t$), and reaction rate (R).

$$D\nabla^2 C = u \cdot \nabla C + \frac{\partial C}{\partial t} + R \tag{8.24}$$

The assumption of constant density and diffusivity is valid in the laminar jet absorber because the change of concentration does not represent a substantial variation in the mole fraction of the diffusant due to the short contact time (Aboudheir et al., 2003). Equation 8.24 can be simplified based on the following assumptions: (a) the penetration theory is applicable for the transport of the gas into liquid in which the reaction takes place by unsteady state molecular diffusion in the liquid; (b) the penetration depth of the absorbed molecule is much smaller than the jet diameter due to the short contact time (created in the laminar jet absorber) between the absorbed gas and liquid jet. Therefore, there is no curvature effect. The absorption of gas into liquid is then considered to be an infinite depth with a flat surface; (c) the diffusion in the flow direction is negligible; (d) the liquid jet is quiescent so that no convection movements affect the transport of the absorbed gas. Regarding these conditions, Equation 8.24 can be simplified to the diffusion equation in Equation 8.25. This equation governs the variation of time and space of the concentration of all reactants and products in the liquid phase (one equation for each component or material balance).

$$D\frac{\partial^2 C}{\partial x^2} = \frac{\partial C}{\partial t} + R \tag{8.25}$$

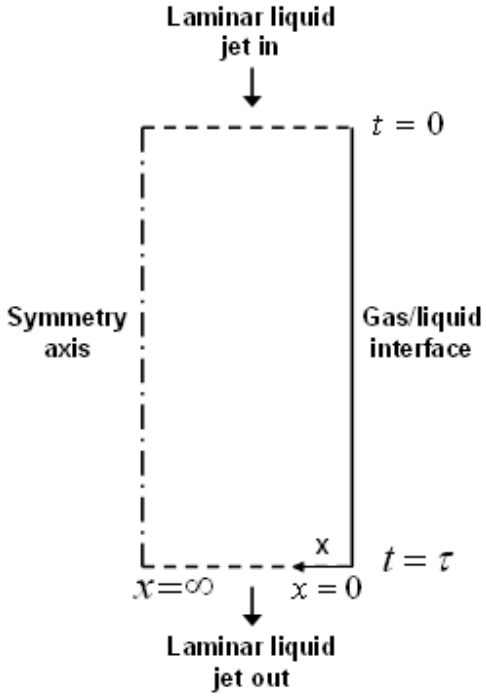

Figure 8.1 Schematic diagram of the liquid jet in the laminar jet absorber.

Thus, the partial differential equations (PDEs) and the nonlinear algebraic equations governing the diffusion-reaction process of Equations 8.1-8.9 can be described as:

CO_2 balance:

$$\frac{\partial C_1}{\partial t} = D_1 \frac{\partial^2 C_1}{\partial x^2} + R_2 + R_4 + R_8 \tag{8.26}$$

Total carbon balance:

$$\frac{\partial C_1}{\partial t} + \frac{\partial C_2}{\partial t} + \frac{\partial C_4}{\partial t} + \frac{\partial C_{10}}{\partial t} = D_1 \frac{\partial^2 C_1}{\partial x^2} + D_2 \frac{\partial^2 C_2}{\partial x^2} + D_4 \frac{\partial^2 C_4}{\partial x^2} + D_{10} \frac{\partial^2 C_{10}}{\partial x^2} \tag{8.27}$$

Total MEA balance:

$$\frac{\partial C_8}{\partial t} + \frac{\partial C_9}{\partial t} + \frac{\partial C_{10}}{\partial t} = D_8 \frac{\partial^2 C_8}{\partial x^2} + D_9 \frac{\partial^2 C_9}{\partial x^2} + D_{10} \frac{\partial^2 C_{10}}{\partial x^2} \tag{8.28}$$

Total DEAB balance:

$$\frac{\partial C_6}{\partial t} + \frac{\partial C_7}{\partial t} = D_6 \frac{\partial^2 C_6}{\partial x^2} + D_7 \frac{\partial^2 C_7}{\partial x^2} \tag{8.29}$$

Total charge balance:

$$\begin{aligned} &\frac{\partial C_2}{\partial t} + \frac{\partial C_3}{\partial t} + 2\frac{\partial C_4}{\partial t} + \frac{\partial C_{10}}{\partial t} - \frac{\partial C_5}{\partial t} - \frac{\partial C_7}{\partial t} - \frac{\partial C_9}{\partial t} = \\ &D_2 \frac{\partial^2 C_2}{\partial x^2} + D_3 \frac{\partial^2 C_3}{\partial x^2} + 2D_4 \frac{\partial^2 C_4}{\partial x^2} + D_{10} \frac{\partial^2 C_{10}}{\partial x^2} \\ &- D_5 \frac{\partial^2 C_5}{\partial x^2} - D_7 \frac{\partial^2 C_7}{\partial x^2} - D_9 \frac{\partial^2 C_9}{\partial x^2} \end{aligned} \tag{8.30}$$

Total carbamate balance:

$$\frac{\partial C_{10}}{\partial t} = D_{10}\frac{\partial^2 C_{10}}{\partial x^2} - R_8 \tag{8.31}$$

All reactions at equilibrium (only the independent equilibrium constants), including $K_2, K_3, K_6,$ and K_7, are given in Equations 8.17, 8.18, 8.20, and 8.21, respectively.

R_2, R_4 and, R_8, which are the reaction rate expressions for reactions 8.2, 8.4, and 8.8, respectively, can be presented as:

$$R_2 = -k_{DEAB}C_1C_6 + \left(\frac{k_{DEAB}}{K_2}\right)C_2C_7 \tag{8.32}$$

$$R_4 = -k_{24}C_1C_3 + \left(\frac{k_{24}}{K_4}\right)C_2 \tag{8.33}$$

$$R_8 = -k_{MEA}C_1C_8 + \left(\frac{k_{MEA}}{K_8}\right)C_5C_{10} \tag{8.34}$$

D_i is the diffusivity of chemical species i into the solution (m^2/s). The diffusivity of CO_2 in aqueous solution of blended MEA-DEAB (D_1) can be calculated from the predictive correlation given in Equation 7.26 (in Chapter 7) via N_2O analogy. Hikita et al. (1980) measured the diffusivity of MEA, DEA, and triethanolamine (TEA) in aqueous solution. They reported that the diffusivity was affected by the group complexity. Since DEAB is a tertiary amine, the same as TEA, it is reasonable to estimate the diffusivity of DEAB from that of TEA (the same assumption has also been made in the case of MDEA by Hagewiesche et al. (1995)). Thus, the diffusivity of DEAB (D_6; cm^2/s) and MEA (D_8; cm^2/s) can be estimated by:

$$D_6 = \left(1.739 \times 10^{-9}\right)\mu^{-0.569842} T \tag{8.35}$$

$$D_8 = \left(2.715 \times 10^{-9}\right)\mu^{-0.559442} T \tag{8.36}$$

where μ is the solution viscosity (g/cm s) and T is the temperature in K. Also, the diffusivity of HCO_3^-, OH^-, CO_3^{2-}, H^+, $RR_2'NH^+$, $R''NH_3^+$, and $R''NHCOO^-$ were assumed to be equal to that of MEA, which is the most abundant species (Hagewiesche et al., 1995).

The forward rate coefficients of Equation 8.4 (k_{24} or k_{DEAB}; m^3/kmol s) are given in Equation 6.37 (in Chapter 6) and those of Equation 8.6 (k_{26}; m^3/kmol s) can be calculated from the correlation developed by Pinsent et al. (1956) as follow:

$$\log\left(k_{26}\right) = 13.635 - \frac{2895}{T} \tag{8.37}$$

Thus, there are 10 partial differential-nonlinear algebraic equations (Equations 8.17, 8.18, 8.20, 8.21, and 8.26-8.31), which can be solved for the concentration of chemical species $C_1 - C_{10}$.

Initial conditions:

for all chemical species, j = 1, 2, 3,…,10

$$C_j(x,0) = C_j^0 \text{ at } t = 0 \text{ and } 0 \le x \ge \infty \tag{8.38}$$

Boundary conditions:

for all chemical species, j = 1, 2, 3,…,10

$$C_j(\infty,t) = C_j^0 \text{ at } x = \infty \text{ and } 0 \le t \ge \tau \tag{8.39}$$

for volatile chemical species, j = 1

$$C_j(0,t) = C_j^* = {P_j}/{He_j} \text{ at } x = 0 \text{ and } 0 \le t \ge \tau \tag{8.40}$$

for non-volatile chemical species, j = 2, 3, 4,…,10

$$\frac{\partial C_j}{\partial t}(0,t) = 0 \text{ at } x = 0 \text{ and } 0 \le t \ge \tau \tag{8.41}$$

where C_1^* is the interfacial concentration of CO_2 in the solution (kmol/m^3), which is defined as the partial pressure of CO_2 in the gas (P_1; kPa) divided by the physical solubility of CO_2 in the solution or Henry's law constant (He_1; kPa m^3/kmol). C_j^0 is the bulk concentration of species j in liquid phase (kmol/m^3), which can be obtained by the vapour-liquid equilibrium model.

For the laminar jet absorber, the contact time (τ) is found to be:

$$\tau = \frac{\pi d^2 h}{4L} \tag{8.42}$$

where d is jet diameter (m), h is jet height (m), and L is volumetric liquid flow rate (m^3/s).

From Higbie's penetration theory, the liquid phase mass transfer coefficient for physical absorption of CO_2 (k_L^0; m/s) is defined as:

$$k_L^0 = 2\sqrt{\frac{D_1}{\pi\tau}} = \frac{4}{d\pi}\sqrt{\frac{D_1 L}{h}} \tag{8.43}$$

The local CO_2 absorption rate per unit area (N; kmol/m^2 s) is given as:

$$N = -D_1\left(\frac{\partial C_j}{\partial t}\right)_{x=0} \tag{8.44}$$

Thus, the average CO_2 absorption rate per unit area (N_{ave}; kmol/m^2 s) is obtained by integrating Equation 8.44 over the contact time τ:

$$N_{ave} = -\frac{D_1}{\tau}\int_0^{\tau}\frac{\partial C_j}{\partial t}(0,t)dt \tag{8.45}$$

The effect of chemical reaction in terms of the enhancement factor, E, which is defined as the ratio of the absorption rate of CO_2 into a reacting liquid to that if there were no reaction, is given by:

$$E = \frac{N_{ave}}{k_L^0 \left(C_1^* - C_1^0 \right)} \tag{8.46}$$

For each absorption rate experiment, Equations 8.17, 8.18, 8.20, 8.21, and 8.26-8.31 were solved using FEM based on COMSOL 4.1 software with 1D time-dependent mode by considering the forward reaction rate constant of Equation 8.8 (k_{MEA}) as an adjustable parameter. The experimental enhancement factor ($E_{\exp}$) can be obtained directly from the experiment using Equation 8.46 (while the N_{ave} was measured experimentally). However, the predicted enhancement factor (E_{pred}) can be obtained numerically by integrating the local CO_2 absorption rate per unit area (N) over contact time τ, as shown in Equation 8.45. $\left(\frac{\partial C_1}{\partial t} \right)_{x=0}$ can be acquired as the result of solving Equations 8.17, 8.18, 8.20, 8.21, and 8.26-8.31 using the COMSOL software. Also, the integration over contact time τ was done using the integration function in the COMSOL software. For each experiment (at different initial amine concentrations, temperatures, initial CO_2 loadings, and contact times), the parameter k_{MEA} was adjusted until $\left| \frac{E_{\exp} - E_{pred}}{E_{\exp}} \right| \leq 1\%$ (Hagewiesche et al., 1995). Then, the forward reaction rate constants k_{MEA} were correlated with the reaction rate constant expression as shown in Equation 8.47.

$$k_{DEAB} = A \cdot \exp\left(-\frac{B}{T}\right) \tag{8.47}$$

8.3. Results and discussion

8.3.1 Vapour-liquid equilibrium model

The VLE model for aqueous solutions of blended MEA-DEAB was developed in order to obtain the bulk concentrations of all chemical species ($C_1 - C_{10}$), which are required for the CO_2 absorption rate/kinetic model. Some results for the bulk concentrations obtained by the VLE model are shown in Figure 8.2. This figure shows the species concentrations at 0 to 1 CO_2 loading for aqueous solution of blended 5 M MEA+1 M MEA at 313 K. It can be seen from Figure 8.2 that the concentration of MEA and DEAB decrease as CO_2 loading increases. This is due to the protonation and the CO_2-amine reactions of both MEA and DEAB, as shown in Equations 8.1, 8.2, 8.7, and 8.8. Thus, $MEAH^+$ and $DEABH^+$ (which are the protonated MEA and protonated DEAB, respectively), are found to increase as CO_2 loading increases. At CO_2 loading of less than 0.53, the concentration of carbamate ($\left[R''NHCOO^-\right]$) is found to increase as CO_2 loading increases because of carbamate formation by CO_2-MEA reaction, as shown in Equation 8.8. However, the $\left[R''NHCOO^-\right]$ decreases as CO_2 loading increases at CO_2 loading higher than 0.53. This is because the reversion of $R''NHCOO^-$ to bicarbonate (HCO_3^-) of Equation 8.9 becomes more important at high CO_2 loading (Hagewiesche et al., 1995). As CO_2 loading increases (which means more CO_2 is introduced to the solution), $\left[HCO_3^-\right]$ is found to increase. This is due to the formation of HCO_3^- from CO_2-DEAB-water, CO_2-water, CO_2-OH^- reactions, and the reversion of $R''NHCOO^-$, as shown in Equations

8.2, 8.3, 8,4, and 8.9, respectively. In addition, the concentration of free CO_2 ($[CO_2]$) is found to increase only at CO_2 loading beyond 0.8 due to the physical solubility of CO_2.

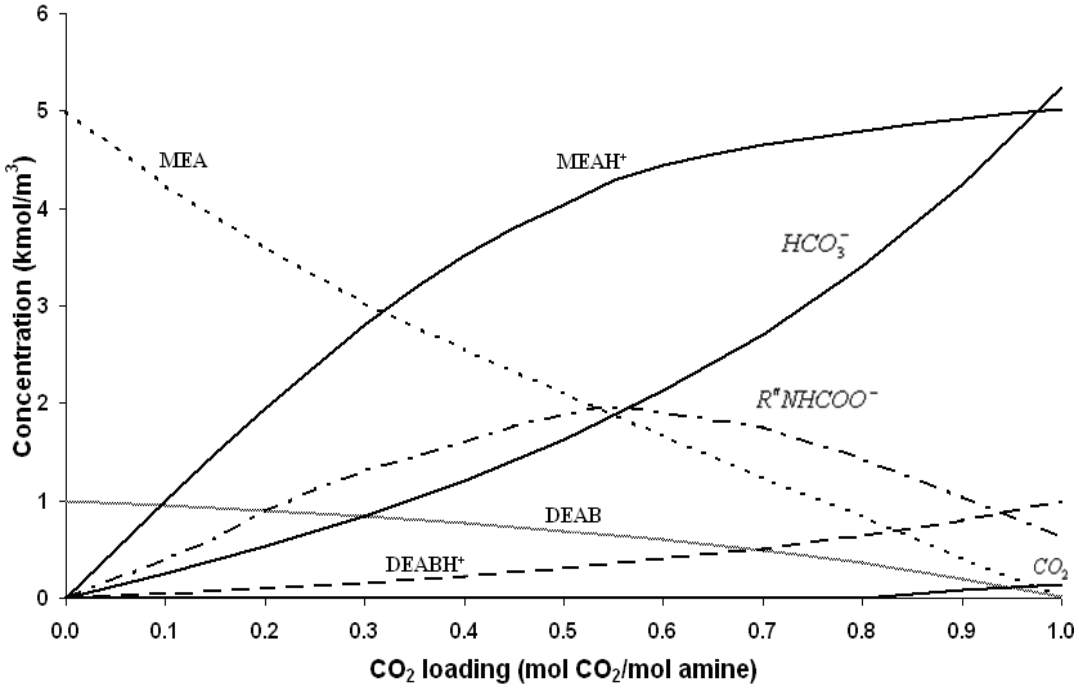

Figure 8.2 Liquid phase speciation and concentration in aqueous solutions of blended MEA-DEAB as a function of CO_2 loading (α) at initial MEA concentration of 5 M, initial DEAB concentration of 1 kmol/m^3, and 313 K (data obtained by vapour-liquid equilibrium model developed in this study).

8.3.2 CO_2 absorption rate/kinetics model

The CO_2 absorption rate in aqueous solutions of blended MEA-DEAB was measured using a laminar jet absorber at atmospheric pressure over a temperature range of 298 K to 323 K, an amine concentration range of 5 M MEA+0.25 M DEAB to 5 M MEA+2 M DEAB, a CO_2 loading range of 0.01 mol CO_2/mol amine to 0.13 mol CO_2/mol amine, and contact time range of 0.0024 s to 0.013 s. These operating conditions were selected because: (1) the regeneration energy of blended MEA-DEAB solution was found to be lower than that of single MEA solution; thus lower absorption temperature is applicable in this case; (2) industrially used MEA concentration is between 5 M to 7 M (mostly at 5 M). Therefore, MEA concentration was kept constant at 5 M, but DEAB concentration was varied from 0.25 M to 2 M in order to observed the effect of adding small amounts of DEAB into aqueous MEA solution; (3) the ideal solution assumption is applicable at low CO_2 loading (Edali, 2010). The experimental results for CO_2 absorption rate in aqueous DEAB solutions are presented in Table B2 (in Appendix B).

The experimental absorption rate data were then interpreted by the numerically solved CO_2 absorption rate/kinetics model using FEM based on COMSOL 4.1 software with 1D time-dependent mode by considering k_{MEA} as an adjustable parameter. The k_{MEA} results were correlated with the reaction rate constant expression of Equation 8.47 as:

$$k_{MEA} = \left(9.15 \times 10^{7}\right) \exp\left(-\frac{2808.1}{T}\right) \tag{8.48}$$

The predicted k_{MEA} at 313 K compared with those in the literature is shown in Table 8.1. The results show that k_{MEA} obtained from the reaction rate/kinetics model developed in this work compares favourably with those in the literature.

The enhancement factors, which represent the ratio of the absorption rate of CO_2 into a reacting liquid to that if there was no reaction, for CO_2 absorption in aqueous solutions of blended MEA-DEAB at 313 K over amine concentration range of 5 M MEA+0.25 M DEAB to 5 M MEA+2 M DEAB are shown in Table 8.2. Also, some predicted enhancement factors obtained from the reaction rate/kinetics model are presented in Table 8.2. Both experimental and predicted data are plotted in Figure 8.3. It can be observed from Figure 8.3 and Table 8.2 that the enhancement factors of blended MEA-DEAB aqueous solutions are higher than those of aqueous MEA solution. Moreover, it was found that the enhancement factor increases as DEAB concentration in the blended solution increases. However, the enhancement factor increases until the concentration of blended solution reaches a specific point (at 5 M MEA+1.25 M DEAB); then, the enhancement factor declines as DEAB concentration in the blended solution increases. Therefore, the maximum enhancement factor for aqueous solutions of blended MEA-DEAB over a concentration range of 5 M MEA+0.25 M DEAB to 5 M MEA+2 M DEAB can be obtained at 5 M MEA+1.25 M DEAB.

It can be observed from Figure 8.3 that the addition of DEAB into aqueous MEA solution can enhance the CO_2 absorption rate in terms of enhancement factor. This could be because there might be a structure-performance relationship between MEA-DEAB-CO_2 that assists the CO_2-MEA/DEAB reaction. This structural interaction between MEA and DEAB allows CO_2 to react with amine easily; thus, the absorption rate is increased.

However, the ratio between MEA and DEAB seems to affect the performance of the blended solution, since the enhancement factor increases as DEAB concentration in the blended solution increases until it reaches 5 M MEA+1.25 M DEAB, then the enhancement factor declines. This can imply that the adequate ratio between MEA-DEAB that leads to the most suitable MEA-DEAB structural interaction is 5 M MEA+ 1.25 M DEAB.

In addition, the reaction rate/kinetics model developed in this study is also able to predict the CO_2 absorption rate in aqueous solutions of blended MEA-DEAB at various temperatures, initial DEAB concentrations, initial CO_2 loadings, and contact times. The CO_2 absorption rate can be obtained numerically by integrating the local CO_2 absorption rate per unit area (N) over contact time τ, as shown in Equation 8.45. $\left(\frac{\partial C_1}{\partial t}\right)_{x=0}$ can be acquired as the result of solving the partial differential-nonlinear algebraic equations of Equations 8.17, 8.18, 8.20, 8.21, and 8.26-8.31 using the COMSOL software. Also, the integration over contact time τ was done using the integration function in the COMSOL software. The predicted CO_2 absorption rates compared with the experimental values are shown in Figure 8.4 as a parity chart with an AAD of 6.8%, which is favourably acceptable. Thus, it can be said that the numerical comprehensive reaction rate/kinetics model for CO_2 absorption into aqueous solution of blended MEA-DEAB developed in this work is adequate and provides accurate results.

Table 8.1 Comparison of k_{MEA} at 313 K with those in literature

k_{MEA} (m^3/kmol s)	References
13,020	Hikita et al. (1977)
11,730	Xiao et al. (2000)
11,592	This work
10,681	Edali et al. (2007)
10,090	Hagewisesche et al. (1995)

Table 8.2 Enhancement factor (E) of aqueous solutions of MEA and blended MEA-DEAB at 313 K

Concentration of amine (M)	Total amine concentration (M)	Enhancement factor
5 M MEA	5	23.1[a]
5 M MEA+0.25 M DEAB	5.25	24.7
5 M MEA+0.5 M DEAB	5.5	26.6[b]
5 M MEA+0.75 M DEAB	5.75	28.1[b]
5 M MEA+1 M DEAB	6	30.2
5 M MEA+1.25 M DEAB	6.25	30.8
5 M MEA+1.5 M DEAB	6.5	29.8
5 M MEA+1.75 M DEAB	6.75	29.6[b]
5 M MEA+2 M DEAB	7	28.9

[a] the experimental enhancement factor for 5 M MEA obtained from Aboudheir (2002).

[b] the predicted enhancement factor obtained from the reaction rate/kinetics model developed in this work.

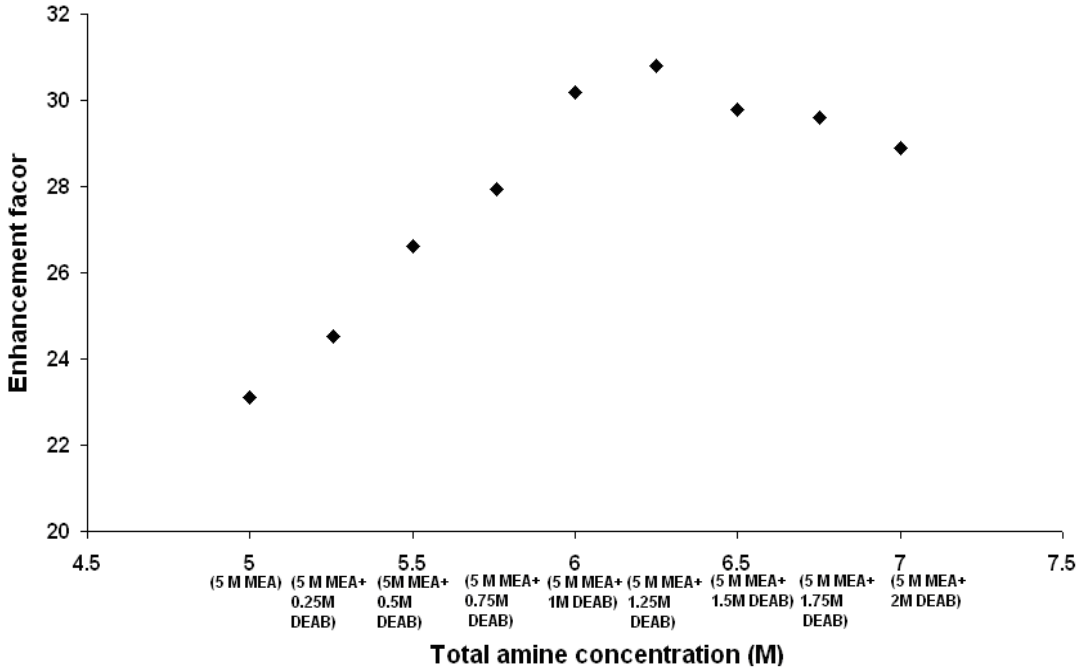

Figure 8.3 Enhancement factor of aqueous solutions of MEA and blended MEA-DEAB at 313 K.

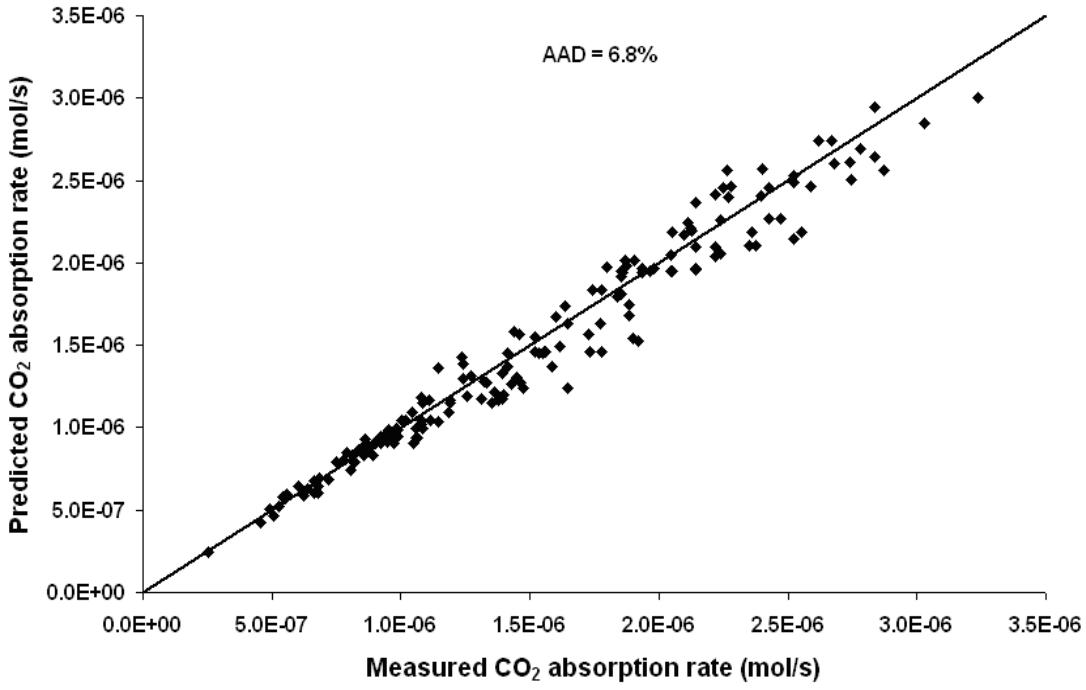

Figure 8.4 Parity chart comparing experimental and predicted CO_2 absorption rate in aqueous solution of blended MEA-DEAB.

8.4 Summaries

1. A comprehensive numerically solved reaction rate/kinetics model for CO_2 absorption into aqueous solutions of blended MEA-DEAB was successfully developed. The rate constant for CO_2 absorption in aqueous solution of blended MEA-DEAB, k_{MEA}, obtained over a temperature range of 298 K to 323 K is:

$$k_{MEA} = \left(9.15 \times 10^{7}\right) \exp\left(-\frac{2808.1}{T}\right)$$

2. Based on the kinetics data in terms of the enhancement factor, it was found that the 5 M MEA+1.25 M DEAB is the best MEA-DEAB combination over a concentration range of 5 M MEA+0.25 M DEAB to 5 M MEA+2 M DEAB.

3. The predicted CO_2 absorption rates obtained from the developed reaction rate/kinetics model fit favourably with the experimental results with an AAD of 6.8%.

8.5 References

1. Aboudheir, A. Kinetics, modeling, and simulation of carbon dioxide absorption into highly concentrated and loaded monoethanolamine solutions; Ph.D. thesis, University of Regina, Regina, Canada, 2002.

2. Aboudheir, A.; Tontiwachwuthikul, P.; Chakma, A.; Idem, R. Kinetics of reactive absorption of carbon dioxide in high CO_2-loaded concentrated aqueous MEA solutions. Chem. Eng. Sci. 2003, 58, 5195-5210.

3. Astarita, G.; Savage, D.; Bisio, A. Gas treating with chemical solvents; Wiley, New York, 1983.

4. Austgen, D.M.; Rochelle, G.T.; Chen, C.C. Model of vapor-liquid equilibria for aqueous acid gas-alkanolamine system. 2. Representation of H_2S and CO_2 solubility in aqueous MDEA and CO_2 solubility in aqueous mixtures of MDEA with MEA or DEA. Ind. Eng. Chem. Res. 1991, 30, 543-555.

5. Chakravaty, T.; Phukan, U.K.; Weiland, R.H. Reaction of acid gases with mixtures of amines. Chem. Engng. Prog. 1985, 81, 32-36.

6. Choi, W.J.; Cho, K.C.; Lee, S.S.; Shim, J.G.; Hwang, H.R., Park, S.W.; Oh, K.J. Removal of carbon dioxide by absorption into blended amines: kinetics of absorption into aqueous AMP/HMDA, AMP/MDEA, and AMP/piperazine solutions. Green Chem. 2007, 9, 594-598.

7. Critchfield, J.; Rochelle, G.T. Absorption of carbon dioxide in aqueous MDEA and MDEA/MEA solutions. The AIChE National Meeting, Houston, Texas, 1987.

8. Edali, M. Kinetics, modeling, and simulation of carbon dioxide absorption into mixed aqueous loaded solution blendes of methyldiethanolamine with monoethanolamine and with piperazine; Ph.D. thesis, University of Regina, Regina, Canada, 2010.

9. Edali, M.; Aboudheir, A.; Idem, R. Kinetics of carbon dioxide absorption into mixed aqueous solutions of MDEA and MEA using laminar jet apparatus and numerically solved absorption-rate/kinetic model. The COMSOL Conference, Boston, 2007.

10. Hagewiesche, D.P.; Ashour, S.S.; Al-Ghawas, H.A.; Sandall, O.C. Absorption of carbon dioxide into aqueous blends of monoethanolamine and N-methyldiethanolamine. Chem Eng. Sci. 1995, 50, 1071-1079.

11. Hikita, H.; Asai, S.; Ishikawa, H.; Honda, M. The kinetics of reaction of CO_2 with MEA, DEA, and TEA by rapid mixing method. Chem. Eng. J. 1977, 13, 7-12.

12. Hikita, H.; Ishikawa, H.; Uke, K.; Murakami, T. Diffusivities of mono-, di-, and tri-ethanolamine in aqueous solutions. J. Chem. Eng. Data 1980, 25, 324-325.

13. Kohl, A.L.; Nielsen, R.B. Gas Purification: 5^{th} Edition; Gulf Publishing Company: Houston, Texas, USA, 1997.

14. Maneeintr, K.; Idem, R. O.; Tontiwachwuthikul, P.; Wee, A. G. H. Synthesis, solubilities, and cyclic capacity of amino alcohols for CO_2 Capture from flue gas streams. Energy procedia 2009, 1, 1327-1334.

15. Naami, A.; Edali, M.; Sema, T.; Idem, R., Tontiwachwuthikul, P. Comprehensive mass transfer studies of CO_2 absorption in aqueous solutions of blended monoethanolamine and 4-diethylamino-2-butanol. Inpress

16. Pinsent, B.R.W.; Pearson, L.; Roughton, F.J.W. The kinetics of combination of carbon dioxide with hydroxide ions. Trans. Faraday Soc. 1956, 52, 1512-1520.

17. Sartori, G.; Savage, D.W. Sterically hindered amines for CO_2 removal from gases. Ind. Eng. Chem. Fundam. 1983, 22, 239-249.

18. Tontiwachwuthikul, P.; Meisen, A.; Lim, J.C. Solubility of CO_2 in 2-amino-2methyl-1-propanol solutions. J. Chem. Eng. Data 1991, 36, 130-133.

19. Tontiwachwuthikul, P.; Wee, A. G. H.; Idem, R. O.; Maneeintr, K.; Fan, G. J.; Veawab, A.; Aroonwilas, A.; Chakma, A. Method for capturing carbon dioxide from gas streams. US Patent Application. US Patent Application, No. US 2008/0050296 A1, 2008.

20. Xiao, J.; Li, C.W.; Li, M.H. Kinetics of absorption of CO_2 into aqueous solutions of 2-AMP + MEA. Chem. Eng. Sci. 2000, 55, 161-175.

21. Zhang, X.; Zhang, C.F.; Liu, Y. Kinetics of absorption of CO_2 into aqueous solution of MDEA blended with DEA. Ind. Eng. Chem. Res. 2002, 41, 1135-1141.

Chapter 9 Overall Conclusions and Recommendations

In this research, comprehensive numerically solved reaction rate/kinetics models for CO_2 absorption into aqueous solutions of DEAB and blended MEA-DEAB have been established in order to develop promising alternative solvents for capturing CO_2. However, the kinetics study of these new formulated solvents first required acquisition of fundamental knowledge such as the Henry's law constant, the physical CO_2 diffusivity, the equilibrium constant that governs CO_2-amine reaction, and the reaction kinetics data. These parameters were determined in this study. Furthermore, the performance of these newly formulated solvents in terms of equilibrium solubility of CO_2 (absorption capacity) was also investigated. From the results, it was found that the aqueous solutions of DEAB and blended MEA-DEAB have good potential to be used as alternative solvents for capturing CO_2.

9.1 Conclusions

The first portion of this research work (Chapters 4-6) focused on CO_2 absorption into aqueous solutions of DEAB about which the following conclusions can be summarized:

9.1.1 The N_2O solubility, which can be used for estimating the Henry's law constant via the N_2O analogy, for DEAB solvent and aqueous DEAB solutions was measured experimentally over ranges of temperatures and DEAB concentrations.

The N_2O solubility in DEAB solvent increases as temperature increases over a temperature range of 298 K to 343 K. The N_2O solubility in DEAB solvent can be estimated by: $He_{N_2O-DEAB} = (1.188 \times 10^7) \exp\left(\frac{-2460.3}{T}\right)$ with an AAD of 3.6%.

The N_2O solubility in aqueous DEAB solutions increases as temperature increases and decreases as DEAB concentration increases over a temperature range of 298 K to 343 K and a DEAB concentration range of 0.68 M to 3.77 M. It was also found that the N_2O solubility in aqueous DEAB solutions can be calculated using the polynomial model with an AAD of 0.1%.

9.1.2 The N_2O diffusivity, which can be used for estimating the physical diffusivity of CO_2 via the N_2O analogy, was experimentally determined over a temperature range of 298 K to 318 K and a concentration range of 1 M to 2.5 M. The results show that the N_2O diffusivity increases as temperature increases and decreases as DEAB concentration increases. Also, the N_2O diffusivity in aqueous DEAB solutions can be calculated using the semiempirical model with an AAD of 3.4%.

9.1.3 The equilibrium solubility of CO_2 in aqueous DEAB solution was found to be very high (comparable with PZ) and higher than that in aqueous solutions of AMP, MDEA, MEA, and DEA, respectively. In addition, the equilibrium solubility of CO_2 in aqueous DEAB solutions decreases as temperature increases and increases as CO_2 partial pressure and DEAB concentration increases over a temperature range of 298 K to 333 K, a CO_2 partial pressure range of 10 kPa to 100 kPa, and a DEAB concentration range of 1 M to 2.5 M.

9.1.4 The chemical equilibrium constant that governs the CO_2-DEAB-water reaction can be determined by the Kent-Eisenberg model or Austgen model.

9.1.5 The developed mathematical model for calculating the equilibrium solubility of CO_2 in aqueous DEAB solutions provides good agreement with the experimental results within the acceptable range of less than 10% AAD.

9.1.6 The estimated heat of CO_2 absorption in aqueous DEAB solution using the derived Gibbs-Helmholtz equation was found to be -41.4 kJ/mol, which is lower than that of MDEA, DEA, and MEA, respectively. Therefore, the regeneration energy for DEAB is lower than that of MDEA, DEA, and MEA, respectively.

9.1.7 The reaction rate constant (k_{DEAB}) for CO_2 absorption into aqueous DEAB solutions at 298 K to 318 K obtained from the developed comprehensive numerically solved reaction rate/kinetics model is $k_{DEAB} = \left(4.01 \times 10^{13}\right) \exp\left(-\frac{7527.7}{T}\right)$.

9.1.8 Based on the reaction rate constant (k), the CO_2 absorption reaction with DEAB is faster than that with MDEA and is comparable with that with AMP and DEA but slower than that with MEA and PZ, respectively.

9.1.9 The predicted CO_2 absorption rates obtained from the developed reaction rate/kinetics model fit favourably with the experimental results with an AAD of 6.5%.

9.1.10 Regarding these outstanding performances over the conventional amines (i.e. very high absorption capacity, fast reaction rate, and low regeneration energy), DEAB is being considered to be a promising alternative solvent for capturing CO_2.

The second part of this research (Chapters 7 and 8) focused on the CO_2 absorption into aqueous solutions of blended MEA-DEAB about which the following conclusions can be summarized:

9.1.11 The N_2O solubility, which can be used for estimating the Henry's law constant via the N_2O analogy, for aqueous solutions of blended MEA-DEAB increases as temperature increases and decreases as DEAB concentration in the blended solution increases over a temperature range of 298 K to 343 K and a concentration range of 5 M MEA+0.25 M DEAB to 5 M MEA+2 M DEAB. The N_2O solubility can be predicted using the semiempirical model with an AAD of 2.7%.

9.1.12 The N_2O diffusivity, which can be used for estimating the physical diffusivity of CO_2 via the N_2O analogy, for aqueous solutions of blended MEA-DEAB increases as temperature increases and decreases as DEAB concentration in the blended solution increases over a temperature range of 298 K to 323 K and a concentration range of 5 M MEA+0.25 M DEAB to 5 M MEA+2 M DEAB. The N_2O diffusivity can be predicted using the semiempirical model with an AAD of 3.6%.

9.1.13 The equilibrium solubility of CO_2 in aqueous solutions of blended MEA-DEAB decreases as temperature increases and increases as CO_2 partial pressure increases. Also, the equilibrium solubility of CO_2 increases as the DEAB concentration in the blended solution increases over a temperature range of 298 K to 333 K, a CO_2 partial pressure range of 10 kPa to 100 kPa, and a concentration range of 5 M MEA+0.25 M DEAB to 5 M MEA+2 M DEAB. Moreover, the equilibrium solubility of CO_2 in the blended solutions of MEA-DEAB was found to be higher than that in 5 M MEA.

9.1.14 Based on the equilibrium solubility of CO_2 in aqueous solutions of blended MEA-DEAB results, it was found that the 5 M MEA+1.5 M DEAB is the best MEA-DEAB formulation over a concentration range of 5 M MEA+0.25 M DEAB to 5 M MEA+2 M DEAB.

9.1.15 The developed mathematical model for calculating the equilibrium solubility of CO_2 in aqueous solutions of blended MEA-DEAB provides good agreement with the experimental results with an AAD of 6.3%.

9.1.16 The reaction rate constant (k_{MEA}) for CO_2 absorption into aqueous solutions of blended MEA-DEAB at 298 K to 323 K obtained from the developed comprehensive numerically solved reaction rate/kinetics model is:

$$k_{MEA} = \left(9.15 \times 10^{7}\right) \exp\left(-\frac{2808.1}{T}\right).$$

9.1.17 Based on the kinetics data in terms of the enhancement factor, it was found that the 5 M MEA+1.25 M DEAB is the best MEA-DEAB combination over a concentration range of 5 M MEA+0.25 M DEAB to 5 M MEA+2 M DEAB.

9.1.18 The predicted CO_2 absorption rates obtained from the developed reaction rate/kinetics model fit favourably with the experimental results with an AAD of 6.8%.

9.1.19 Based on the equilibrium solubility of CO_2 and the kinetics data in terms of the enhancement factor, it can be concluded that 5 M MEA+1.25 M DEAB is the best MEA-DEAB combination over a concentration range of 5 M MEA+0.25 M DEAB to 5 M MEA+2 M DEAB. This is because the maximum enhancement factor is obtained at 5 M MEA+1.25 M DEAB. Even though the best equilibrium solubility of CO_2 is found at 5 M MEA+1.5 M DEAB, the equilibrium solubility of CO_2 at 5 M MEA+1.25 M DEAB is almost the same as that at 5 M MEA+1.5 M DEAB. Another advantage of using 5 M

MEA+1.25 M DEAB is the amounts of amine used in the CO_2 capturing process are lower than with 5 M MEA+1.5 M DEAB.

9.2 Recommendations for future work

It has been demonstrated through this research that these new formulated solvents (i.e. DEAB and blended MEA-DEAB) are promising alternative solvents for capturing CO_2 in terms of their of absorption capacity, absorption rate, and regeneration energy. However, for industrial applications, more research needs to be done. The following investigations are recommended for future research:

9.2.1 The experimental data for the vapour-liquid equilibrium (VLE) model of aqueous solutions of DEAB and blended MEA-DEAB are essential in order to (i) produce more accurate liquid phase speciation, (ii) develop more comprehensive reaction rate/kinetics models, and (iii) obtain greater understanding of the reaction mechanisms of the new formulated solvents.

9.2.2 Develoing comprehensive reaction rate/kinetics models at various partial pressures of CO_2, including 10% CO_2 (from a natural gas reboiler), 15% CO_2 (from coal fired power plant), and 30% CO_2 (reformate gas from hydrogen production), is suggested for a better representation of the kinetics data in industrial applications.

9.2.3 One of the main problems for CO_2 treating plants is corrosion. Therefore, investigating the corrosion characteristics of the newly formulated solvents (i.e. DEAB and blended MEA-DEAB), as well as potential corrosion inhibitors, is suggested.

9.2.4 The investigation of the degradation characteristics of the newly formulated solvents (i.e. DEAB and blended MEA-DEAB) and potential degradation inhibitors is suggested.

9.2.5 The investigation on compatibility of rubber and plastic sealant with the newly formulated solvents (i.e. DEAB and blended MEA-DEAB) is suggested.

9.2.6 The reboiler heat duties for the regeneration of the newly formulated solvents (i.e. DEAB and blended MEA-DEAB) are essential for the full assessment of solvent suitability.

9.2.7 It would be worthwhile to extend investigation of new solvent formulations to blended DEAB-PZ, since PZ is a very effective promoter in terms of both capacity and absorption rate.

Appendix A1 Procedure for simultaneously solving the coupled nonlinear algebraic equations using 0D stationary solver mode in COMSOL software

The coupled nonlinear algebraic equations have been simultaneously solved using 0D stationary solver mode in COMSOL software in many aspects throughout this research such as (i) for determining the chemical equilibrium constant in Chapter 5, (ii) for calculating the equilibrium solubility of CO_2 in Chapters 5 and 7, and (iii) for determining the liquid bulk concentrations and equilibrium partial pressure of CO_2 (the vapour-liquid equilibrium (VLE) model) in Chapters 6 and 8. These applications used the same procedure, which is solving the n equations for the n unknowns. Therefore, only one example of the determination of bulk concentrations and equilibrium partial pressure of CO_2 for the VLE model for CO_2-DEAB aqueous system, as describe in Chapter 6, is presented.

The VLE model CO_2-DEAB aqueous system is governed by the following equations:

$$[DEAB]_0 = C_6 + C_7 \tag{1A}$$

$$\alpha[DEAB]_0 = C_1 + C_2 + C_4 \tag{2A}$$

$$C_5 + C_7 = C_2 + C_3 + 2C_4 \tag{3A}$$

$$K_2 = \frac{C_2 C_7}{C_1 C_6} \tag{4A}$$

$$K_3 = \frac{C_2 C_5}{C_1} \tag{5A}$$

$$K_4 = \frac{C_2}{C_1 C_3} \tag{6A}$$

$$K_6 = C_3 C_5 \tag{7A}$$

$$He_{CO_2} = P_{co_2} \Big/ C^*_{CO_2} \tag{8A}$$

List of unknowns: $C_1 - C_7$ and P_{co_2}

List of operation parameters or constants: α, $[DEAB]_0$, $[DEAB]_0$, K_2, K_3, K_4, K_6, He_{CO_2}, and $C^*_{CO_2}$

The solutions of 8 coupled nonlinear algebraic equations (1A-8A) will yield the value of 8 unknowns ($C_1 - C_7$ and P_{co_2}).

Procedure of simultaneously solving the 8 coupled nonlinear algebraic equations for the 8 unknowns using 0D stationary solver in COMSOL 4.1 software:

1. select Space Dimension of 0D → select Stationary study type

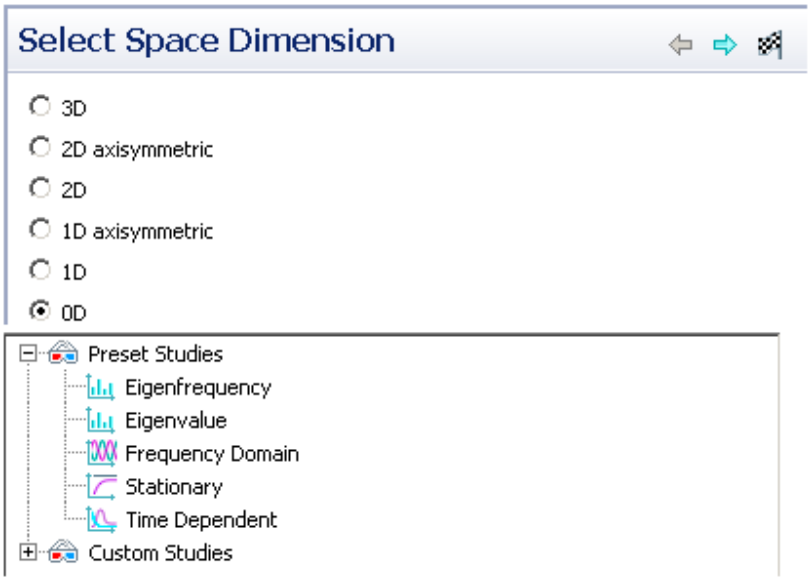

2. select Global Definitions → select Parameters → input all the operation parameters or constants (i.e. α, $[DEAB]_0$, $[DEAB]_0$, K_2, K_3, K_4, K_6, He_{CO_2}, and $C^*_{CO_2}$), as well as the initial guesses for $C_1 - C_7$ and P_{co_2}

Parameters

Name	Expression	Value	Description
Alpha	0.10	0.1	
K2	2.2404E+03	2240	
K3	9.0323E-09	9.032E-9	
K5	1.0789E-12	1.079E-12	
K6	9.2836E-18	9.284E-18	
HeS	2896.04023	2896	
PCO2guess	2.0153E-02	0.02015	
C1guess	1.6827E+00	1.683	
C2guess	7.6029E-13	7.603E-13	

3. select Global Equations → input all the equations (i.e. Equation 1A-8A)

Global Equations

$f(u,u_t,u_{tt},t) = 0, \quad u(t_0) = u_0 \quad u_t(t_0) = u_{t0}$

Name	f(u,ut,utt,t)	Initi...(u_0)	Initi..._t0)	Description
C1	C0-C1-C3	C1guess	0	
C2	K3-((C2*C5)/C4)	C2guess	0	
C3	C3+C2-C...(2*C7)	C3guess	0	
C4	(Alpha*...4-C5-C7	C4guess	0	
C5	K2-((C3...1*C4))	C5guess	0	
C6	K6-(C2*C6)	C6guess	0	

4. select Study → Compute

5. The obtained values of $C_1 - C_7$ and P_{co_2} are subsequently used as the new initial guesses for solving the 8 unknowns. This process is repeated until percentage deviation of the results of each unknown for successive attempts is less than 0.01%

Appendix A2 Procedure for solving the partial differential-nonlinear algebraic equations using 1D time dependent mode in COMSOL software

In this research, the partial differential-nonlinear algebraic equations have been solved using 1D time dependent mode in COMSOL 4.1 software for the aid of developing the reaction rate/kinetics models for the CO_2 absorption into aqueous solutions of DEAB and MEA-DEAB as describe in Chapters 6 and 8, respectively. Both models have been developed using the same procedure; thus, only one example of aqueous DEAB solutions is presented.

The diffusion equations that govern the CO_2 absorption into aqueous solutions of DEAB in terms of the CO_2 balance, total carbon balance, total DEAB balance, total charge balance, and independent equilibrium constant are given in the following equations:

$$\frac{\partial C_1}{\partial t} = D_1 \frac{\partial^2 C_1}{\partial x^2} - k_{DEAB} C_1 C_6 + \left(\frac{k_{DEAB}}{K_2} \right) C_2 C_7 - k_{24} C_1 C_3 + \left(\frac{k_{24}}{K_4} \right) C_2 \tag{9A}$$

$$\frac{\partial C_1}{\partial t} + \frac{\partial C_2}{\partial t} + \frac{\partial C_4}{\partial t} = D_1 \frac{\partial^2 C_1}{\partial x^2} + D_2 \frac{\partial^2 C_2}{\partial x^2} + D_4 \frac{\partial^2 C_4}{\partial x^2} \tag{10A}$$

$$\frac{\partial C_6}{\partial t} + \frac{\partial C_7}{\partial t} = D_6 \frac{\partial^2 C_6}{\partial x^2} + D_7 \frac{\partial^2 C_7}{\partial x^2} \tag{11A}$$

$$\frac{\partial C_2}{\partial t} + \frac{\partial C_3}{\partial t} + 2\frac{\partial C_4}{\partial t} - \frac{\partial C_5}{\partial t} - \frac{\partial C_7}{\partial t} = D_2 \frac{\partial^2 C_2}{\partial x^2} + D_3 \frac{\partial^2 C_3}{\partial x^2} + 2D_4 \frac{\partial^2 C_4}{\partial x^2} - D_5 \frac{\partial^2 C_5}{\partial x^2} - D_7 \frac{\partial^2 C_7}{\partial x^2} \tag{12A}$$

$$K_2 = \frac{C_2 C_7}{C_1 C_6} \tag{13A}$$

$$K_3 = \frac{C_2 C_5}{C_1} \tag{14A}$$

$$K_6 = C_3 C_5 \tag{15A}$$

List of unknowns: $C_1 - C_7$

List of operation parameters or constants: $D_1 - D_7$, k_{24}, K_2, K_3, K_6, N_{ave}, k_L^0, C_1^*, C_1^0, and $E_{\exp}$

The solutions of 7 partial differential-nonlinear algebraic equations (9A-15A) will yield the value of 7 unknowns ($C_1 - C_7$).

The k_{DEAB} is the adjustable parameter. It will be adjusted until $\left| \frac{E_{\exp} - E_{pred}}{E_{\exp}} \right| \leq 1\%$ as describe in Chapter 6.

Procedure of solving the partial differential-nonlinear algebraic equations using 1D time dependent mode in COMSOL software

1. select Space Dimension of 1D → select PDE (c),coefficient form, → add dependent variable ($C_1 - C_7$) → select Time Dependent

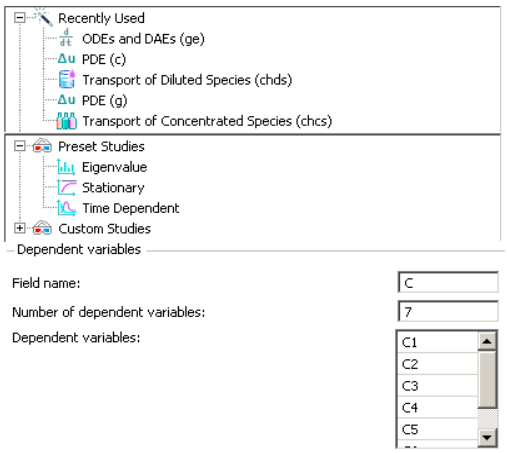

2. select Geometry → select Interval → draw straight line → input length (liquid jet radius)

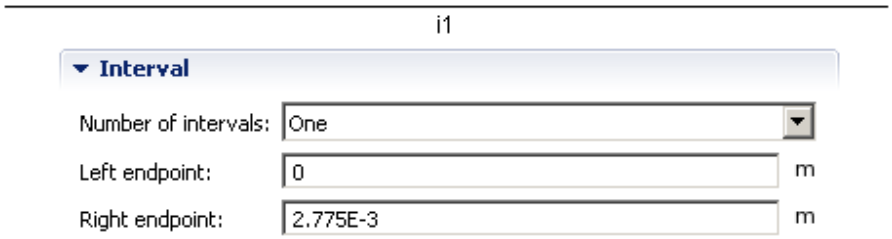

3. input all operating parameters, constants, bulk concentrations, and adjustable k_{DEAB}

Parameters

Name	Expression	Value	Description
kDEAB	1429	1429	m3/ kmol s
k24	8.3221377E3	8322	m3/ kmol s
K2	3.4987E3	3499	unitless
K3	7.8659E-9	7.866E-9	kmol/m3
K4	2.4418E9	2.442E9	m3/kmol
K6	3.2213E-18	3.221E-18	kmol^2/m3^2
D1	1.1194E-9	1.119E-9	m2/s
D2	3.02079E-10	3.021E-10	m2/s
D3	3.02079E-10	3.021E-10	m2/s
D4	3.02079E-10	3.021E-10	

4. select PDE (c) → select Coefficient form → input all partial differential-nonlinear algebraic equations (i.e. 9A-15A) → set coefficients e_a, α, γ, β, α, and a to be zero

$$e_a\frac{\partial^2\mathbf{u}}{\partial t^2}+d_a\frac{\partial\mathbf{u}}{\partial t}+\nabla\cdot(-c\nabla\mathbf{u}-\alpha\mathbf{u}+\gamma)+\beta\cdot\nabla\mathbf{u}+a\mathbf{u}=f$$

$$\mathbf{u}=[C1,C2,C3,C4,C5,C6,C7]^T$$

Diffusion Coefficient

c

	D1	0	0	0	0	0	0
	0	0	0	0	0	0	0
	0	0	0	0	0	0	0
c	D1	D2	0	D4	0	0	0
	0	D2	D3	2*D4	-D5	0	-D7
	0	0	0	0	0	D6	D7
	0	0	0	0	0	0	0

Damping or Mass Coefficient

d_a

	1	0	0	0	0	0	0
	0	0	0	0	0	0	0
	0	0	0	0	0	0	0
d_a	1	1	0	1	0	0	0
	0	1	1	2	-1	0	-1
	0	0	0	0	0	1	1
	0	0	0	0	0	0	0

5. select PDE (c) → input initial and boundary conditions as given in Chapter 6
6. select Study → select Compute

Appendix B Experimental data for CO_2 absorption into aqueous solutions of DEAB and blended MEA-DEAB

Table B1 Experimental data for CO_2 absorption into aqueous solutions of DEAB

DEAB concentration (M)	Temperature (K)	Loading (mol CO_2/ mol amine)	Jet diameter (mm)	Jet height (mm)	CO_2 absorption rate (ml/min)
2	298	0.0014	0.555	4.39	0.82
2	298	0.0014	0.555	5.64	0.93
2	298	0.0014	0.555	7.73	0.96
2	298	0.0014	0.555	9.03	0.97
2	298	0.0014	0.555	11.92	1.05
2	298	0.0014	0.555	12.08	1.06
2	298	0.0014	0.555	14.66	1.08
2	298	0.0361	0.55	15.61	1.09
2	298	0.0361	0.55	14.63	1.02
2	298	0.0361	0.55	13.77	1.05
2	298	0.0361	0.55	12.40	0.97
2	298	0.0361	0.55	11.73	0.95
2	298	0.0361	0.55	10.35	0.93
2	298	0.0361	0.55	10.24	0.93
2	298	0.0894	0.55	14.29	1.02
2	298	0.0894	0.55	13.04	1.00
2	298	0.0894	0.55	11.49	0.89
1.5	298	0.0818	0.52	12.95	0.93
1.5	298	0.0818	0.52	12.01	0.92
1.5	298	0.0818	0.52	9.74	0.84
1.5	298	0.0818	0.52	7.85	0.82
1.5	298	0.0818	0.52	6.62	0.79
1.5	298	0.0818	0.52	5.21	0.77
1.5	298	0.1154	0.56	12.50	0.92
1.5	298	0.1154	0.56	12.26	0.91
1.5	298	0.1154	0.56	10.54	0.89
1.5	298	0.1154	0.56	10.35	0.89
1.5	298	0.1154	0.56	9.21	0.86
1.5	298	0.1154	0.56	9.04	0.85
1.5	298	0.1154	0.56	7.27	0.79
1.5	298	0.1154	0.56	6.36	0.76
1.5	298	0.1505	0.42	9.22	0.79
1.5	298	0.1154	0.56	6.36	0.76
1.5	298	0.1505	0.42	9.22	0.79

Table B1 Experimental data for CO_2 absorption into aqueous solutions of DEAB

(continued)

DEAB concentration (M)	Temperature (K)	Loading (mol CO_2/ mol amine)	Jet diameter (mm)	Jet height (mm)	CO_2 absorption rate (ml/min)
1.5	298	0.1505	0.42	6.19	0.68
1	298	0.1082	0.53	10.40	0.62
1	298	0.1082	0.53	9.84	0.59
1	298	0.1082	0.53	8.93	0.55
1	298	0.1082	0.53	7.22	0.51
1	298	0.1082	0.53	5.57	0.48
1	298	0.1406	0.54	11.21	0.50
1	298	0.1406	0.54	10.10	0.47
1	298	0.1406	0.54	8.71	0.45
1	298	0.1406	0.54	6.36	0.41
1	298	0.1825	0.555	6.51	0.39
1	298	0.1825	0.555	7.31	0.42
1	298	0.1825	0.555	8.63	0.48
1	298	0.1825	0.555	9.91	0.57
1	298	0.1825	0.555	10.81	0.61
2	308	0.0014	0.56	15.19	1.33
2	308	0.0014	0.56	12.77	1.21
2	308	0.0014	0.56	12.70	1.20
2	308	0.0014	0.56	10.01	1.19
2	308	0.0014	0.56	9.31	1.14
2	308	0.0014	0.56	7.29	1.04
2	308	0.0014	0.56	7.19	1.01
2	308	0.0036	0.55	12.84	1.19
2	308	0.0036	0.55	12.13	1.18
2	308	0.0036	0.55	10.25	1.07
2	308	0.0036	0.55	10.18	1.05
2	308	0.0036	0.55	9.89	1.04
2	308	0.0036	0.55	9.72	1.03
2	308	0.0036	0.55	7.32	0.95
2	308	0.0894	0.55	12.11	1.11
2	308	0.0894	0.55	11.60	1.06
2	308	0.0894	0.55	9.52	1.00
1.5	308	0.0818	0.52	12.45	1.09

Table B1 Experimental data for CO_2 absorption into aqueous solutions of DEAB

(continued)

DEAB concentration (M)	Temperature (K)	Loading (mol CO_2/ mol amine)	Jet diameter (mm)	Jet height (mm)	CO_2 absorption rate (ml/min)
1.5	308	0.0818	0.52	7.40	0.89
1.5	308	0.1154	0.56	13.28	1.09
1.5	308	0.1154	0.56	12.29	1.04
1.5	308	0.1154	0.56	11.43	0.97
1.5	308	0.1154	0.56	11.42	0.96
1.5	308	0.1154	0.56	10.09	0.92
1.5	308	0.1154	0.56	9.42	0.90
1.5	308	0.1505	0.42	10.95	0.84
1.5	308	0.1505	0.42	9.95	0.96
1.5	308	0.1505	0.42	8.96	0.83
1.5	308	0.1505	0.42	7.96	0.77
1.5	308	0.1505	0.42	7.72	0.65
1	308	0.1082	0.52	9.54	0.63
1	308	0.1082	0.52	8.74	0.61
1	308	0.1082	0.52	8.53	0.60
1	308	0.1082	0.52	6.83	0.53
1	308	0.1406	0.54	7.28	0.56
1	308	0.1406	0.54	6.02	0.52
1	308	0.1406	0.54	5.54	0.49
1	308	0.1406	0.54	4.38	0.36
1	308	0.1825	0.53	10.86	0.65
1	308	0.1825	0.53	10.34	0.61
1	308	0.1825	0.53	6.80	0.44
2	318	0.0014	0.57	14.71	1.39
2	318	0.0014	0.57	13.47	1.31
2	318	0.0014	0.57	11.51	1.25
2	318	0.0014	0.57	9.51	1.21
2	318	0.0014	0.57	8.24	1.14
2	318	0.0014	0.57	5.45	1.03
2	318	0.0361	0.55	12.84	1.19
2	318	0.0361	0.55	12.13	1.18
2	318	0.0361	0.55	10.25	1.07
2	318	0.0361	0.55	10.18	1.05

Table B1 Experimental data for CO_2 absorption into aqueous solutions of DEAB

(continued)

DEAB concentration (M)	Temperature (K)	Loading (mol CO_2/ mol amine)	Jet diameter (mm)	Jet height (mm)	CO_2 absorption rate (ml/min)
2	318	0.0894	0.59	12.99	1.17
2	318	0.0894	0.59	12.79	1.16
2	318	0.0894	0.59	11.36	1.06
2	318	0.0894	0.59	9.94	1.04
1.5	318	0.0818	0.52	8.79	0.99
1.5	318	0.0818	0.52	7.54	0.94
1.5	318	0.0818	0.52	7.43	0.91
1.5	318	0.1154	0.55	11.80	0.99
1.5	318	0.1154	0.55	9.73	0.94
1.5	318	0.1154	0.55	6.90	0.88
1.5	318	0.1154	0.55	6.41	0.87
1.5	318	0.1505	0.42	10.33	0.89
1.5	318	0.1505	0.42	8.04	0.82
1.5	318	0.1505	0.42	6.59	0.78
1.5	318	0.1082	0.53	7.94	0.67
1.5	318	0.1082	0.53	6.10	0.56
1.5	318	0.1082	0.53	5.77	0.52
1.5	318	0.1082	0.53	4.38	0.46
1.5	318	0.1406	0.54	9.32	0.75
1.5	318	0.1406	0.54	7.90	0.68
1.5	318	0.1406	0.54	6.02	0.61
1.5	318	0.1406	0.54	5.43	0.54
1.5	318	0.1825	0.53	11.30	0.89
1.5	318	0.1825	0.53	9.93	0.78
1.5	318	0.1825	0.53	7.88	0.65

Table B2 Experimental data for CO_2 absorption into aqueous solutions of blended MEA-DEAB

Concentration (M)		Temperature (K)	Loading (mol CO_2/ mol amine)	Jet diameter (mm)	Jet height (mm)	CO_2 absorption rate (ml/min)
MEA	DEAB					
5	0.25	298	0.0157	0.49	9.30	2.09
5	0.25	298	0.0157	0.49	8.40	1.87
5	0.25	298	0.0157	0.49	7.59	1.54
5	0.25	298	0.0157	0.49	6.87	1.32
5	0.25	298	0.0157	0.49	6.04	1.10
5	0.25	298	0.1018	0.45	10.40	1.78
5	0.25	298	0.1018	0.45	9.73	1.67
5	0.25	298	0.1018	0.45	8.74	1.40
5	0.25	298	0.1018	0.45	7.75	1.20
5	0.25	298	0.1305	0.55	13.30	2.53
5	0.25	298	0.1305	0.55	12.62	2.32
5	0.25	298	0.1305	0.55	11.81	2.17
5	0.25	298	0.1305	0.55	10.92	1.85
5	0.25	298	0.1305	0.55	9.86	1.76
5	0.25	298	0.1305	0.55	9.12	1.42
5	0.25	298	0.1305	0.55	8.45	1.31
5	0.25	298	0.1305	0.55	7.68	1.12
5	1	298	0.0117	0.51	11.63	2.20
5	1	298	0.0117	0.51	10.92	1.93
5	1	298	0.0698	0.42	10.53	1.42
5	1	298	0.0698	0.42	9.90	1.27
5	1	298	0.0698	0.42	9.19	1.08
5	1	298	0.0698	0.42	8.34	0.97
5	1	298	0.1174	0.49	12.68	1.80
5	1	298	0.1174	0.49	12.13	1.55
5	1	298	0.1174	0.49	11.54	1.43
5	1	298	0.1174	0.49	10.04	1.41
5	1	298	0.1174	0.49	9.30	1.16
5	1	298	0.1174	0.49	8.43	0.92
5	1.5	298	0.0289	0.45	8.72	1.16
5	1.5	298	0.0289	0.45	7.89	1.06
5	1.5	298	0.0289	0.45	7.52	0.91
5	1.5	298	0.0289	0.45	7.06	0.86

Table B2 Experimental data for CO_2 absorption into aqueous solutions of blended MEA-DEAB (continued)

Concentration (M)		Temperature (K)	Loading (mol CO_2/ mol amine)	Jet diameter (mm)	Jet height (mm)	CO_2 absorption rate (ml/min)
MEA	DEAB					
5	1.5	298	0.0567	0.6	7.20	1.09
5	1.5	298	0.1085	0.56	9.61	2.50
5	1.5	298	0.1085	0.56	8.96	2.39
5	1.5	298	0.1085	0.56	7.84	2.04
5	1.5	298	0.1085	0.56	7.01	1.45
5	1.5	298	0.1085	0.56	6.58	1.16
5	1.5	298	0.1085	0.56	5.85	0.89
5	2	298	0.0289	0.5	7.32	0.91
5	2	298	0.0289	0.5	6.43	0.84
5	2	298	0.0289	0.5	5.23	0.68
5	2	298	0.0567	0.48	7.31	0.89
5	2	298	0.0567	0.48	6.52	0.74
5	2	298	0.0567	0.48	5.23	0.71
5	2	298	0.0567	0.48	4.13	0.61
5	2	298	0.1085	0.51	7.42	0.81
5	2	298	0.1085	0.51	6.14	0.73
5	2	298	0.1085	0.51	5.15	0.66
5	0.25	313	0.0157	0.49	13.07	4.35
5	0.25	313	0.0157	0.49	11.79	3.86
5	0.25	313	0.0157	0.49	10.15	3.32
5	0.25	313	0.0157	0.49	8.85	2.88
5	0.25	313	0.0157	0.49	8.10	2.55
5	0.25	313	0.0157	0.49	6.75	2.13
5	0.25	313	0.0157	0.49	5.66	1.82
5	0.25	313	0.1018	0.45	12.33	3.16
5	0.25	313	0.1018	0.45	11.74	3.01
5	0.25	313	0.1018	0.45	11.15	2.75
5	0.25	313	0.1018	0.45	10.35	2.52
5	0.25	313	0.1018	0.45	8.02	1.87
5	0.25	313	0.1018	0.45	7.50	1.60
5	0.25	313	0.1018	0.45	6.58	1.28
5	0.25	313	0.1305	0.55	13.22	3.60
5	0.25	313	0.1305	0.55	12.34	3.39

Table B2 Experimental data for CO_2 absorption into aqueous solutions of blended MEA-DEAB (continued)

Concentration (M)		Temperature (K)	Loading (mol CO_2/ mol amine)	Jet diameter (mm)	Jet height (mm)	CO_2 absorption rate (ml/min)
MEA	DEAB					
5	0.25	313	0.1305	0.55	9.90	2.49
5	0.25	313	0.1305	0.55	13.22	3.60
5	1	313	0.0117	0.41	12.61	3.26
5	1	313	0.0117	0.41	11.97	2.98
5	1	313	0.0117	0.41	11.57	2.76
5	1	313	0.0117	0.41	10.65	1.98
5	1	313	0.0117	0.41	9.91	2.21
5	1	313	0.0117	0.41	9.29	2.21
5	1	313	0.0117	0.41	8.48	1.95
5	1	313	0.0698	0.42	12.85	3.00
5	1	313	0.0698	0.42	12.14	2.73
5	1	313	0.0698	0.42	11.58	2.53
5	1	313	0.0698	0.42	10.94	2.33
5	1	313	0.0698	0.42	9.98	1.92
5	1	313	0.0698	0.42	9.42	1.88
5	1	313	0.0698	0.42	6.86	1.28
5	1	313	0.1174	0.49	12.62	2.84
5	1	313	0.1174	0.49	12.01	2.76
5	1	313	0.1174	0.49	11.07	2.56
5	1	313	0.1174	0.49	10.31	2.49
5	1	313	0.1174	0.49	9.91	2.34
5	1	313	0.1174	0.49	9.07	1.96
5	1	313	0.1174	0.49	8.63	1.71
5	1	313	0.1174	0.49	8.20	1.67
5	1.5	313	0.0289	0.45	7.57	1.49
5	1.5	313	0.0289	0.45	7.34	1.45
5	1.5	313	0.0289	0.45	6.87	1.21
5	1.5	313	0.0289	0.45	6.44	1.15
5	1.5	313	0.0567	0.6	9.71	2.39
5	1.5	313	0.0567	0.6	8.89	2.10
5	1.5	313	0.0567	0.6	8.09	1.90
5	1.5	313	0.0567	0.6	7.59	1.79
5	1.5	313	0.0567	0.6	6.37	1.69

Table B2 Experimental data for CO_2 absorption into aqueous solutions of blended MEA-DEAB (continued)

Concentration (M)		Temperature (K)	Loading (mol CO_2/ mol amine)	Jet diameter (mm)	Jet height (mm)	CO_2 absorption rate (ml/min)
MEA	DEAB					
5	1.5	313	0.1085	0.46	8.29	1.28
5	1.5	313	0.1085	0.46	5.48	0.34
5	2	313	0.0372	0.47	10.38	1.59
5	2	313	0.0372	0.47	8.53	1.46
5	2	313	0.0372	0.47	6.43	1.32
5	2	313	0.0635	0.51	9.52	1.37
5	2	313	0.0635	0.51	7.53	1.28
5	2	313	0.0635	0.51	6.48	1.21
5	2	313	0.0635	0.51	5.32	1.04
5	2	313	0.1204	0.46	8.54	1.24
5	2	313	0.1204	0.46	6.87	1.16
5	0.25	323	0.0157	0.49	11.02	4.07
5	0.25	323	0.0157	0.49	10.28	3.81
5	0.25	323	0.0157	0.49	9.17	3.39
5	0.25	323	0.0157	0.49	8.04	2.88
5	0.25	323	0.0157	0.49	7.28	2.42
5	0.25	323	0.0157	0.49	6.00	1.35
5	0.25	323	0.0157	0.45	13.95	3.81
5	0.25	323	0.0157	0.45	13.37	3.59
5	0.25	323	0.0157	0.45	12.69	3.26
5	0.25	323	0.0157	0.45	11.86	3.22
5	0.25	323	0.0157	0.45	11.24	2.85
5	0.25	323	0.0157	0.45	10.38	2.60
5	0.25	323	0.1305	0.55	12.47	3.74
5	0.25	323	0.1305	0.55	11.90	3.69
5	0.25	323	0.1305	0.55	10.54	3.02
5	0.25	323	0.1305	0.55	9.71	2.88
5	0.25	323	0.1305	0.55	8.29	2.51
5	0.25	323	0.1305	0.55	7.34	2.04
5	1	323	0.0117	0.41	12.05	3.52
5	1	323	0.0117	0.41	11.61	3.48
5	1	323	0.0117	0.41	10.93	3.43
5	1	323	0.0117	0.41	10.37	3.39

Table B2 Experimental data for CO_2 absorption into aqueous solutions of blended MEA-DEAB (continued)

Concentration (M)		Temperature (K)	Loading (mol CO_2/ mol amine)	Jet diameter (mm)	Jet height (mm)	CO_2 absorption rate (ml/min)
MEA	DEAB					
5	1	323	0.0117	0.41	8.06	2.49
5	1	323	0.0117	0.41	7.70	2.20
5	1	323	0.0117	0.41	6.93	1.90
5	1	323	0.0698	0.42	13.33	3.68
5	1	323	0.0698	0.42	12.32	2.88
5	1	323	0.0698	0.42	11.21	2.66
5	1	323	0.0698	0.42	10.81	2.60
5	1	323	0.0698	0.42	10.10	2.47
5	1	323	0.0698	0.42	9.61	2.38
5	1	323	0.0698	0.42	8.77	2.06
5	1	323	0.0698	0.42	7.47	1.83
5	1	323	0.1174	0.49	11.94	3.17
5	1	323	0.1174	0.49	11.28	2.98
5	1	323	0.1174	0.49	10.73	2.88
5	1	323	0.1174	0.49	10.17	2.58
5	1	323	0.1174	0.49	9.63	2.08
5	1	323	0.1174	0.49	9.09	1.97
5	1.5	323	0.0289	0.45	11.80	3.23
5	1.5	323	0.0289	0.45	11.32	3.06
5	1.5	323	0.0289	0.45	11.05	2.82
5	1.5	323	0.0567	0.6	8.74	3.04
5	1.5	323	0.0567	0.6	7.98	2.98
5	1.5	323	0.0567	0.6	7.15	2.15
5	1.5	323	0.1085	0.46	7.29	1.60
5	1.5	323	0.1085	0.46	6.63	1.33
5	1.5	323	0.1085	0.46	6.02	1.24
5	1.5	323	0.1085	0.46	5.13	1.01
5	2	323	0.0316	0.49	8.93	1.45
5	2	323	0.0316	0.49	6.72	1.36
5	2	323	0.0316	0.49	5.27	1.18
5	2	323	0.0593	0.51	7.79	1.46
5	2	323	0.0593	0.51	6.23	1.27